Hydroplaning With Lightly-Loaded Truck Tires

Final Report

Robert D. Ervin
Luis Balderas

March 1990

UMTRI The University of Michigan Transportation Research Institute

Technical Report Documentation Page

1. Report No.	2. Government Accession No.	3. Recipient's Catalog No.

4. Title and Subtitle
HYDROPLANING WITH
LIGHTLY-LOADED TRUCK TIRES

5. Report Date
January 1990

6. Performing Organization Code

7. Author(s)
Robert D. Ervin, Luis Balderas

8. Performing Organization Report No.
UMTRI-90-6

9. Performing Organization Name and Address
The University of Michigan
Transportation Research Institute
2901 Baxter Road, Ann Arbor, Michigan 48109

10. Work Unit No. (TRAIS)

11. Contract or Grant No.
R49/CCR 502401-02

12. Sponsoring Agency Name and Address
Department of Health and Human Services
Centers for Disease Control
Atlanta, GA 30333

13. Type of Report and Period Covered
Final: 4/1/88 - 6/30/89

14. Sponsoring Agency Code

15. Supplementary Notes

16. Abstract

A mobile dynamometer device was used to make measurements of the traction performance of truck tires operating at very light loads on wetted pavements. A baseline set of tests covered the influences of velocity, inflation pressure, pavement type, tire type and tire model on traction levels. The tests employed either single or dual tires mounted ahead of the test specimens in order to "wipe" water from the paths of the test specimen tires in a manner analagous to actual truck installation. A second set of tests employed a large sample of tires that had been worn through normal usage in trucking fleets. The tests using fleetworn specimens covered a range of tread depths, providing results upon which to consider the appropriateness of federal regulations stipulating minimum tread depth values for interstate trucking.

Results indicate that hydrodynamic phenomena do indeed influence the traction performance of lightly-loaded truck tires on wet pavement at conventional highway speeds. These influences are observed for rear-mounted tires despite the wiping action resulting from tires mounted at front-axle positions. Lightly-loaded truck tires were seen to lose 50 to 70% of their "as-new" traction capability when approaching the federally-stipulated minimum in tread depth.

17. Key Words	18. Distribution Statement
truck tires, hydroplaning, wet pavement, traction, braking, testing	

19. Security Classif. (of this report)	20. Security Classif. (of this page)	21. No. of Pages	22. Price
		89	

TABLE OF CONTENTS

Acknowledgements

The authors wish to acknowledge the generous participation of the United Parcel Service and Roadway Express for providing fleet-worn tires for use in the measurement program conducted here. Mr. Michael Campbell of the UMTRI staff provided all of the instrumentation support for the project and Mr. Tom Dixon of UMTRI served as the driver of the test vehicle. Modification of the test vehicle was supervised by Mr. John Koch.

Coordination of the traction measurement activity at the Transportation Research Center of Ohio was provided by Ms. Teri Elliot.

1.0 Introduction

This document constitutes the final report on a study entitled, "Hydroplaning with Lightly-Loaded Truck Tires", sponsored under grant no. R49/CCR502401-01-02 from the U.S. Department of Health & Human Services under its program focussing upon injury control. The study was conducted by the University of Michigan Transportation Research Institute (UMTRI).

The project addressed a specific area of concern involving the control of heavy duty trucks on wetted pavement. The concern deals with the lightly-loaded, or near-empty condition in which truck, tractor, and semitrailer tires are less capable of providing good wet-traction performance. The traction handicap derives from the fact that the lightly-loaded truck tire contacts the ground with a footprint which is rather short relative to its width such that there is risk on wet pavements of developing significant hydrodynamic pressures over a substantial portion of the tire's contact length.

Since the tire rolls in the longitudinal direction, a very short contact length dimension implies a very short time interval during which water on the roadway must be expelled from beneath the footprint. If the contact shape is short, but wide, a long escape path is presented for water flowing laterally while the short available time implies that very high water velocities must prevail if the fluid is to escape and thus allow the tire tread to engage the pavement. When tread depth is also low, even thin films of water will result in high levels of hydrodynamic pressure beneath the tire, since the groove volume available for receiving the water bulk is very limited. In deep water, classical hydroplaning appears to be possible within normal highway speeds, regardless of the tread depth condition.

This study has attempted to quantify the "bottom line" posed by this phenomenon in terms of the traction performance of lightly-loaded truck tires, particularly under the influence of reduced values of tread depth. Recognizing that commercial vehicles accumulate mileage rapidly and that tire costs are significant to the profitability of trucking operations, the tread depth issue addresses a classic tradeoff between safety and economics. Thus the study results are intended to aid in the formulation of government policies and industry practices which seek an informed balance to this tradeoff.

Section 2.0 of this report reviews the research which forms the basis for the wet-traction hypothesis espoused above, in the context of the classical work on hydroplaning which first addressed the problem of aircraft landings on wet runways.

The focus of this study involved an experimental program by which direct measurement was made of truck tire traction performance under the conditions described. A mobile test device was modified for these experiments such that the wet pavement condition encountered by the test tires was representative of that encountered by the lightly-loaded tires located on the rear axles of near-empty trucks and tractors under moderate rainfall. A matrix of tire tests was conducted both to define the parametric sensitivities of

the light-load traction problem and to specifically quantify the influence of tread depth on actual fleet-worn tires. Tread depth is of special interest as an obviously dominant tire parameter influencing wet traction performance, and is also a variable regulated by federal statute for trucks in interstate transportation. To a substantial degree, the results of this study speak to the suitability of the federal statute that is involved. Section 3.0 of the report describes the various elements of the test program conducted here, including the test apparatus, the tire sample, the test matrix, and the procedures employed.

The data collected on board the mobile test device were later processed to produce measures of the tire's traction response. Section 4.0 addresses the data processing methods.

The results of the study are presented as quantitative levels of traction force, relative to tire load, which the sample tires exhibited under the selected conditions. These results are useful both for indication of the nominal force levels produced and the variation in performance which prevails among tire specimens which are essentially identical. The experimental results are presented and discussed in Section 5.0.

Section 6.0 presents the conclusions of the work, with emphasis upon the implications of the findings for trucking practice.

Four Appendices are also provided as follows:

Appendix A, showing histograms characterizing the sample of fleet-worn tires, as it covered the range of tread depth values;

Appendix B, presenting a complete tabular listing of the measured traction performance values for each tire and test condition;

Appendix C, showing traction response curves obtained for both of the tire location arrangements in a dual tire pair (contrasting the case of tire A on the inside/tire B on the outside with the converse, tire A on the outside/tire B on the inside of the dual assembly);

Appendix D, presenting alternative groupings of the various tire types and makes for illustrating the influence of tread depth on traction performance, over the fleet-worn sample.

2.O Background

The bulk of the prior research involving partial and total hydroplaning of pneumatic tires has been experimental. Attempts to model the hydrodynamic effect on tire traction have been mainly of an empirical nature. Analytical fits to experimental data have been developed to determine frictional limits as a function of velocity and to determine a critical hydroplaning speed as a function of inflation pressure. In general, rather little work to develop a basic theory on hydroplaning has been done. An overview of the hydroplaning issue as it pertains to lightly-loaded truck tires is presented in section 2.1 which follows.

Subsequently, in Section 2.2, reference is made to an additional issue concerning the dynamic load borne on lightly-loaded truck axles, a situation making wheel lockup more likely than is implied simply by the reduced traction levels of the lightly-loaded tire itself.

2.1 Overview of the technical issues vis-a-vis hydroplaning potential

Investigators have identified two types of hydroplaning, namely:

- *Viscous Hydroplaning* which occurs when the removal of the water film from beneath the tire contact area is resisted by internal friction within the fluid layer. Since the viscosity of water is relatively low, this hydrodynamic component tends to dominate under thin rather than thick water films. The formation of this layer can occur on smooth or macro-textured roads at any speed. The removal of a thin water film from between the tire footprint and the road surface requires flow paths in the tread and/or the road surfaces and localized slip so as to open up siped cuts in the tread.

- *Dynamic Tire Hydroplaning* which occurs in the region of the footprint where the water depth is relatively deep and in which rapid changes in flow direction occur. In this phenomenon the inertial effects of the fluid are dominant, producing changes in momentum which cause a reaction force normal to the tire tread. As with the viscous mechanism, the inertial effect is also dependent upon speed. Increasing speed causes an increase in the hydrodynamic pressure which provides a net lifting force, beginning at the forward edge of the footprint. The support of the tire footprint on a water wedge penetrates, in full hyrdroplaning, through to the rear of the contact patch.

A generalized summary of the literature relating tire and condition parameters to the occurrence of hydroplaning is presented in Appendix E. The research forming the immediate background for this study, however, is discussed below.

A paper by Horne [1] in 1984 stipulated the hypothesis that truck tires can indeed hydroplane under conditions of light load at highway speeds on wetted pavements due to both viscous and dynamic hydroplaning mechanisms. This hypothesis broadened prior work by recognizing that the aspect ratio of the contact area, length over width, is

instrumental in determining hydrodynamic pressure development in addition to the traditionally-recognized role of tire inflation pressure. Horne specifically predicted a more rapid loss of ground contact, due to hydrodynamic pressures, under lightly-loaded truck tires due to the peculiarly fore shortened shape of the tread contact patch which results in a shortened time interval available for water expulsion.

Ivey [2] confirmed that the so-called "complete hydroplaning" of lightly loaded truck tires does relate to the aspect ratio of the contact patch as had been predicted by Horne's analysis. In this regard, truck tires were found to be unique among all types of highway and aircraft tires in their ability to develop high values of this aspect ratio at light loads. Not only is it unusual that the truck tire's contact area tends to shorten without narrowing, as load reduces, but the light-load condition that trucks achieve when empty results in absolute tire loads which are a much smaller fraction of the tire's rated load than is attained with other vehicles.

Even short of the conditions needed for so-called "complete hydroplaning," great losses in traction level appear to occur due to hydrodynamic phenomena with lightly-loaded truck tires. For example, Sakai [3] showed an approximate 50% loss in traction level, due to hydrodynamic effects, for a full-tread lug-type truck tire operating at a speed of 60 mph, under full rated load. While Sakai did not operate truck tires at empty-equivalent loads, he did show that the wet-traction level fell another 15% when the load was reduced to 0.6 times the rated load value. Moreover, although no definitive experiments had been reported prior to this study showing the wet-traction performance of truck tires at "empty"-level loads, there was every reason to believe that the performance values would be exceedingly low for highway-speed operation.

There is also support for the hypothesis that reduced traction performance by empty vehicles on wet pavement adversely influences the safety record. In a 1985 study of truck accident data, Chira-Chavala [4] showed that empty trucks account for some 39% of the single-vehicle truck accidents on wet pavements, but only 14% of the single-vehicle truck accidents occurring on dry pavement. Single-vehicle accidents have been traditionally recognized as constituting a prime category for studying vehicle controllability problems and, of course, also speak to the potential for occupational injury to the truck driver, himself. Even in the case of car/truck impact accidents, where the influence of truck controllability problems is less able to rule the overall statistic, empty trucks account for 37% of the accidents on wet pavements and 29% of the accidents on dry pavement. While it is true that truck braking systems are poorly proportioned for the empty case, making when the vehicle is empty, so wheel lockup more likely, Chira-Chavala surmised that the low wet-traction capability of lightly-loaded truck tires ranked as a strong contributing factor in these apparent over involvements.

In another recent study of truck accidents on exit ramps, Ervin [5] identified various individual ramp sites as having frequent loss-of-control accidents with trucks, many involving jackknife under wet pavement conditions. At one site, all 44 truck accidents occurring over a two-year period on a freeway connection ramp involved rainy conditions, apparently as a result of a poor level of pavement texture, together with the marginal ability

of truck tires to operate under such conditions. Moreover, there is persuasive statistical, as well as anecdotal, evidence that a substantial incidence of truck accidents in wet weather occurs as a result of the unusual behavior of lightly-loaded truck tires on wet pavement.

Notwithstanding such evidence, persons in the trucking community, as well as tire engineers, tend to disbelieve suggestions of hydroplaning potential because of the fact that on an empty truck, the lightly loaded rear tires are preceded by rather heavily loaded front tires, thus presumably "wiping" the water from the rear tire paths. Because the front tires in question are installed as single tires, however, while rear tires are mounted in dual wheel assemblies, the authors believe that this hypothesis doesn't "hold water." Namely, the single front tires are typically installed somewhat toward the projected center of the dual-tire pair, such that the outer dual tire is only partially "masked" by the front-axle tire and the inner dual tire is in a path which is likely to experience increased water depths due to the lateral flow from beneath the front tire. It is noteworthy that Horne [6] reported measurements of the improved traction levels, due to "wiping," at rear tires on the tandem landing gear bogies of aircraft. Although such measurements are quite analogous to the wiping that should be expected ahead of the trailing axle in truck tandem suspensions, they do not address the partial masking effects, plus the possible buildup of a fluid film, at the dual tires following the steering axle on heavy trucks.

Moreover, this study was designed to address the combined phenomena which influence both (a) the effective water depths encountered by the lightly-loaded, rear-placed tires, as well as (b) the response of the lightly loaded tire to the wet-pavement condition. The measurements were thus confined to the range of conditions experienced by rear tires on either the leading or trailing tandem axle of a lightly-loaded truck or tractor.

2.2 Dynamic axle hop on lightly-loaded trucks

Because the focal interest of this study is on lightly-loaded operating conditions, it was deemed pertinent to examine a coincident issue that might further aggravate the problem of braking such trucks on wet pavements. A simulation effort was undertaken to study the dynamic behavior of a truck while braking at empty load on rough pavement, in order to determine whether an increased tendency for premature wheel lockup due to axle bounce would prevail. The UMTRI pitch plane ride model was employed for computing dynamic tire load histories as an input to a wheel spin computation. The spin degree of freedom was then acted upon by a brake torque input, with the tire's braking force response modelled conventionally as a continuous μ-slip curve, given the instantaneous tire load.

The purpose of the computation was to generate the longitudinal force time history, under both smooth and rough road scenarios, to determine whether, during the rebound phase of the wheel-hop cycle, the lightened tire load would enable the tire to spin down rapidly enough to pass prematurely across the peak condition and thus toward lockup. To the degree that such a response would occur, it was supposed that braking of empty trucks might be even further compromised than previously thought.

This task showed that no discernible reduction in total vehicle deceleration capability is produced due to axle bounce in the frequency and amplitude ranges excited by the real road profiles that were studied. Accordingly, the task is not discussed further in this report.

3.0 Tire Test Program

This section describes the details of the test equipment, tires, conditions, and test procedure employed in collecting the experimental data. The experimental data were confined to measurements of tire traction levels on wetted surfaces of a selection of tires having different stages of tread wear. Two different tire tread designs were considered; rib-tread and lug tread. The test data were collected by using the UMTRI mobile truck tire dynamometer, described below.

A baseline series of tests involved new tires that were subjected to a matrix of conditions examining sensitivities to operating variables. A so-called "worn tire" sample was then subjected to a narrowly-defined set of conditions in order to examine the influence of tread depth, per se, using authentically fleet-worn tires. Specimens for the worn tire study were obtained through the cooperation of two large national fleets, Roadway Express and the United Parcel Service (UPS.)

The tire tests were all conducted at the facilities of the Transportation Research Center of Ohio, TRC. The test dates were divided into two periods, (fall, 1987 and spring, 1988) in order to accommodate the availability of the fleet-worn tires.

3.1 Test Apparatus.

The UMTRI mobile traction dynamometer, shown in figure 3.1, is a tractor-semitrailer combination equipped for measuring the vertical load, braking force, and wheel spin velocity of the test wheels while travelling at a constant speed. The mobile dynamometer was modified for this project to accommodate a dual pair of specimen tires in the trailer-mounted test wheel position, and to add an axle for situating the so-called "wiping" tires ahead of the test specimens. As diagrammed in Figure 3.2, the fixture for the wiping tire(s) was mounted at the rear extremity of the tractor portion of the dynamometer. As such, the longitudinal space between the wiping tire(s) and the test specimen is approximately 11 feet--equivalent to the wheelbase of a short 2-axle tractor. The fixture itself constitutes a trailing arm suspension incorporating a spindle for tire mounting. The fixture is loaded by an air spring to achieve precalibrated tire loads on the basis of regulated air pressure. When a single wiping tire is employed, to represent a steering-axle tire running ahead of a dual-rear pair, the lateral position of the single tire is adjusted to reflect the axle-track geometry prevailing on typical tractors in the U.S.

The test wheels as well as the "wiping" tires are loaded by means of air springs. The angular velocity of the test wheels is measured by a tachometer. The braking torque is applied to the test wheels by means of an air-actuated friction brake whose actuation pressure is controlled and regulated though the use of pneumatic valves.

In order to preserve an undisturbed water condition up to the location of the wiping tire (i.e., free from spray churned up by the dynamometer tractor's own tires) a skirted tunnel was installed beneath the dynamometer tractor. The tunnel incorporated plywood

Figure 3.1 UMTRI Mobile Traction Dynamometer

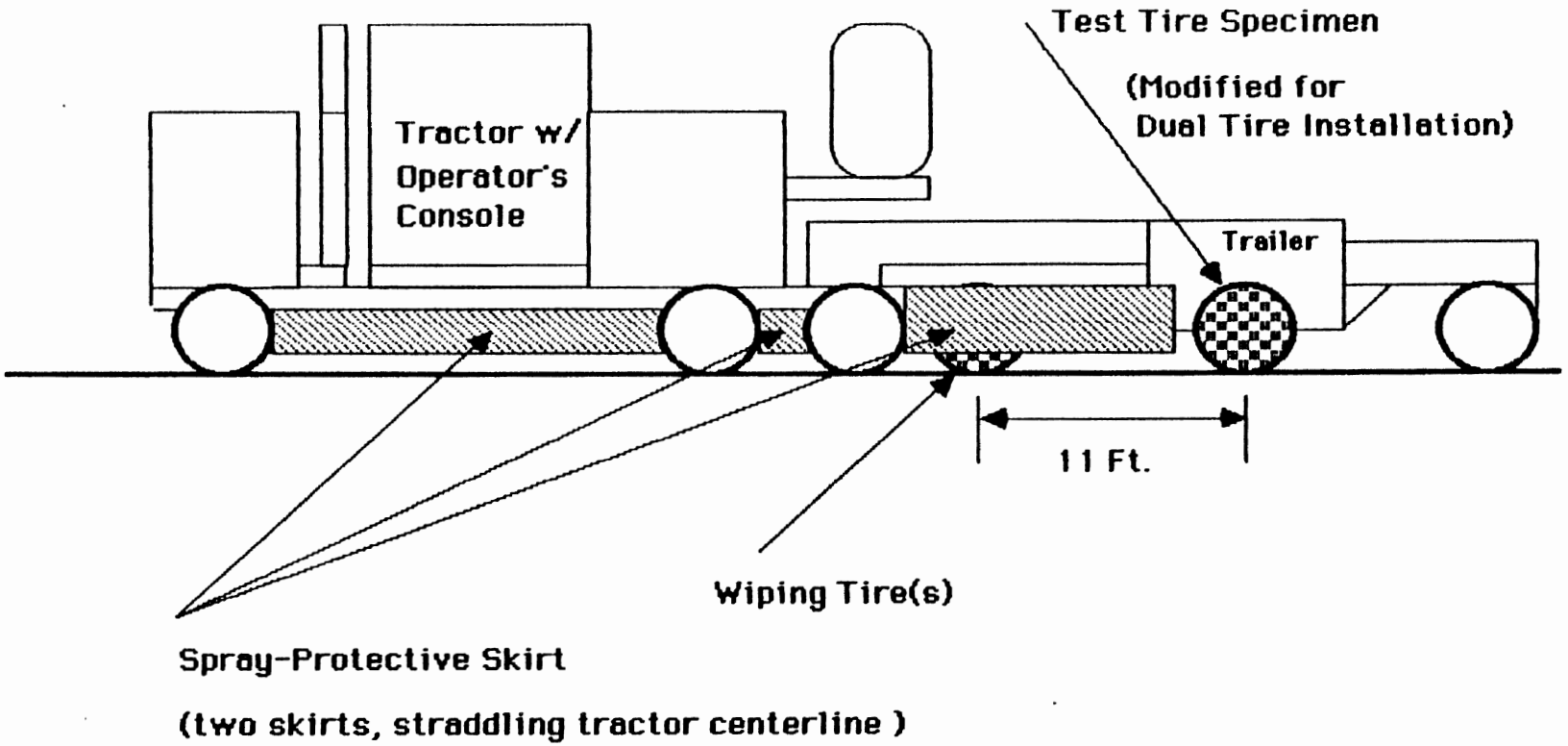

Figure 3.2 Modification to the UMTRI dynamometer for conduct of the wet-traction experiments

panels as the horizontal "roof" elements plus long strips of road-sweeper brushes positioned just above the pavement surface as its longitudinal "skirt". The overall tunnel structure was thus intended to isolate the pavement beneath the center of the vehicle from splash disturbances. Further, the tunnel appeared to be effective in assuring a tranquil water layer at the wipe-and-test station of the dynamometer.

The tire reaction forces are transduced on the dynamometer through a multicomponent strain-gauged load cell. A matrix of influence coefficients for the respective channels of the load cell were derived through a complete laboratory calibration of the system both prior to and just following each of the two phases of the traction test program.

The data acquisition system provides anti-alias filtering, plus a high sampling rate, thence storing the digital data on magnetic tape for later analysis. Further, a test-control computer also provides for electronic calibration and zero adjustment of the analog input channels prior to each individual test run.

3.2 Test Tires

Two groups of tire tests were conducted, a "baseline" series and a "worn-tire" series. The two test groups differed both in the test conditions which were employed and in the nominal state of the tires themselves. A description of the tire sets is given below and their test conditions are explained in section 3.3.

The tires were arranged and tested as dual pairs. The "pairing" was based on matching a tire with another of the same tread design having the closest available value of tread depth. The tread depth value which is reported for each dual pair is then the average of the depth values for the two specimens involved.

All the tires from the baseline and worn-tire groups were numbered sequentially. Figure 3.3 shows a chart with the different types of tires used within both groups. Tires in the overall program are identified by distinctions in tread configuration, nominal tread depth, and the dual vs. single installation arrangement in the "wipe-tire" position. A complete listing of all of the test tires, tread depths, wipe tire arrangements, and processed results is presented in the summary data sheets of Appendix B.

3.2.1 Baseline tires.

The baseline test group consisted of a total of 16 individual tires which were distributed among wiping and test specimen roles. A total of 6 pairs of tires were matched up as dual, test specimen assemblies. These tires were examined in both a new, full-tread condition, and at lesser levels of tread depth achieved through mechanical removal of tread on a buffing machine. Further, the test tires represented rib-type and lug-type tread designs in differing conditions of tread depth.

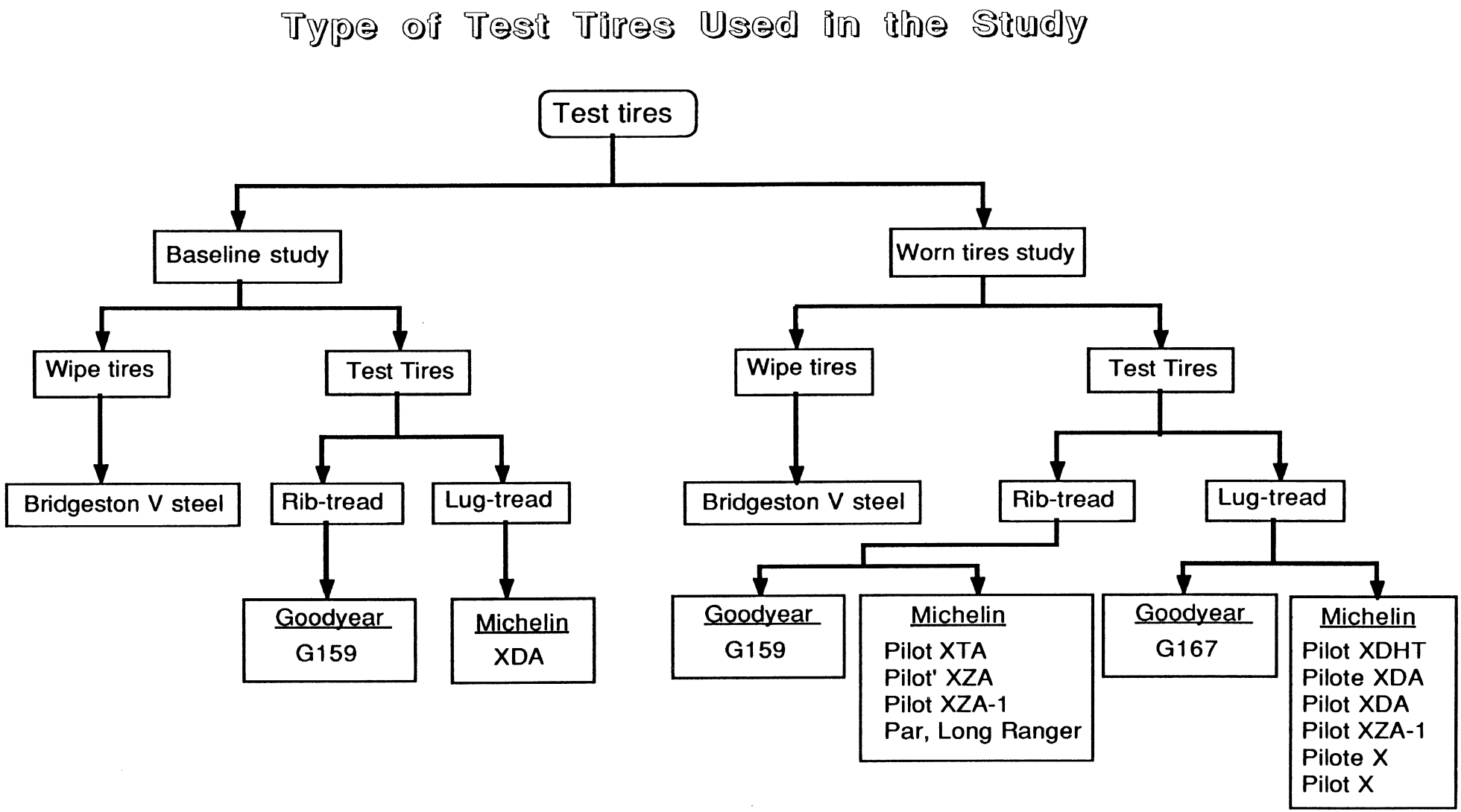

Figure 3.3 Matrix of tire types and models tested

The baseline tires included the following:

- Goodyear G159 295/75R22.5, a low-profile, rib-tread tire, tested at tread depths of 18, 10, and 8/32's of an inch.

- Michelin XDA 275/80R22.5, a low profile, lug-tread tire, tested at tread depths of 24, 16, and 2/32's of an inch

- Bridgestone V Steel R6 R290 11R22.5, a rib tire employed as the wipe tire at tread depths of 18 and 14/32's of an inch.

In the baseline test series, the wiping tires were installed in both single and dual configurations in order to illustrate the influence of the wipe configuration on results.

3.2.2 Fleet-worn tires

A total of 112 "fleet-worn" tires were also tested. Each tire was numbered sequentially and matched with a similar tire, as explained above, to make a test pair. These tires were provided by the Roadway Express and UPS fleets in the tread state that prevailed when tires had been removed for recapping. That is, the tires were not deliberately selected by the fleets but rather were simply accumulated in a batch for traction testing instead of being forwarded to the recapper.

In general, these fleet-worn specimens had developed very irregular wear patterns during service. Photos showing examples of uneven tread surfaces are presented in Figure 3.4. Many of the tires showed undulatory surfaces with indentations spaced such that 10 to 16 wavelengths appeared around the circumference of the tire. Localized variations in the undulation amplitude of the tread depth value were on the order of 0.050 to 0.10 inches (i.e., with peak-to-peak variations as high as 0.20 inches, or 6/32'nds of an inch.) Since the tire rotates at approximately 7 rotations per second at the nominal 53 mph test speed employed throughout the worn-tire test series, the tread surface undulations imposed a 70- to 112-Hz excitation in vertical load. Recognizing that the mobile dynamometer exhibits a wheel-hop natural frequency of approximately 7 Hz, a very substantial variation in tire contact pressure must have developed throughout the full wheel rotation (as the test wheel spindle failed to respond to the high-frequency, undulation-induced excitation).

The implication of such phenomena on the wet traction behavior of the tire is certainly unknown. Nevertheless, since it was the intent of the study to capture the performance of tires coming out of authentic fleet usage, the undulatory nature of the wear conditions was simply accepted as characteristic of a fleet-worn tire sample and was not quantified in any way in the test log.

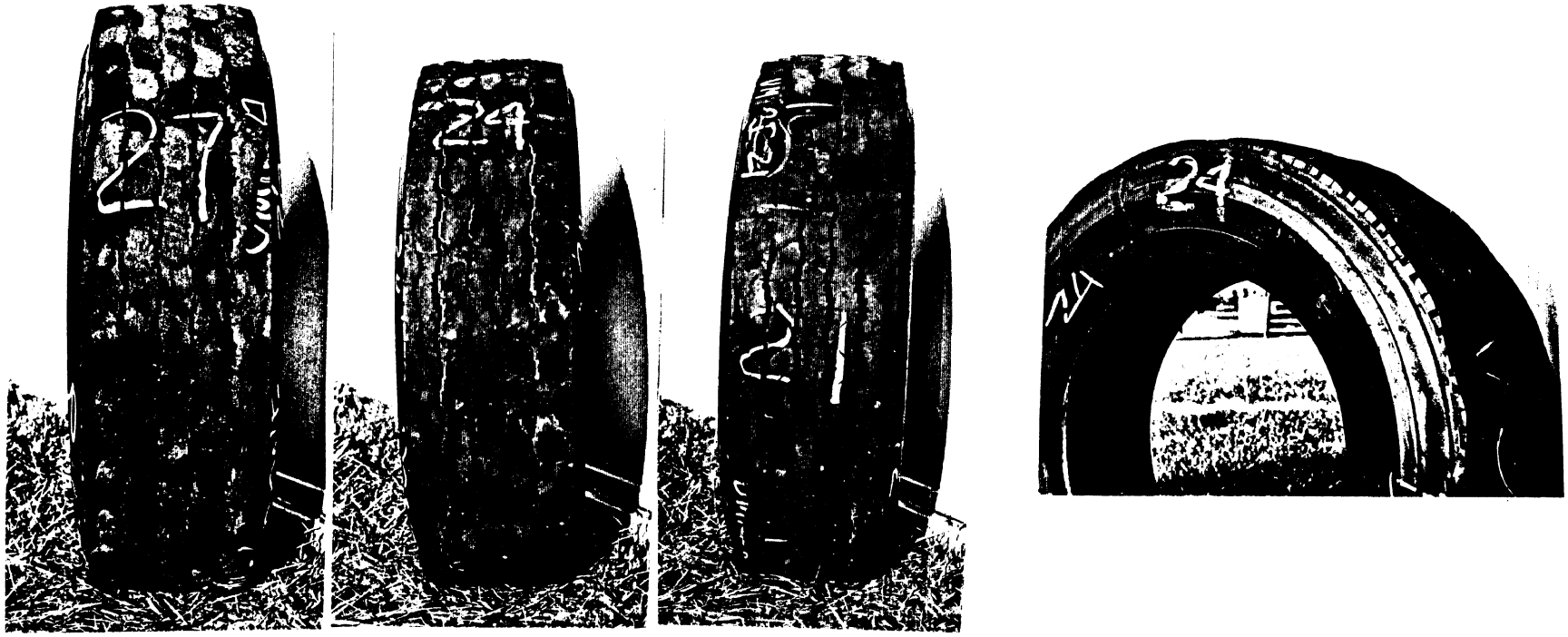

Figure 3.4 Photo of irregular tread surfaces prevaling on the feet-worn test tires

The actual wear patterns accruing in fleet service are thus incorporated here as a prevalent factor which may or may not significantly influence the wet traction behavior of these specimens or the at-large population of truck tires. Nevertheless, there is good reason to believe that the uneven tread surfaces are responsible for much of the remarkable nonuniformity that was seen in the shapes of μ-slip curves for differing tires (see section 4.1.5 and Appendix C.)

3.2.3 Pairs of tires tested

As was mentioned above, all tire tests were run in dual pairs incorporating specimens having nominally the same tread depth. In the worn-tire study, however, there were a few cases in which the tread depth values of three individual tires were close to one another but quite different from that of the next-closest value among the other specimens. In such cases, it was necessary that two pairs be created through a repeat usage of one of the tires (Considering the case of same-depth tires, x,y and z, for example, it was necessary to create a first pair, x-y, and a second pair, y-z.) Except for such a special case, all of tire specimens were tested in only one dual pair.

In the worn tire study, each dual tire pair was tested in both of the mirror image configurations of the dual. That is, the inner and outer tires of the dual pair were "swapped" for one another to create a meaningful repeat condition. As shown below in figure 3.5, a test tire pair was examined both in the arrangement with A outside and B inside, as illustrated and in another arrangement with specimen B outside and A inside. Data representing this "swapped" configuration of the dual are reported as an independent test pair, since:

- The direction of rotation of the tires is reversed, and,
- The positioning of the wiped path relative to each tire in the dual pair is reversed between the two arrangements (note again that only a single wipe tire was employed throughout the worn-tire series.)

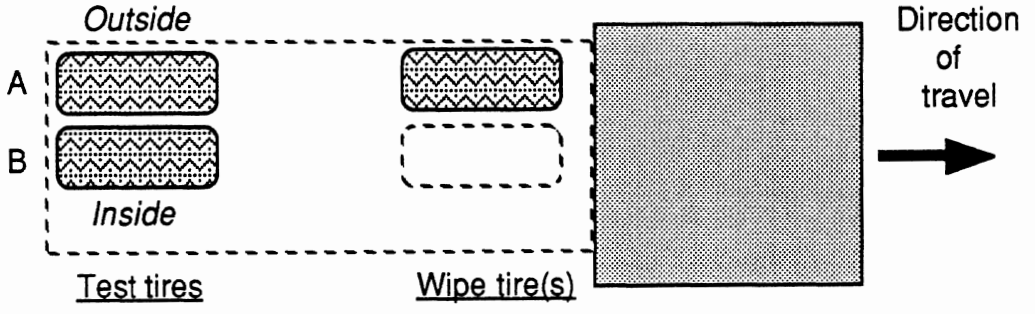

Figure 3.5.

Appendix A presents histograms showing the distribution of the test tire sample by nominal tread depth value. The figures show that the great majority of the fleet-worn tires had tread depth values lying between 4/32" and 8/32", with an overall mean value of tread depth at 6.85/32". Recognizing that the federal regulation for minimum tread depth is 2/32's on steering axles and 4/32's on all other axles, the sample histograms reveal that the two cooperating fleets employ a rather conservative practice of pulling tires from service for recapping. On the other hand, the distribution of tires was somewhat unfortunate from the perspective of the study objectives, since it provided for only 15 tests of dual pairs at tread depths below 3/32".

The overall sample contained 20 Goodyear-lug tires, 26 Goodyear-rib, 41 Michelin-lug tires and 25 Michelin-rib tires, for a total of 112 tires. Breaking down the sample into each of its constituent subsets, the average tread depths (TDavg), for each group of test pairs were as follows:

Subset of tires-pairs	TDavg
All Goodyear pairs (47)	7.04/32"
All Michelin pairs (63)	6.14/32"
Goodyear-lug pairs only (22)	4.69/32"
Goodyear-rib pairs only (25)	9.11/32"
Michelin-lug pairs only (39)	6.21/32"
Michelin-rib pairs only (24)	6.03/32"
All Lug-pairs (61)	5.66/32"
All Rib-pairs (49)	7.60/32"

3.3 Test procedure

This section describes the test conditions and procedures employed in the measurement program .

3.3.1 Type of surfaces

Two widely differing surface friction conditions were provided by the two selected pavement surfaces at the TRC facilities in Ohio. These surfaces, coded PA and PS in the summary listing of results in Appendix B, corresponded to:

• **PA** = Uncoated asphalt, showing a nominal ASTM (wet) skid number of 55. This surface is situated on the Vehicle Dynamics Area of TRC. The relatively open macrotextured surface was wetted by a watering truck which made repeat passes ahead of each test pass of the mobile dynamometer. This surface was employed only in the baseline test series (and not in the study of fleet-worn tires.)

• **PS** = Polished concrete, showing a nominal ASTM (wet) skid number of 26. This rather smooth, machine-polished surface was wetted by an in-place sprinkling system.

3.3.2 Tire Loading

The test tire pair was loaded to a steady state value of 2000 lbs, or 1000 lbs per tire. This level represents the load that would typically prevail on the rear tires of a tandem-axle tractor in the bobtail condition. The single "wipe" tire was loaded to 4000 lbs corresponding to a typical steering tire load for a bobtail tractor or a tractor with empty semitrailer attached.

3.3.3 Warm-up Procedure.

A warmup lap was performed upon each installation of a fresh dual pair of test tires. The warmup procedure consisted of running one four-mile lap of the test track with the test tires rolling on the ground. After the warmup lap, the mobile tester was stopped in order to calibrate and adjust zero offsets on all of its analog input channels.

3.3.4 Baseline test matrix.

The baseline tests were conducted on both surfaces described above as **PA** and **PS**. Both dual and single wipe configurations were employed at test speeds of 43 mph, 48 mph, and 53 mph. The highest speed value was determined by the maximum speed which could be attained by the mobile dynamometer within the physical constraints of the facility.

For each of the six tire pairs, comprised of three pairs of Goodyear specimens at tread depth values of 18, 10, and 8/32's, respectively, and three pairs of Michelin specimens at 24, 16, and 2/32's, respectively, traction measurements were conducted under each of the following test conditions (where RB1 and RB.5 denote full- and half-treaded wipe tires, respectively, and the "S" and "D" designations refer to the installation of the wipe tires in either single or dual configurations):

Wipe	Wipe conf.	Speeds	Surfaces	Total tests per pair
RB1	S,D	43, 48, 53 mph	**PA, PS**	12
RB.5	S,D	43, 48, 53 mph	**PA, PS**	12

Each test condition was examined by means of a set of four lockup cycles. The data processing scheme then employed an averaging technique over the four lockups to produce a net traction performance value. When taking data on the asphalt surface, **PA**, the physical constraints of the facility were such that all four lockup cycles could be obtained in a single pass of the dynamometer. In the case of the concrete surface, **PS**, it was necessary to make two passes in order to collect data over the four lockup cycles.

3.3.Study of Fleet-worn tires

The testing of fleet-worn tires was designed with a priority interest in measurement of a large number of specimens. Accordingly limitations in overall program scope required that only one test condition be employed for characterization of the entire worn-tire sample. The single condition involved simply the four-lockup sequence on the concrete surface, **PS**, at a single speed of 53 mph. The "wipe" tire configuration was set at the single half-worn (**RB.5**) case. In this series, due to the low levels of tread depth prevailing in many of the tests, the spin-up transient following lockup and release of the test brake was so slow that only one lockup cycle could be accomplished per pass over the limited-length test surface. Accordingly, all of the data in the worn tire series were collected with one lockup cycle per pass. After a fresh pair of tires was tested in configuration "AB", the dynamometer was stopped for swapping to the "BA" configuration, and the remaining sequence on that dual pair was concluded.

The total tests covering the worn tire series can be summarized as:

(112 test pairs) X (1 test speed) X (1 test surface) X (1 wipe configuration) = **112** tests

In the worn tire study there were five pairs that were also tested for inflation pressure variations when they were in configuration "BA". This was done for those pairs having the maximum and minimum tread depth values within each group.

3.3.6 Control tire.

An extra run sequence, using a single control tire, was conducted in the middle of every test day throughout the worn-tire study. The control tire was selected as a full tread, new tire at the beginning of the test series. As the worn-tire series covered a total of nine days, however, considerable wear of the control tire's tread was experienced, with the original sipes and sharp-edged tread blocks being substantially rounded on their "upstream" edges as the sequence proceeded. As a result, the traction performance of the control tire fell continuously over the nine-day sequence to a final value that was 43% below the first measurement. Noting that no visually-observable change had occurred in this machine-polished test surface and that ASTM skid number measurements throughout the test period showed only minor variations, the control tire data were pronounced "anomalous" as a descriptor of the test surface and were not employed for normalization of the test data. Rather, the traction data are presented with the assumption that the pavement friction qualities remained essentially constant throughout the test sequence.

4.0 Test Data Analysis

By means of computer processing from digital tape, the traction test data were reduced to the following formats:

- tables of traction force level vs.longitudinal slip
- plots of μ_i vs. slip, and
- numeric values of μ_p and μ_s, where,

"μ_i " is the normalized longitudinal braking force defined by the ratio:

$$\mu_i = \frac{F_{Xi}}{F_Z}$$

F_{xi}, is the the value of the longitudinal or braking force delivered by the tire,

F_z, is the normal load on the tire,

μp is the peak or maximum value of μ_i produced by a tire,

μs is the locked-wheel value, that is, the value of μ_i prevailing when the spin velocity is zero. See Figure 4.1, below.

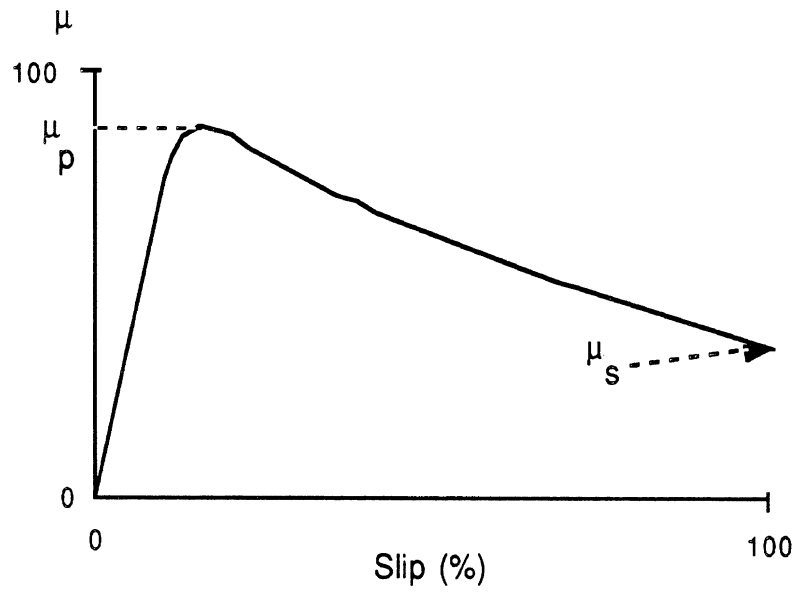

Figure 4.1. The μ-slip curve.

Assuming constant forward speed throughout the slip test cycle, the longitudinal slip, s, is defined as:

$$s = 1 - \frac{\omega}{\omega_0}$$

where:

ω is the angular velocity of the slipping wheel,

ω_0 is the angular velocity of the wheel when rolling freely at a forward speed V,

Thus, "s" is positive when braking, and reaches its maximum value of 1 when the wheel locks up.

4.1 The μ-slip curves

This section describes the processing of "raw" experimental data in order to produce μ-slip curves and determine numeric values for μ_p and μ_s. Different stages in the processing procedure were employed to obtain the final values. These stages are explained below.

4.1.1 Smoothing the raw data.

The raw data were filtered at the analog level to prevent anti-aliasing and then sampled for digitization and digitally filtered. Fairly aggressive filtering was required to deal with the large quantity of noise, shown in figures labeled as "raw" data below. Different degrees of filtering severity were examined in order to select a filter that would retain the important frequency content residing in the highly-transient portion of the μ vs. slip curve while otherwise cleaning the curve as much as possible.

Figures 4.2 through 4.5 show a comparison of raw data vs. filtered data gathered on a full-tread tire on the concrete skid pad (**PS**). The plots display the following time histories through a slip sequence involving one full lockup cycle and the beginning of a second cycle:

- The longitudinal or braking force, F_X,
- The tire load, F_Z,
- The forward velocity of the test vehicle, V,
- The rotational speed of the test tire, ω,

In the F_X curve, for example, the application of the brake at time 3.3 seconds causes the peak to be reached around 3.8 seconds, following which the tire dwells at the locked wheel condition from 3.9 through 4.8 seconds. The digital filtering removes approximately 90% of the mechanical noise in the system (predominating from the 7 Hz wheel hop response which is excited by pavement and tread surface irregularity.) All of the data gathered in the test program were filtered (as shown in these examples) with a constant filter setting, before reduction to μ-slip curves and μ_p and μ_s values.

4.1.2 Examination of a dynamic vertical load error

A brief examination was made of the influence on the vertical load *measurement* (in contrast to the *actual* load) of the inertial contribution of the test wheel and spindle mass which is situated outboard of the load cell, as shown in Figure 4.6. The presence of a dynamic tire load deriving from the vertical acceleration of this mass was of particular

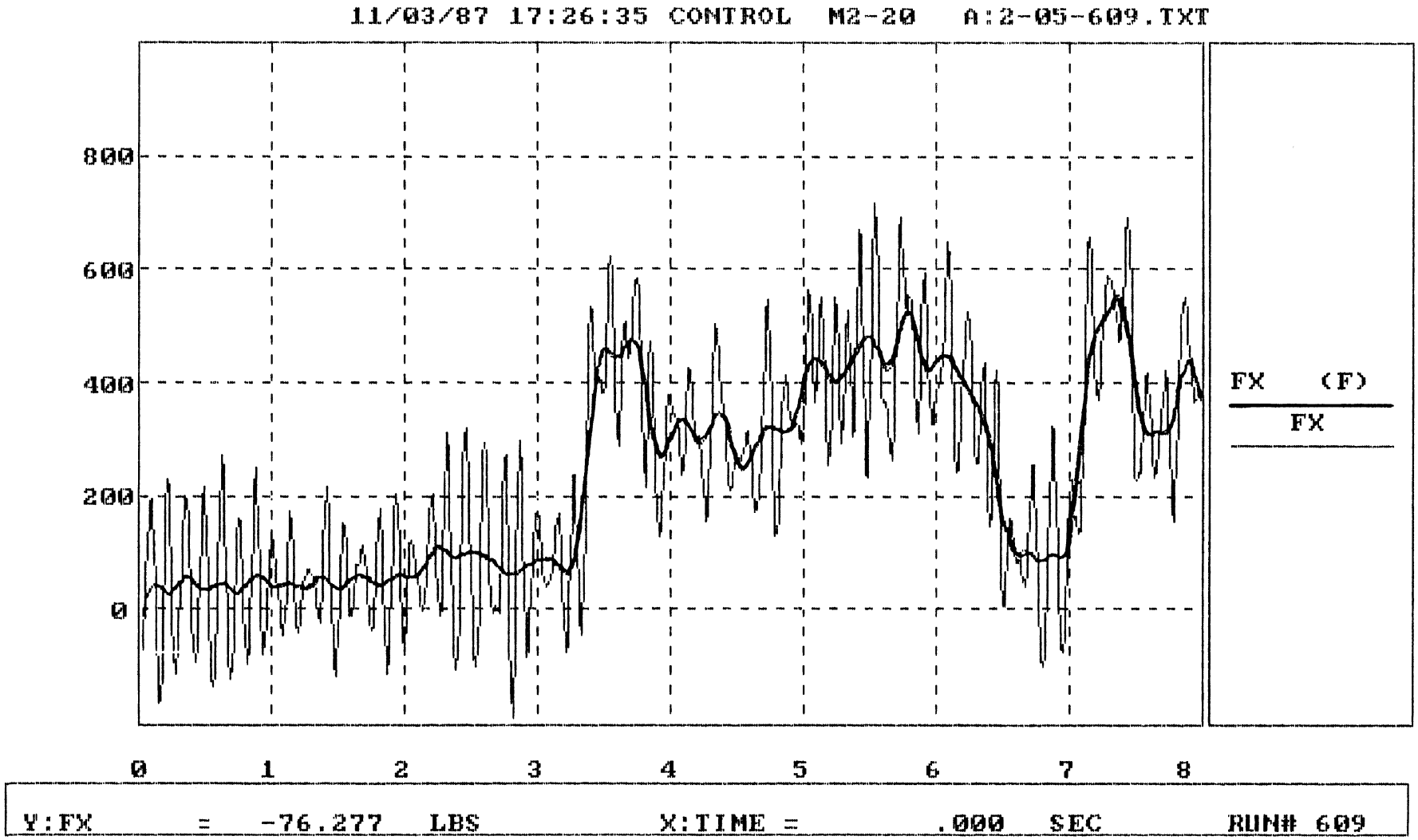

Figure 4.2 Comparison of raw, Fx, and filtered, Fx (F),data signals

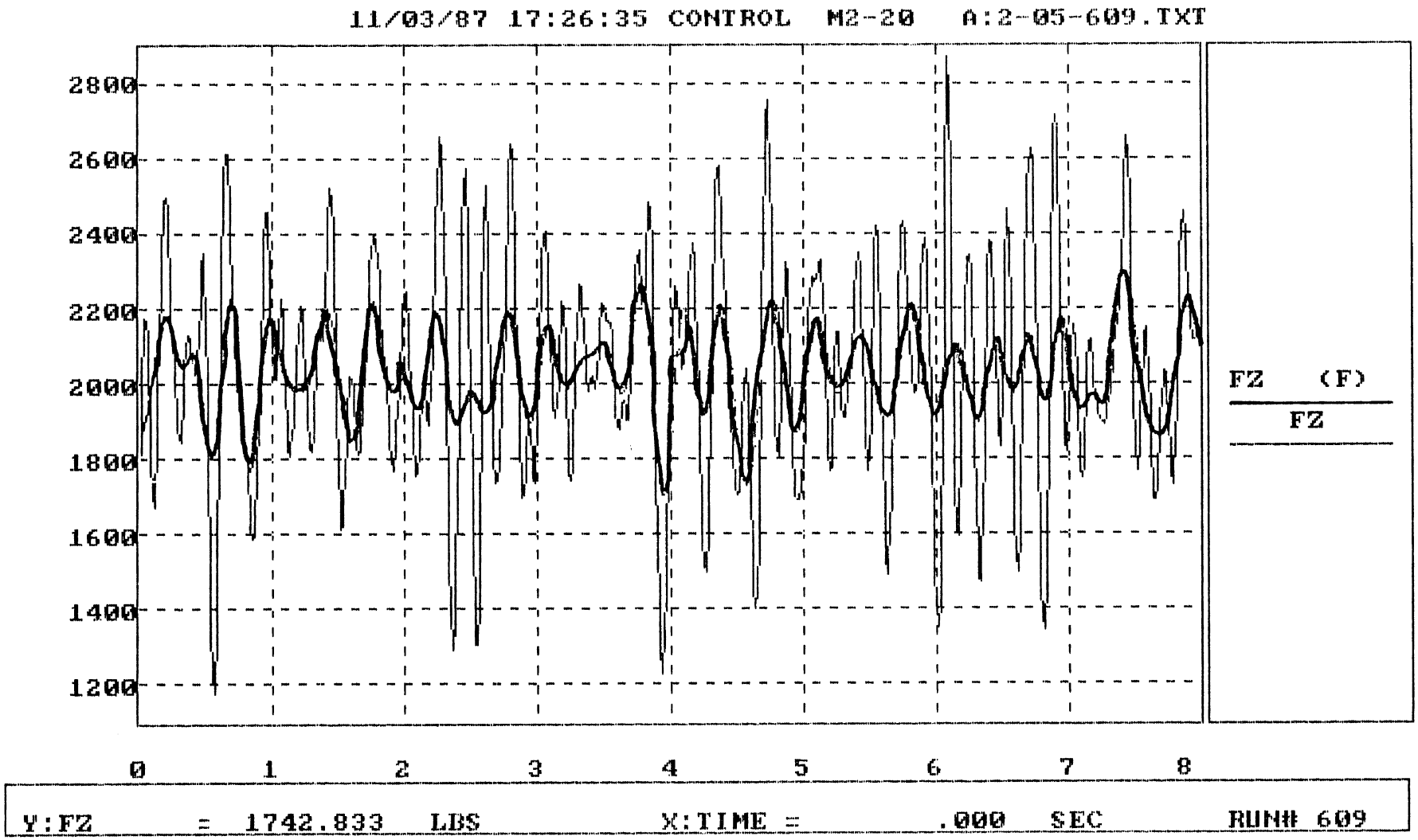

Figure 4.3 Comparison of raw, Fz, and filtered, Fz (F), data signals

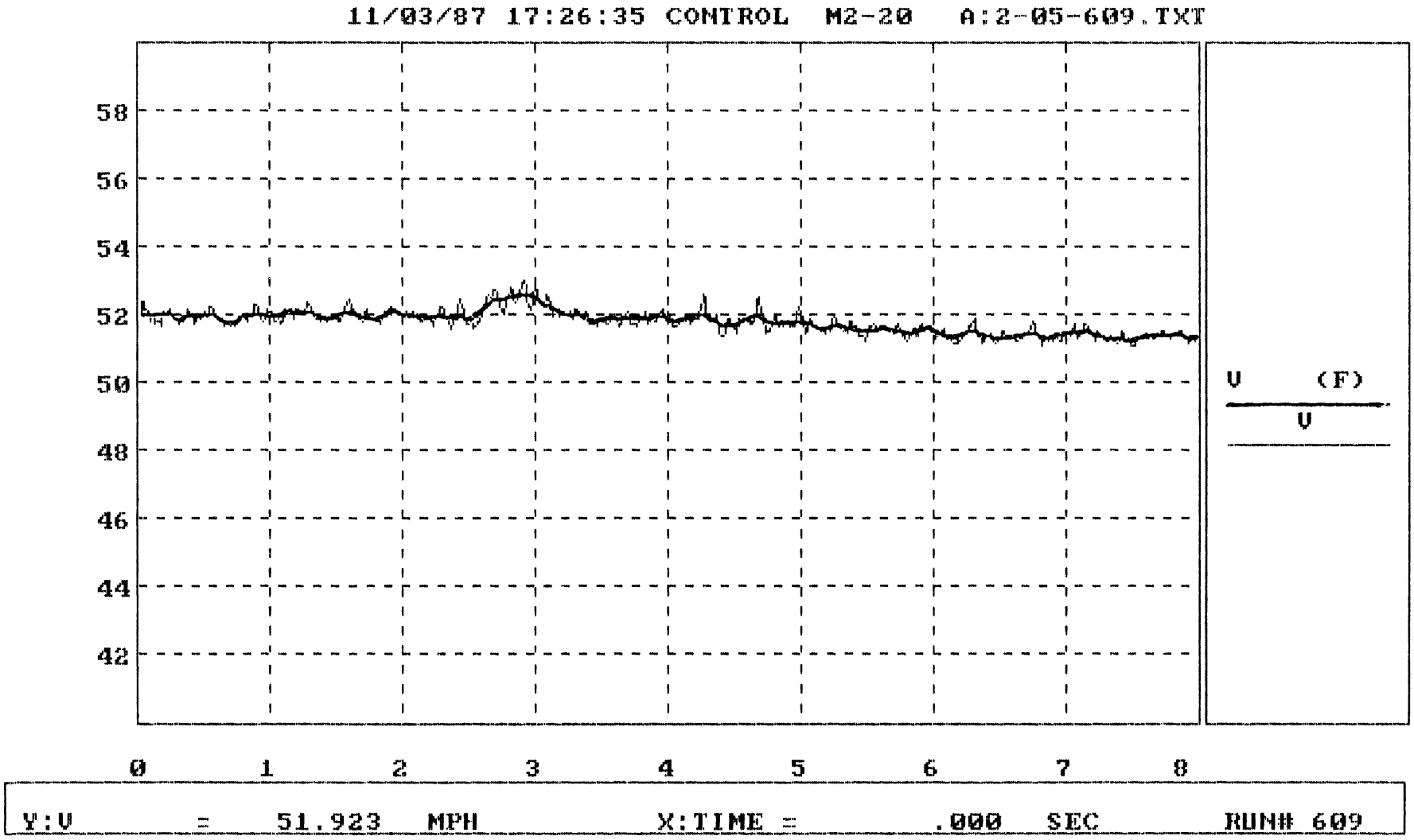

Figure 4.4 Comparison of raw, V, and filtered, V (F), data signals

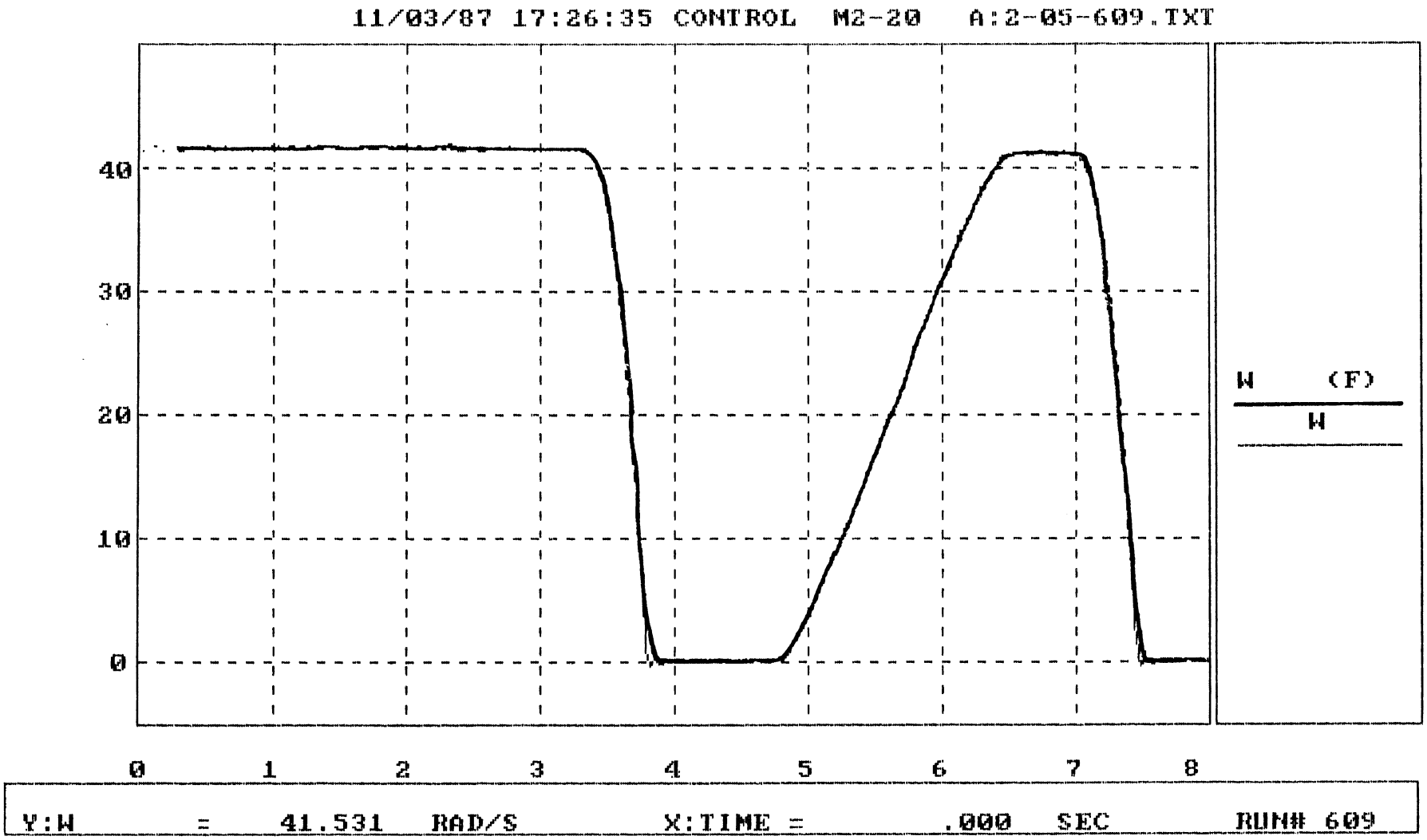

Figure 4.5 Comparison of raw, W, and filtered, W (F), data signals

interest due to the large mass of the dual wheel assembly and the light-load focus of this test program. To characterize this contribution, the vertical acceleration, A_Z, of the mass system described above was measured using an accelerometer on the spindle.

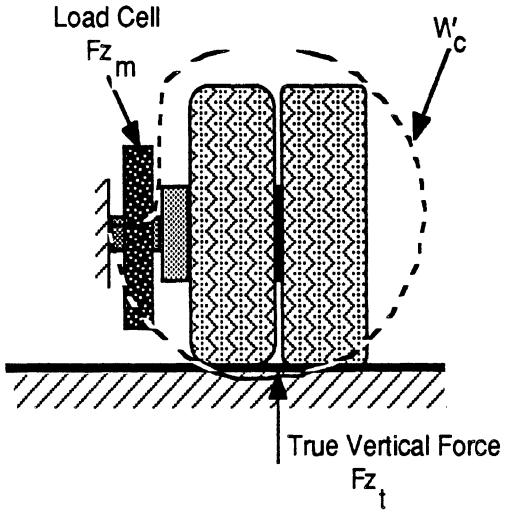

Figure 4.6. Schematic representation of the test wheel assembly.

The vertical load was then corrected as follows:

$$F_{Zt}=F_{Zm}-w_c*A_Z$$

where:

- $w_c \approx 900$ lbs (weight of the spindle, brake, dual wheel & tires, etc).
- F_{Zt} = True vertical load on the dual tire pair,
- F_{Zm} = Measured total tire load.
- A_Z = Measured vertical acceleration, in g's.

Figure 4.7 depicts time histories of the acceleration-corrected and measured values of vertical load, F_{ZC} and F_{Zm}. From these plots we can see that a small in-phase adjustment has been made, relative to the directly-measured signal and that peak values of the corrected load are generally of smaller magnitude than the measured values.

Analysis of data from most of the worn-tire series revealed that the influence of these differences on the magnitude of the normalized μ value in a single slip cycle involved a mean error of approximately 1% of μ_p values (and, of course, 0 % of μ_s values since the locked wheel result is computed from a continuous 0.25 second-sample of data at zero spin velocity.) Because measurements defining the spindle accelerations were not available throughout all of the conducted tire tests, the inertial correction was not made to the data reported from this study. Nevertheless, since the magnitude of the μ_p error in any given lockup cycle is the random result of the phasing of the wheel hop vibration cycle to the slip transient while passing through μ_p, no methodical error is encountered from run to run due to the inertial error source. Further, the practice of averaging four lockup cycles to define peak and slide values of μ reduces the error in processed data to negligible proportions.

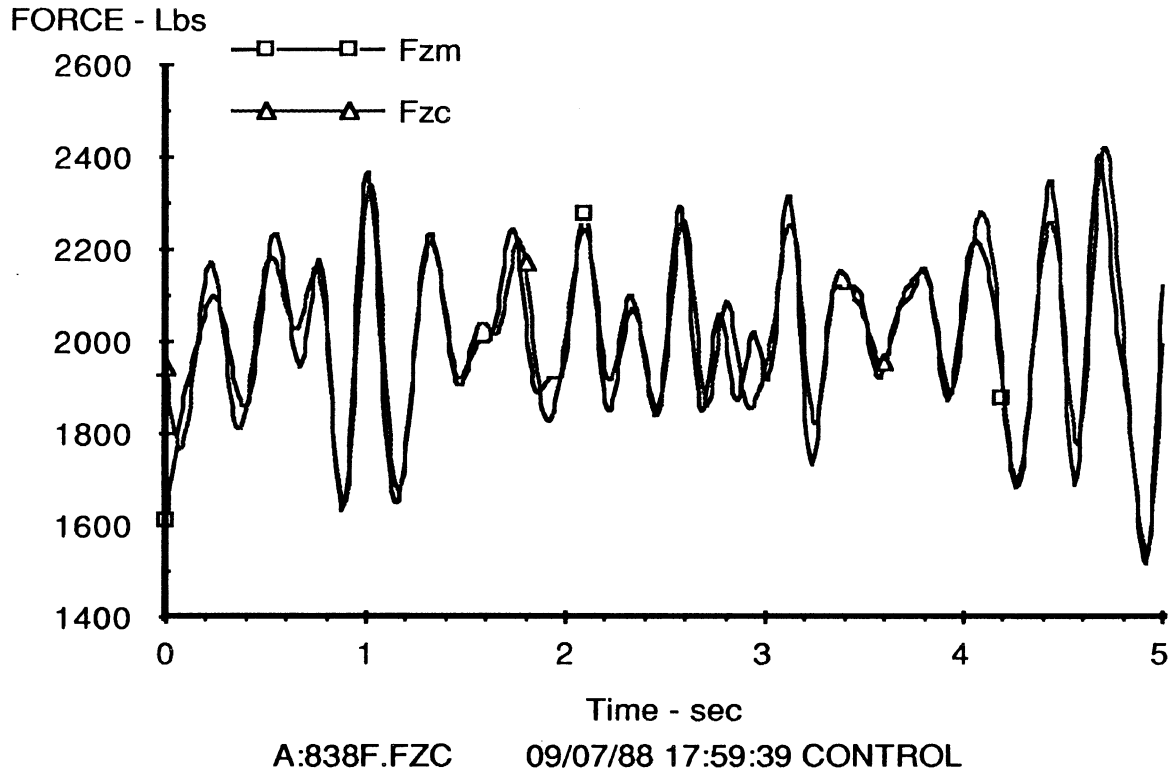

Figure 4.7 **Contrast in filtered data signals showing directly-measured vertical load, F_{zm}, and a corrected load Signal, F_{zc}, employing an instantaneous measurement of vertical acceleration of the test wheel**

4.1.4 Data reduction.

A computerized data reduction program was employed for automatic processing of the raw data and computation of normalized traction results. This program performs the following functions:

1) reads in a raw data file,

2) identifies the number of lockups in the data file,

3) calculates the average speed and vertical load of the experiment,

4) obtains the instantaneous values of μ, F_X/F_Z, and slip throughout each lockup cycle within the data file,

5) for each lockup cycle obtains the μ_p and μ_s values as well as the slip at the peak,

6) generates an average μ-slip curve for the set of lockup cycles found in the file,

7) calculates the overall μ_p and μ_s values from the average μ-slip curve,

4.1.5 Combining Individual μ-slip Curves

As discussed earlier, four lockup cycles were obtained to produce a set of data describing a dual tire specimen under a specific set of conditions. Although the data processing program determined the peak and slide values of μ from the average μ-slip curve, thence discarding the individual curves from each cycle, the study included some inspection of the individual cycles so as to examine the qualitative nature of the results. Shown in Figure 4.8 is a fairly representative set of four lockup cycles, in this case for a Michelin tire with minimal (1.43/32's of an inch) tread depth, as tested on the polished concrete pavement. The figure shows major variation in response from cycle to cycle, presumably resulting from the combined irregularities of the tire's tread face, as worn in fleet service, and the textural patterns of the paved surface. Recognizing that the portion of the μ-slip curve from 20 to 100% is typically covered in approximately .100 seconds in these tests, the observed variation in this range is occurring in less that one full revolution of the tire.

For the illustrated case, the averaging program deduced that $\mu_p = 0.105$ and $\mu_s = 0.075$. All such reduced data for μ_p and μ_s values are presented in tabular form in Appendix B.

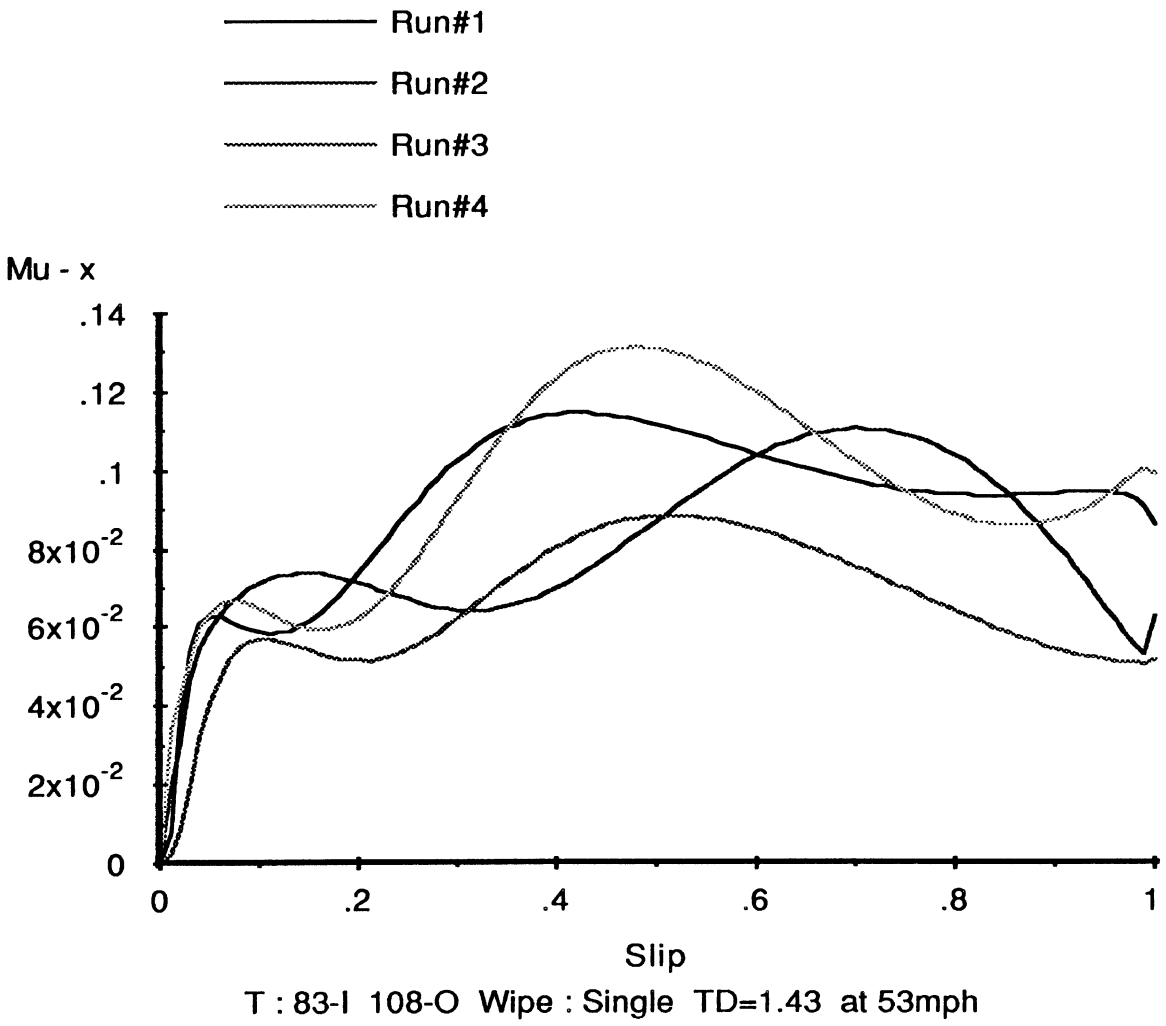

Figure 4.8 Four lockup cycles for Michelin dual pair having a nominal tread depth of 1.43/32nds of an inch

5.0 Discussion of Results

The results of the study are discussed in this section as they elucidate the braking traction of truck tires at light loads on wetted pavements. The results address the following issues:

- the influence of velocity on peak and slide traction levels,
- differences seen between rib and lug treads in the sample,
- the influence of the wipe tire configuration,
- the influence of inflation pressure,
- variation observed upon "swapping" the two tires in a dual pair, and
- the influence of tread depth.

5.1 The influence of velocity

Shown in Figure 5.1 through 5.4 are data from the baseline test series for single and dual-wipe configurations, respectively, showing the influence of velocity on peak and slide traction levels. The plots show dark lines to indicate data taken on the higher friction (asphalt) test surface, PA, and grey lines for the data gathered on the polished concrete surface, PS. The data show the expected reduction in traction level with velocity over the set of conditions and tire specimens illustrated.

A statistical sampling of all of the data in these plots yields a velocity sensitivity of (-.009 units of peak μ per mph) and (-.014 units of slide μ per mph.) While such linear coefficients describe the velocity sensitivity over the narrow speed range examined here, it should be noted that the hydrodynamic influence, per se, is driven by the square of the velocity, per classical analyses.

As will be shown subsequently, the rather large spread in traction levels seen for the two indicated pavement conditions is due primarily to differences in tread depth across the sample of tires in the baseline group.

5.2 Differences seen between Rib & Lug tires in the sample

Figures 5.1 through 5.4 also denote the rib and lug type tread patterns in the sample. The crude designations refer to the rib-style Goodyear G159 tires, with its distinctly circumferential tread pattern, and the lug-style Michelin XDA, a tire designed for

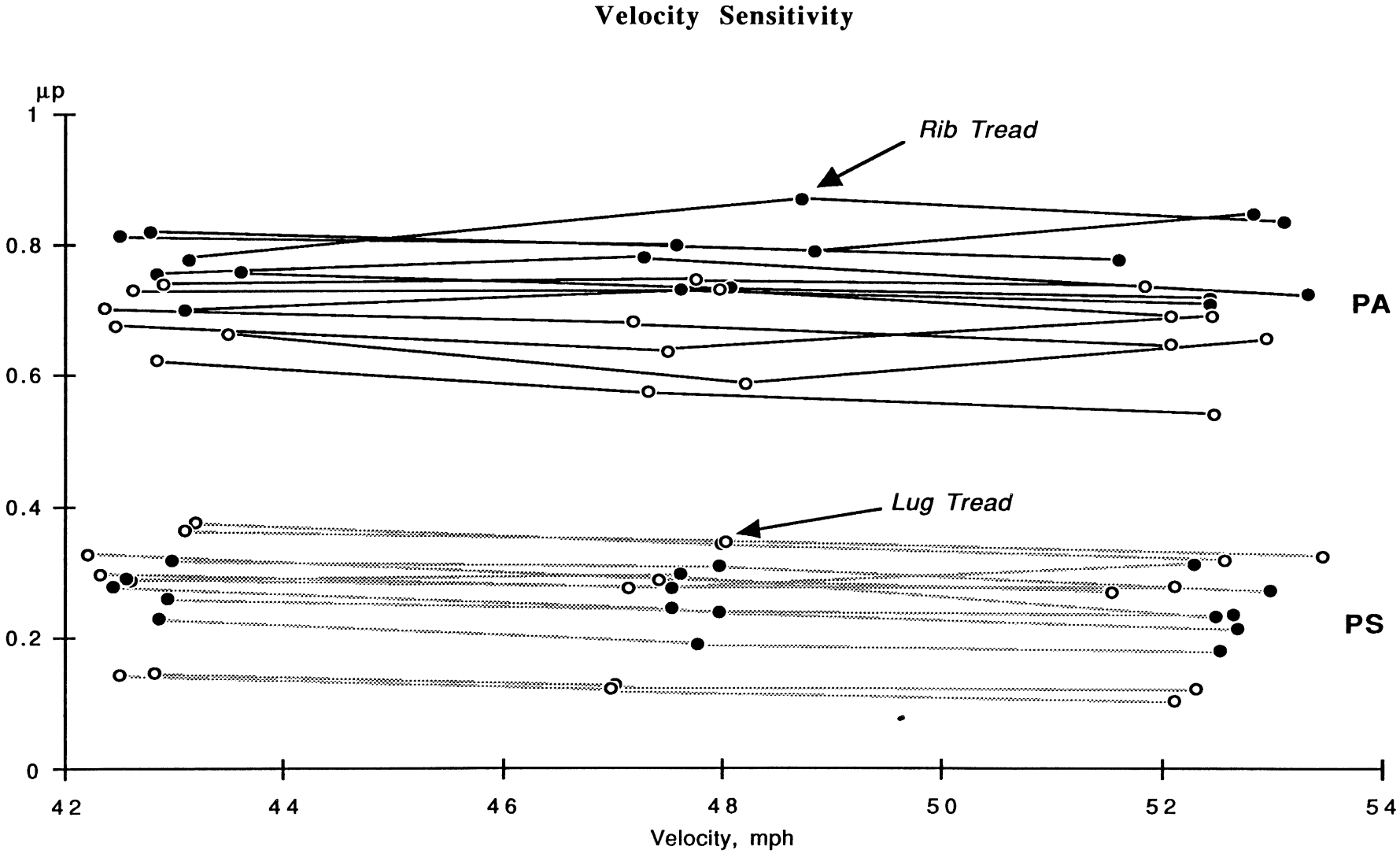

Figure 5.1 Velocity sensitivity in μ_p values, on both asphalt (PA) and concrete, (PS), pavements with a dual wipe tire configuration

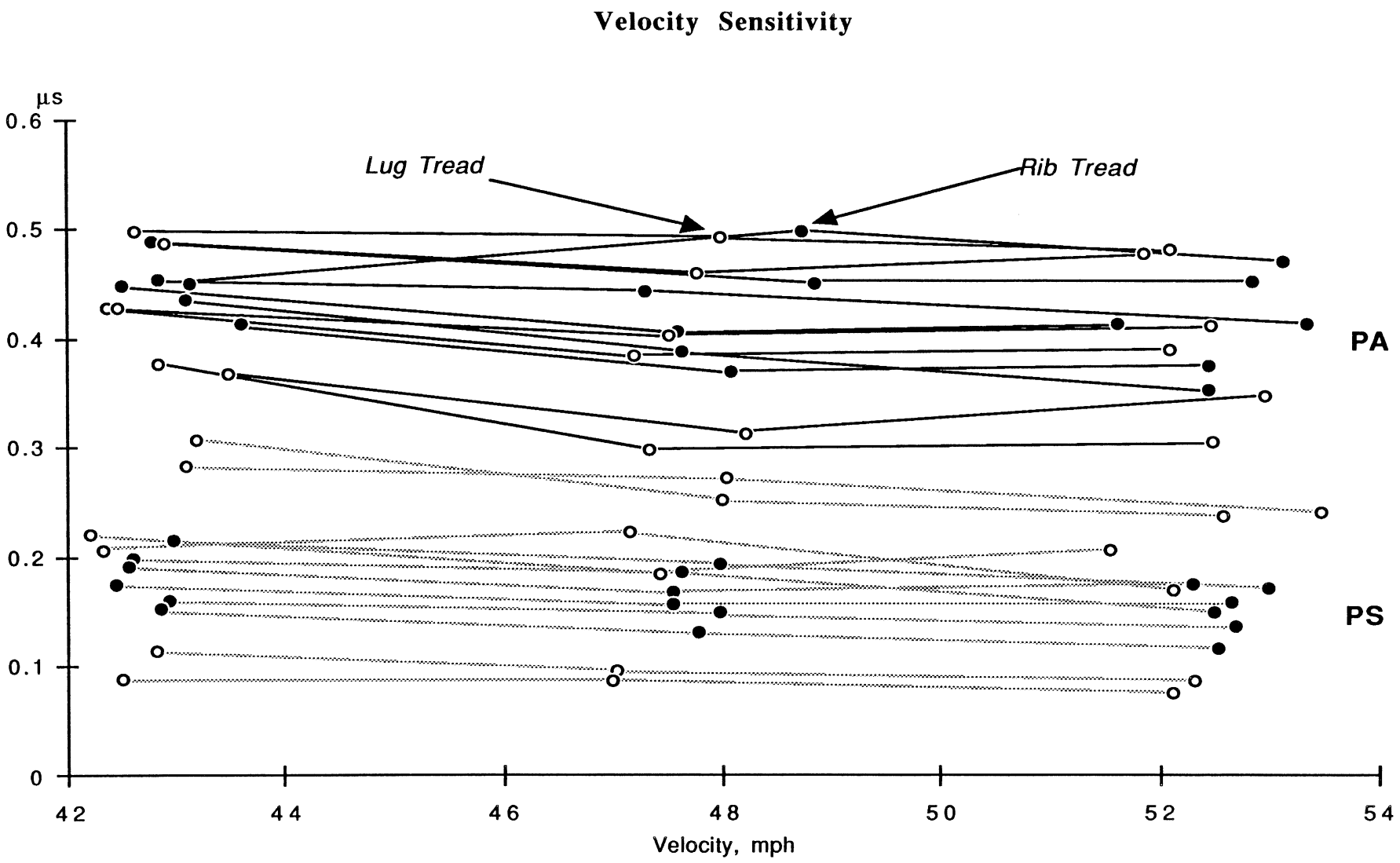

Figure 5.2 **Velocity sensitivity in μ_s values, on both asphalt (PA) and concrete, (PS), pavements with a dual wipe tire configuration**

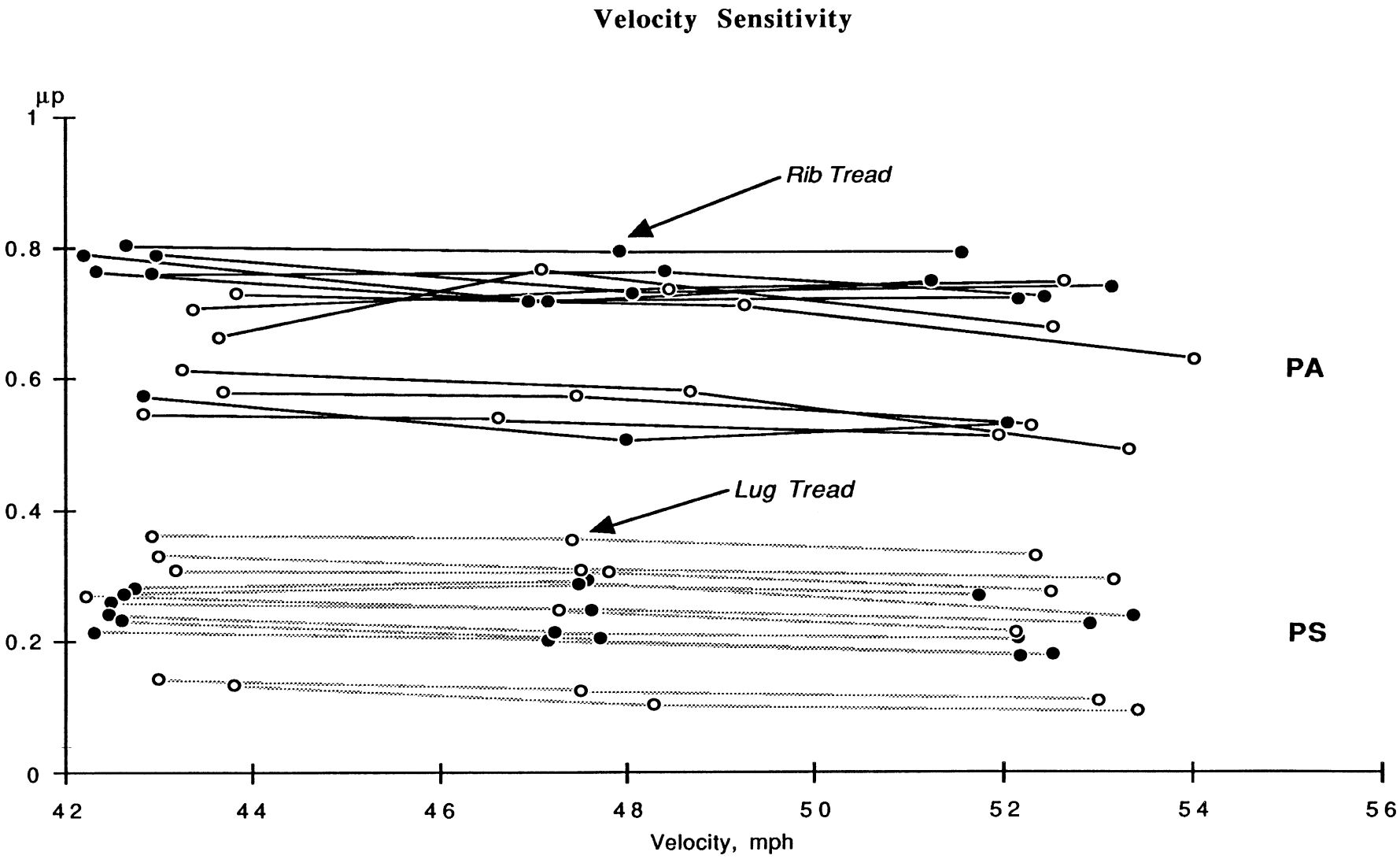

Figure 5.3 Velocity sensitivity in μ_p values, on both asphalt (PA) and concrete, (PS), pavements with a single wipe tire configuration

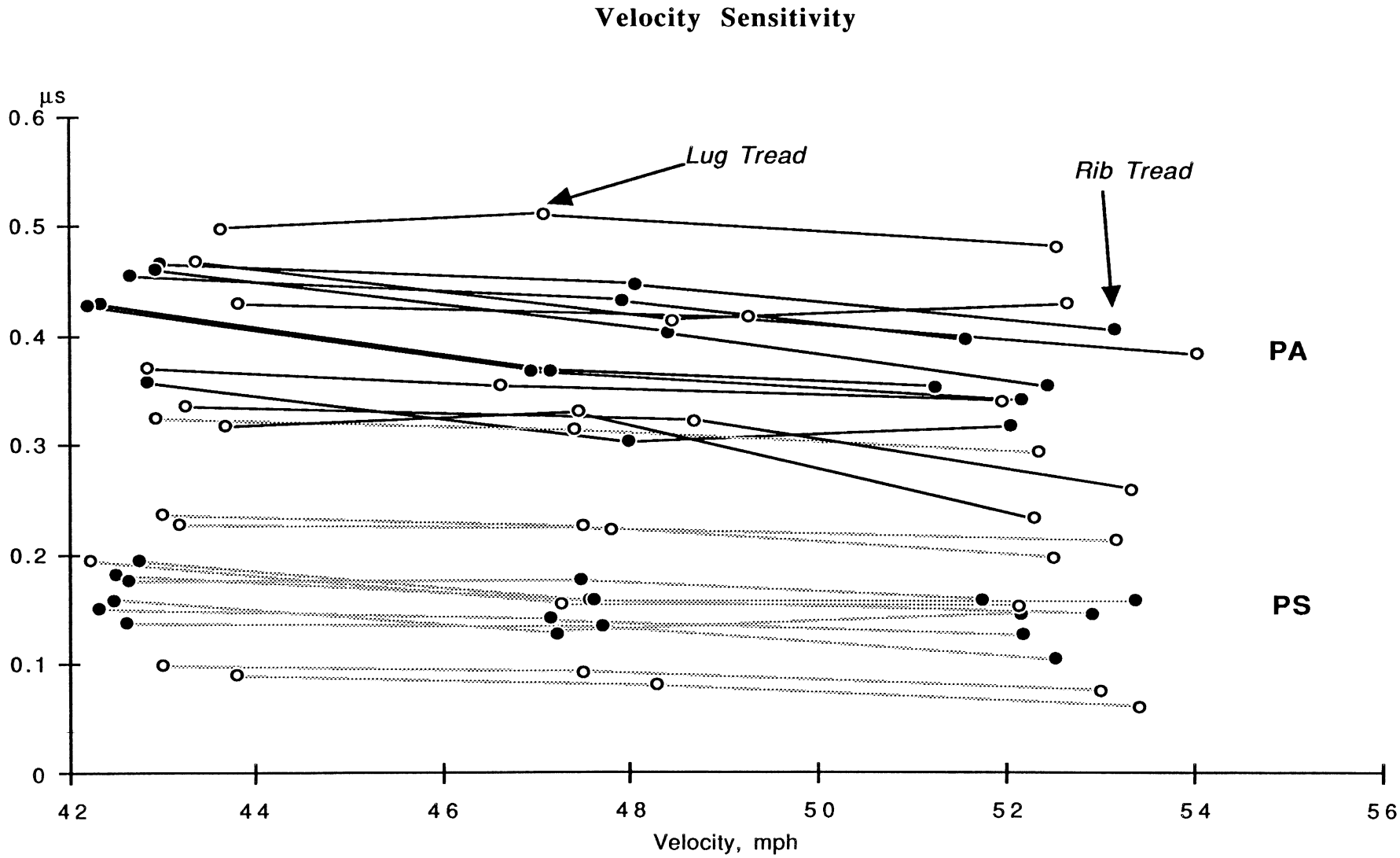

Figure 5.4 **Velocity sensitivity in μ_s values, on both asphalt (PA) and concrete, (PS), pavements with a single wipe tire configuration**

use on truck and tractor drive axles, with a distinctly "blocky" tread pattern. The data suggest that no general basis exists for distinguishing the traction levels of these two tires. Differences which do appear under one set of test conditions or the other seem to derive more from differences in tread depths of the corresponding rib and lug tires employed in the sample.

5.3 The influence of the wipe tire configuration

The influence of the wipe tire configuration appears to be negligible. Shown in Figures 5.5 and 5.6 are overlays of data taken with single- and dual-wipe tires on both asphalt and concrete test surfaces. The data show an effectively random relationship with the single/dual distinction. Furthermore, inspection of the numerical results attending the half-tread vs. full-tread wipe tire condition shows no correspondence with the traction levels reached by the trailing test specimen tires. Unfortunately, no tests were run in the "no-wipe" configuration. Nevertheless, the hypothesis that lightly-loaded truck tires will not suffer low absolute traction performance due to hydrodynamics on wet pavement, because the path travelled by the light rear tires has already been wiped by front-axle tires, seems patently refuted by the exceedingly low traction levels exhibited by the more worn tires in the sample on the low-macrotexture pavement.

5.4 The influence of inflation pressure

Shown in Figure 5.7 and 5.8 are peak and slide traction values, respectively, collected on five tires from the fleet-worn group covering the range of inflation pressures from 80 through 100 psi. The data were all taken on the polished concrete surface at a velocity of 53 mph. The pressure range was selected to cover typical trucking practice with modern radials installed in dual pairs.

The results show an effectively negligible influence of inflation pressure over the examined range. The reader should note that classical hydroplaning analyses will show a positive influence of inflation pressure on the value of speed needed to reach full hydroplaning, as a consequence of the increasing contact pressures at high inflation pressures. With the heavy truck tire, the crucial issue appears to involve the contact shape change in aspect ratio with inflation pressure may be greatly important, but was not studied here.

5.5 Variation observed upon "swapping" the two tires in a dual pair

Shown in figure 5.9 is a sample of the μ-slip curves representing "swapped" tires in a dual pair. The full complement of swapped pairs from the worn-tire test series is presented in Appendix C. The figure indicates substantial variations in both the shape of the curve and the nominal peak and slide values that are obtained. It is assumed, again, that the primary factor determining these variations is the remarkable variation in tread wear

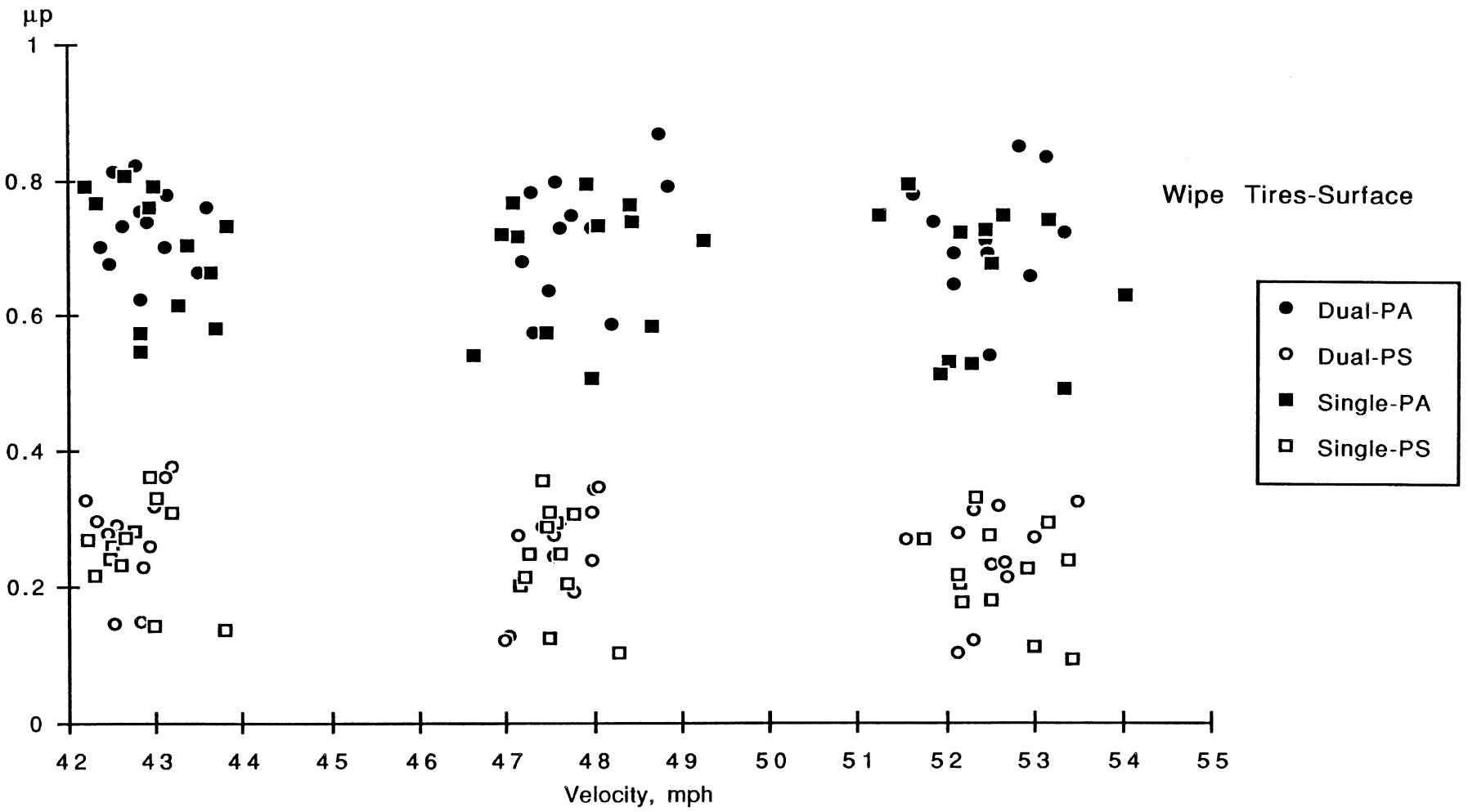

Figure 5.5 Influence of single vs. dual wipe tire arrangement on μ_p values

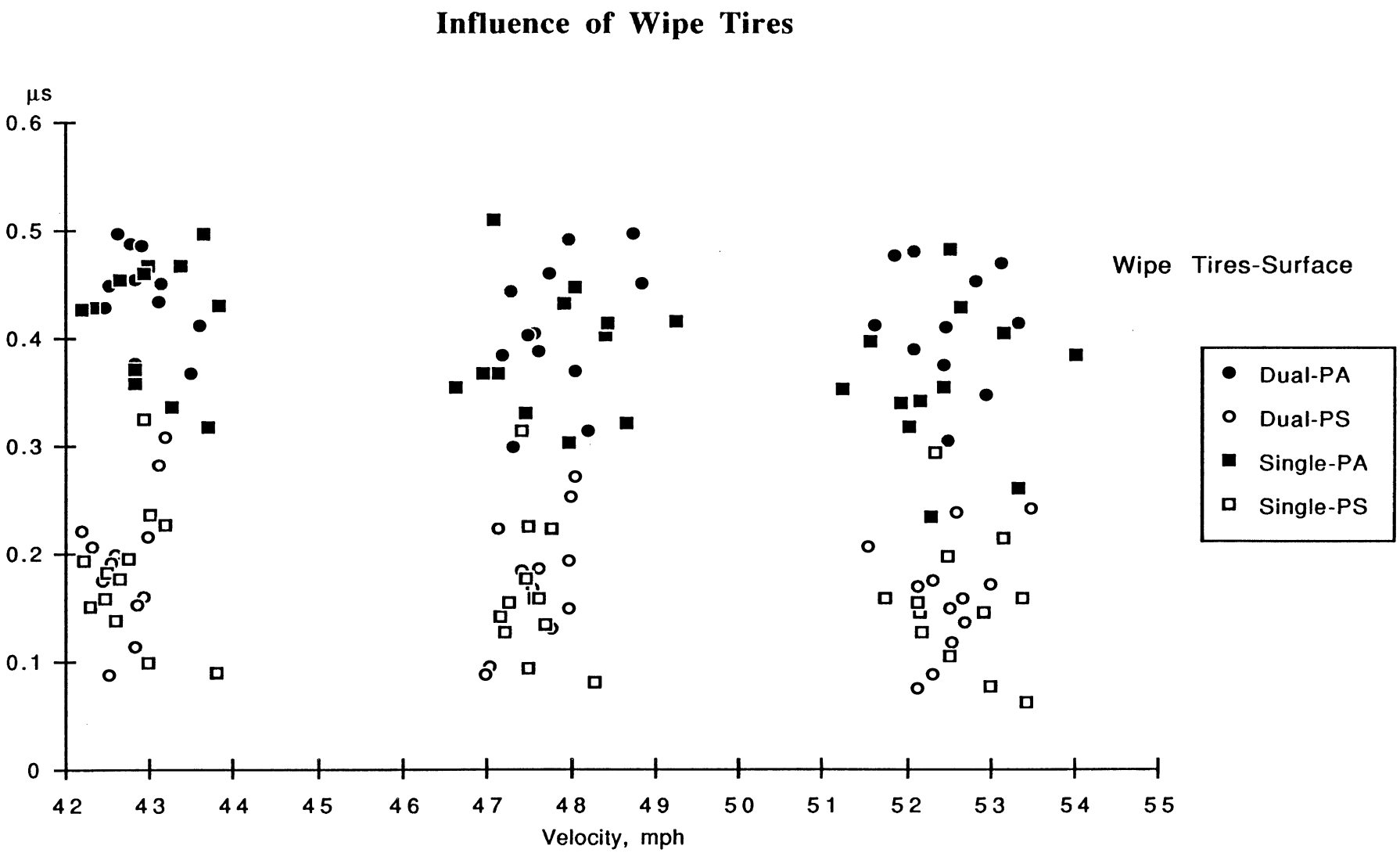

Figure 5.6 Influence of single vs. dual wipe tire arrangements on μ_s values

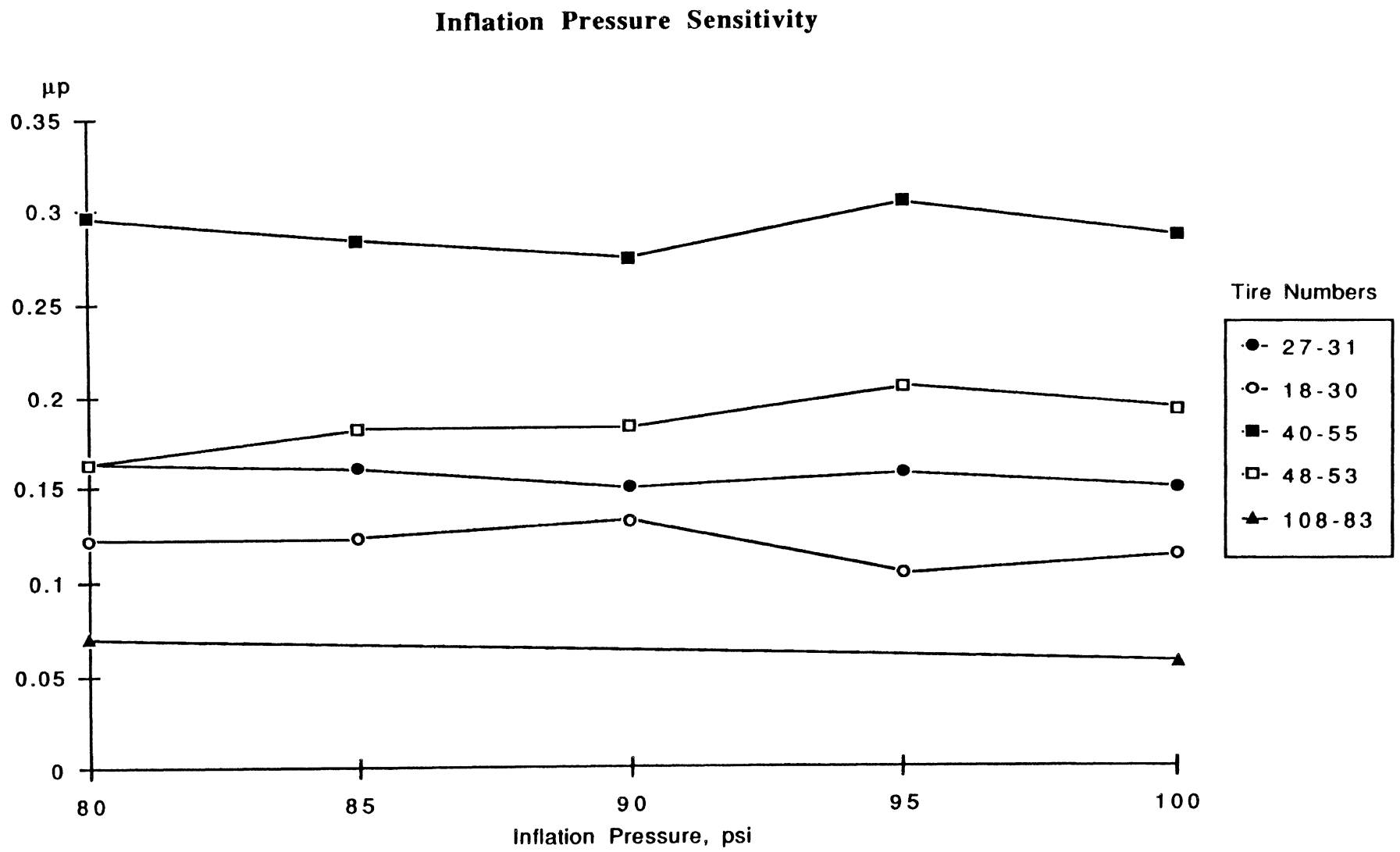

Figure 5.7 Influence of inflation presure on μ_p values for polished concrete, at 53 mph

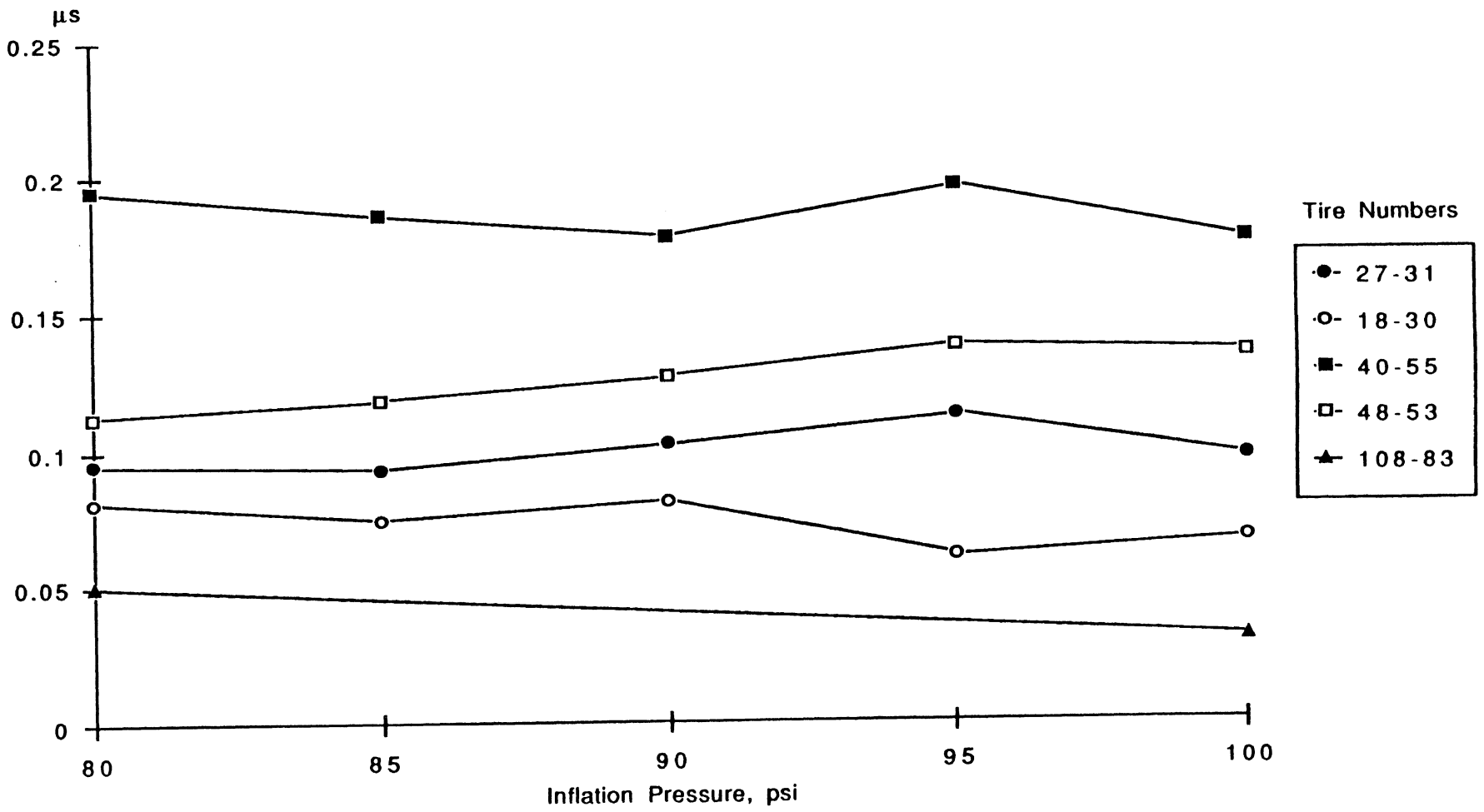

Figure 5.8 Influence of inflation pressure on μ_s values for polished concrete at 53 mph

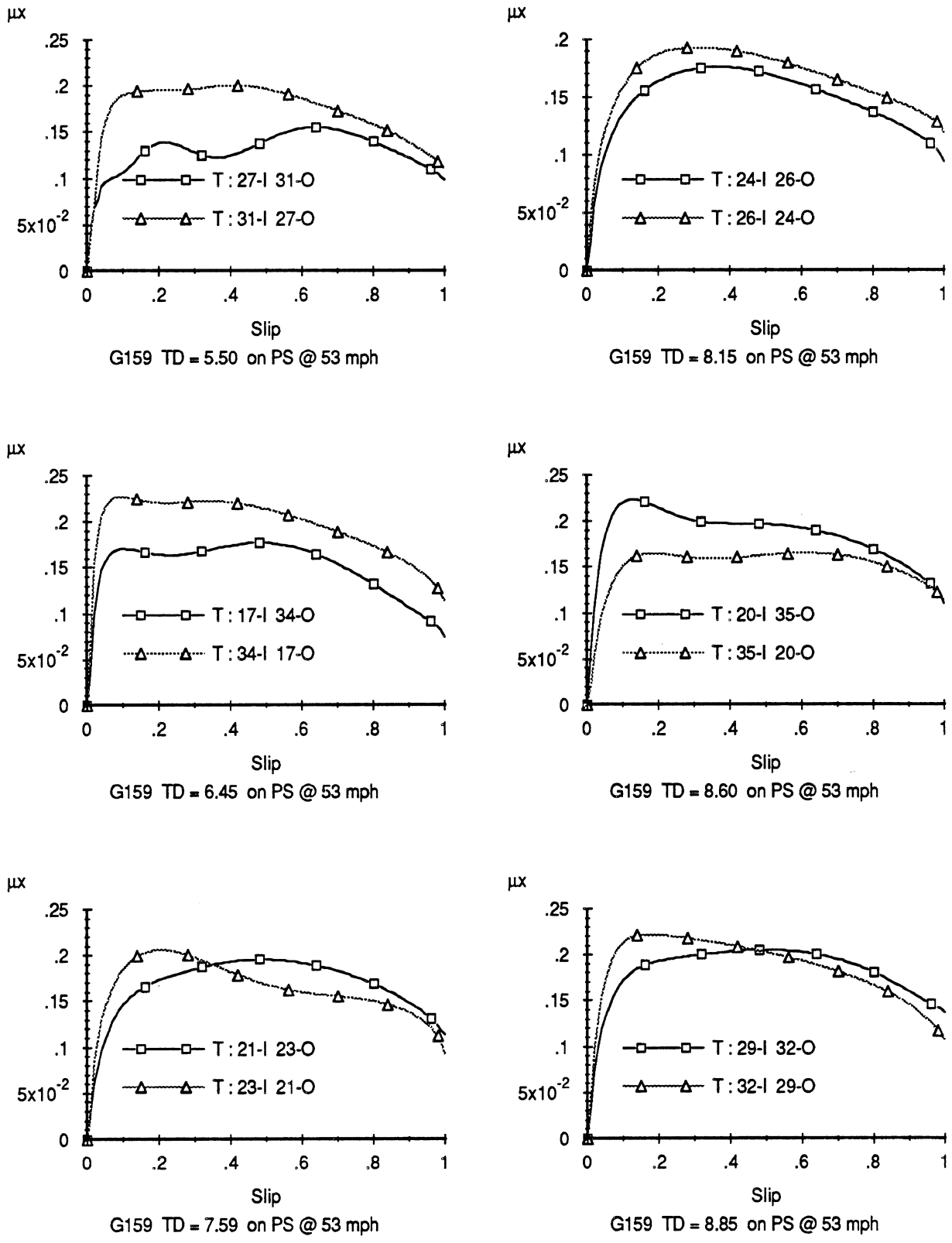

Figure 5.9 **Differences in μ-slip curves obtained for dual pairs with tires installed A-B, and then B-A. Curves are designated by tire specimen no. mounted "inside" (I) and specimen no. mounted "outside" (o).**

patterns which are developed under authentic fleet operations. Even the slide traction values can vary markedly due to such localized wear differences, depending upon the specific portion of the tread that comes to a halt under the tire as the locked wheel condition is reached.

5.6 The influence of treadwear

In the baseline tire test series, both the Michelin XDA and the Goodyear G159 were tested in three states of machine-produced treadwear. Curves showing the resulting μ-slip behavior of these two tire models on the polished concrete surface, at 53 mph, are presented in Figures 5.10 and 5.11, respectively. The data show that, while the Goodyear specimen (Figure 5.10) having the higher (18/32") value of tread depth shows a somewhat lower traction level than does the intermediate (10.25/32") case for the same tire model, the rest of the data on both models follows a trend toward lower traction level with declining tread depth. Conspicuously, the Michelin tire (Figure 5.11) at a tread depth of only 2/32's of an inch shows a much-reduced traction level—less than 30% of the peak traction level of the tire in its full-tread condition.

These data obtained on a small sample of uniformly-worn tires complement the larger data set obtained from fleet-worn tires. Obviously, the collection of fleet-worn tires was prompted by a desire to obtain a relatively large sample of data on the influence of authentic treadwear on traction performance. The processed data for the fleet-worn sample appear in various plotted formats in Appendix D. Shown in Figure 5.12 is a scatterplot of the peak and slide values measured on the fleet-worn sample, from which the following observations can be made.

- The data show wide variability, resulting in poor correlation coefficients when common statistical fitting methods are applied.

- Over all tread depths, the mean value of the slide data is at less than 50% of the ASTM skid number (expressed as a %) for this pavement. Even the mean of the peak traction level is at less than 75% of the ASTM-measured skid traction level. (This observation simply addresses the gross traction performance of these truck tires relative to a measurement, albeit crude, of the traction capability of car tires on this surface.)

- The distribution of tread depth values across the sample has the heaviest concentration between depth values of 4 and 8/32's of an inch. Nevertheless, nineteen specimens were tested at tread depths below 4/32's of an inch.

- The sketched-in envelope of the data suggests a peculiar trend as a function of tread depth, with an apparent drop in the upper boundary at tread depth values below 4/32's of an inch.

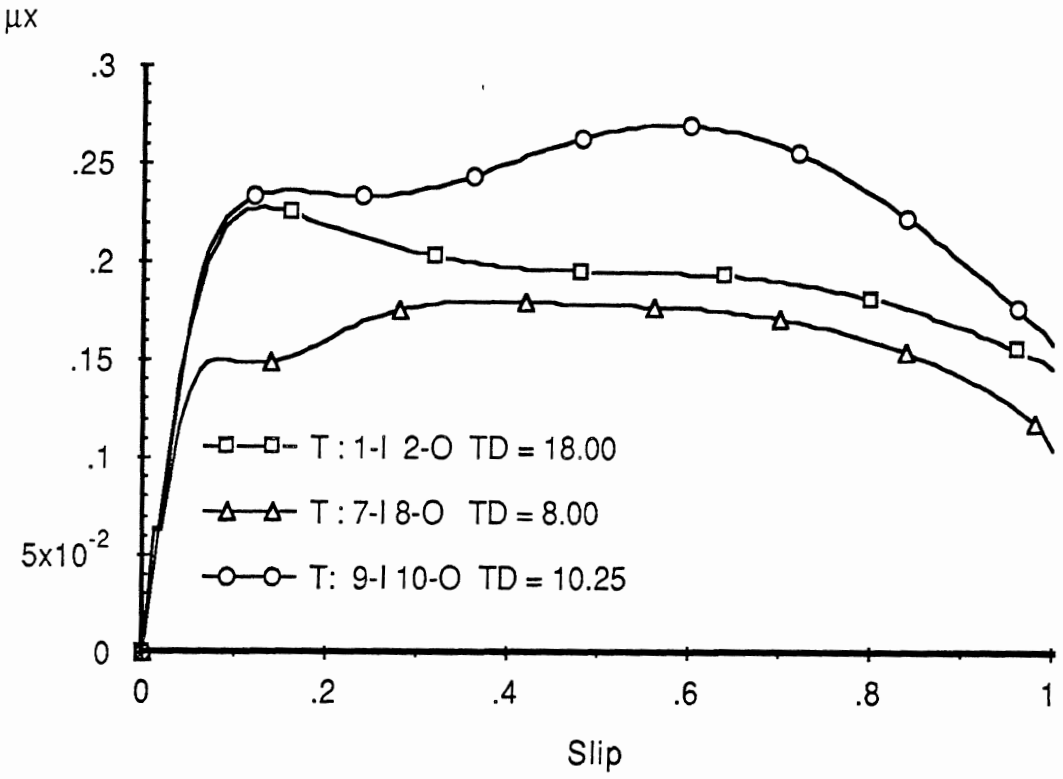

Figure 5.10 **The influence of tread depth (TD) on the μ-slip response of the Goodyear G159 tire as tested on the polished concrete surface at 53 mph**

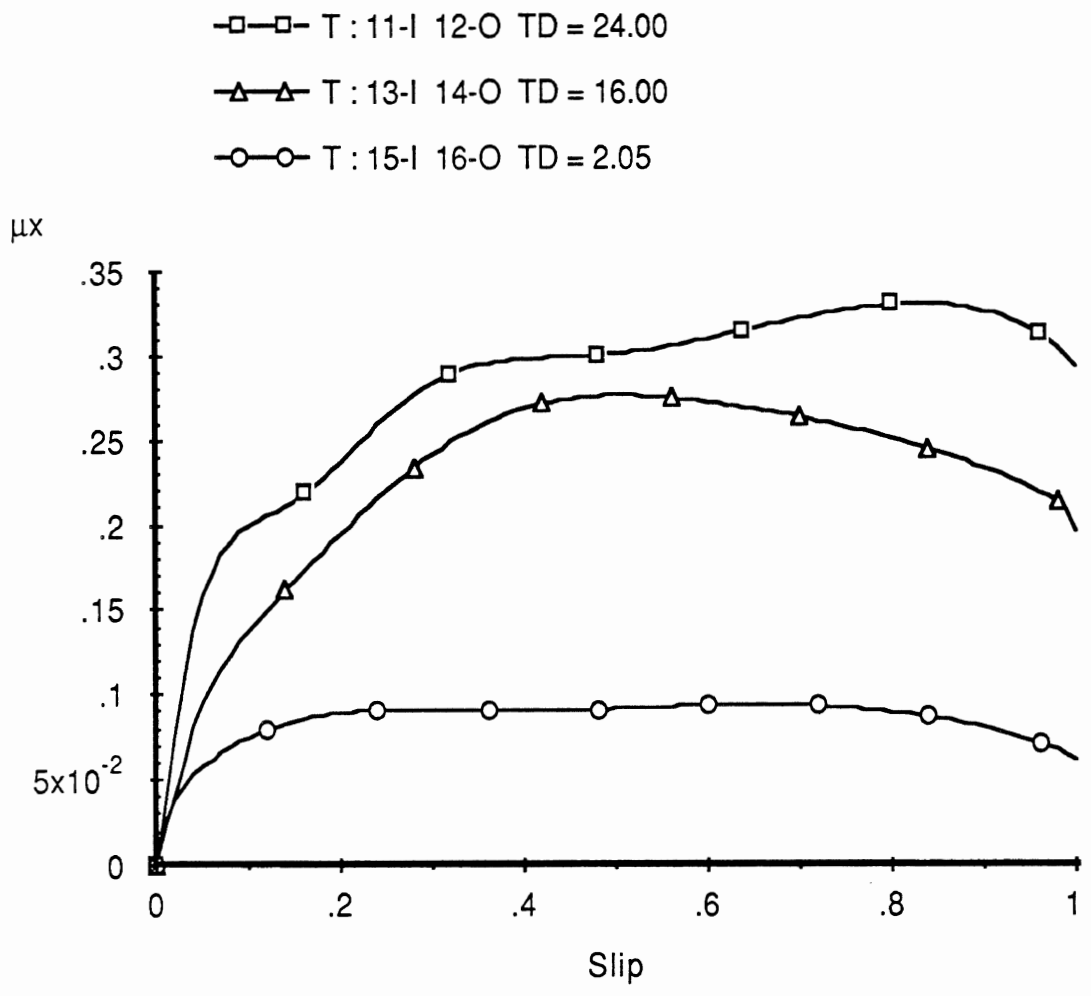

Figure 5.11 The influence of tread depth (TD) on the μ-slip response of the Michelin XDA tire as tested on the polished concrete surface at 53 mph

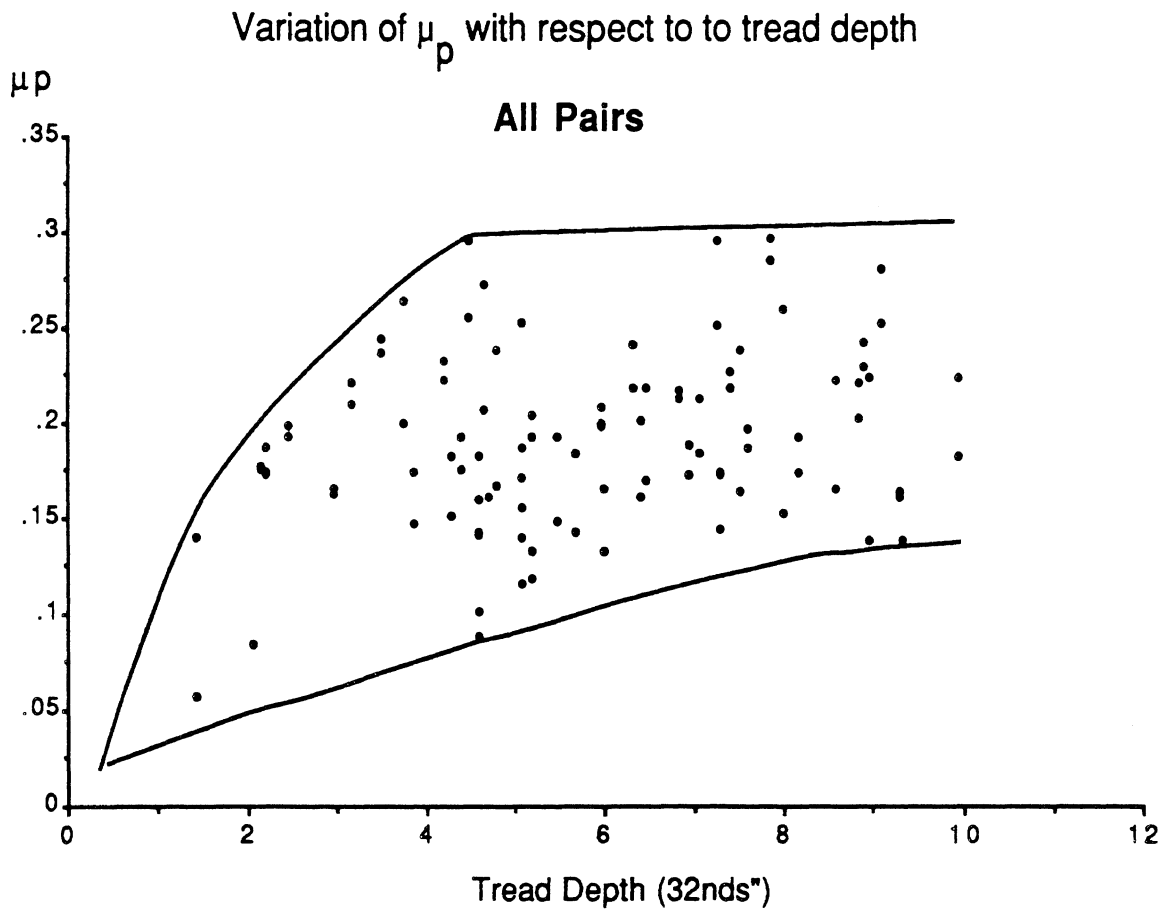

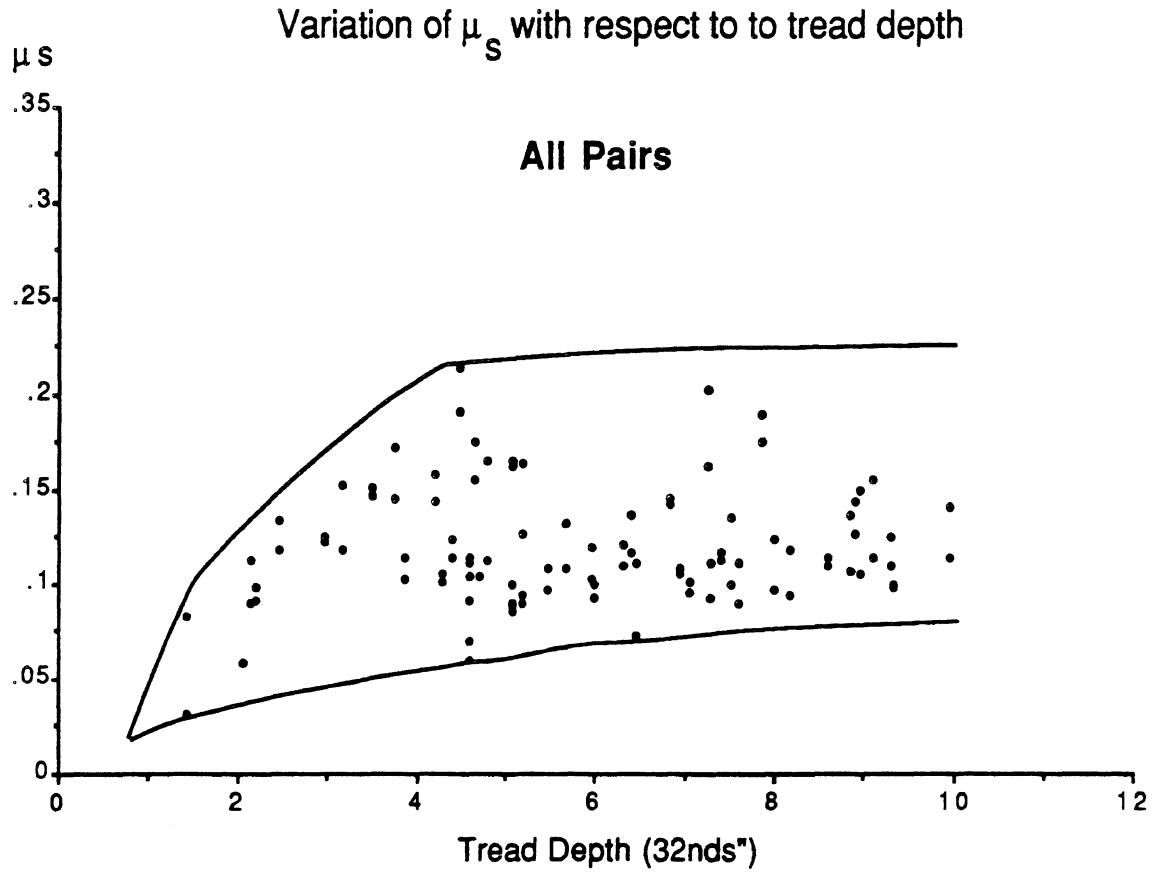

Figure 5.12 Scatter plots of μ_p and μ_s values as a function of tread depth in the fleet-worn sample

The overall data set presents something of a conundrum. Namely, while a much steeper sensitivity to tread depth appears at depth values of 4/32's and below, the traction data in this range are not well distributed. For example, we note an obvious "hole" in μp values below 0.15 (and in μs values below 0.10) for tread depths between 2 and 4/32's of an inch. Thus, a continuous, nicely distributed data set covering the range of tread depths did not materialize. Addressing this issue further, Figures 5.13 and 5.14 show linear regressions to the peak and slide data on, respectively, (a) all worn tires and (b) only those tires having tread depth values below 4/32's of an inch. The two plots show regression lines that differ by five to one. Thus, the peak data in Figure 5.13 show a correlation coefficient of 0.37 for the best-fit slope of -0.0059 units of μp per 32nd of an inch of tread depth, while the plot of Figure 5.14 shows a correlation coefficient of 0.65 for the best-fit slope of -0.030 units of μp per 32nd of an inch.

On the one hand, hydroplaning theory certainly supports the finding that traction level will fall off precipitously as tread depth approaches zero on thin water films. On the other hand, the peculiar distribution of the tread depths across the tire sample, plus the large degree of scatter driven apparently by the severely-undulated tread wear patterns, provides less than an ideal statistical case for quantifying this fall-off.

In Appendix D, the various subsets of the total tire sample are broken out for individualized plotting of the traction levels as a function of tread depth. One such plot is presented here as Figure 5.15. This Figure presents only the data for the fleet-worn, Michelin lug-tread tires, over the range of tread depths. The fitted regression line in this case is -0.009 units of peak traction level per 32nd of an inch with a correlation coefficient of 0.75. When the portion of this curve below 4/32's of an inch is fitted with a regression line, a slope of -0.039 units of μp `per 32nd is obtained, with a correlation coefficient of 0.53.

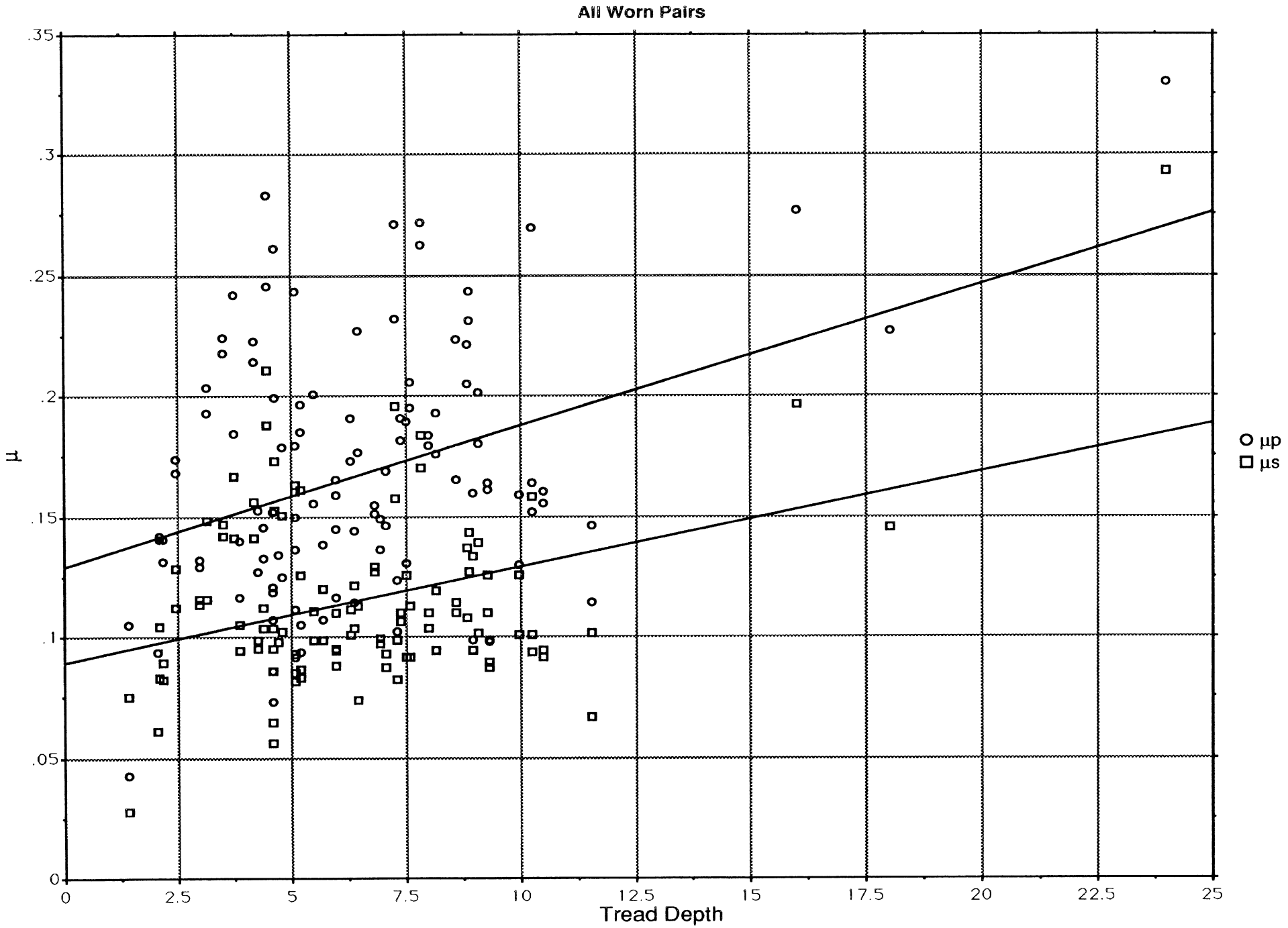

Figure 5.13 Linear regression lines fitted to μ_p data (circles) and μ_s data (squares) as a function of tread depth over the entire range of tread depth values.

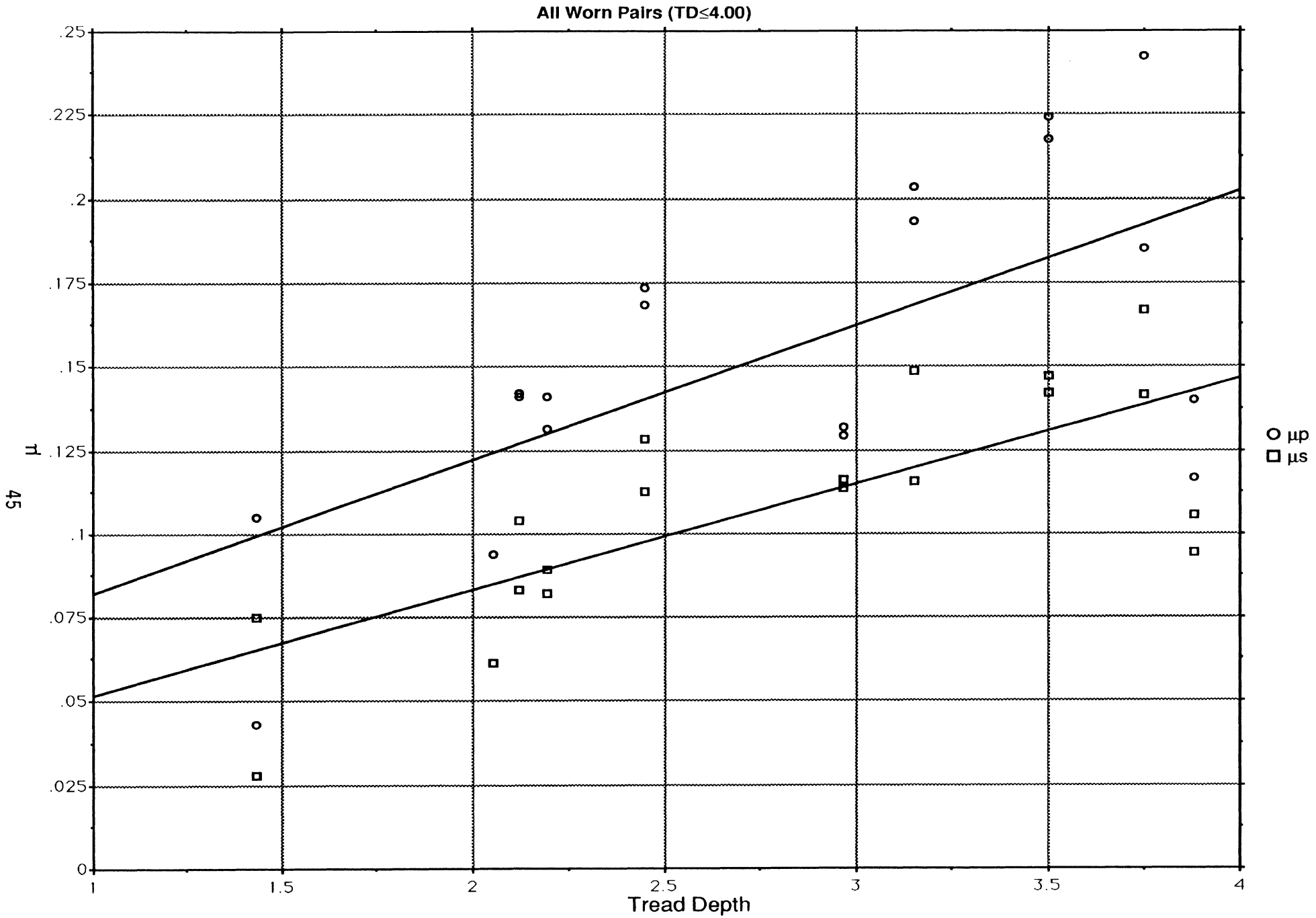

Figure 5.14 Linear regression lines fitted to μ_p data (circles) and μ_s data (squares) as a function of tread depth over the range of tread depth values below 4/32nds of an inch.

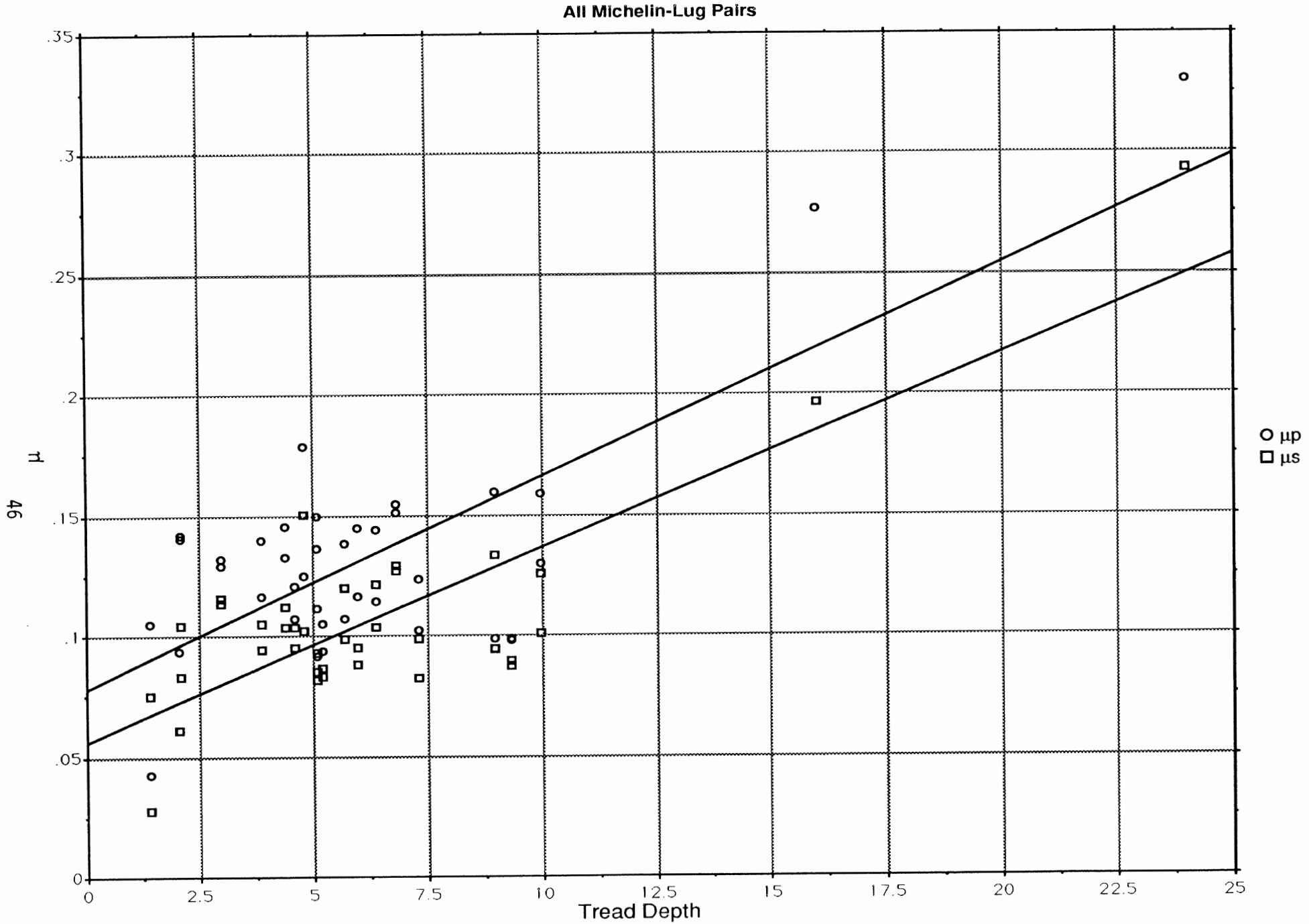

Figure 5.15 Linear regression lines fitted to the μ_p peak and μ_s slide values for the Michelin-lug samples only

6.0 Conclusions

This study has produced quantitative measurements of the braking traction performance of truck tires operating on wet pavement at light load. The data represent the type of water cover conditions that would prevail on reasonably drained roadways under heavy rainfall conditions without flooding. The primary findings of significance pertain to the loss in absolute traction performance levels as a result of treadwear. The findings are as follows:

1) Traction performance levels do degrade under the influence of strong hydrodynamic mechanisms, as the wear accrued in actual fleet usage reduces tread depth toward the values specified as minimums under federal regulation.

2) Hydrodynamic mechanisms dominate the traction performance of lightly-loaded, worn, rear-mounted truck tires on heavily-wetted pavements despite the wiping action of front-axle tires.

3) Lightly-loaded truck tires were seen to lose on the order of 50 to 70% of the traction performance they had attained when new, as they approached 2/32's of an inch of remaining tread depth. For the case of a wet, polished concrete surface, the traction performance achieved under the minimum tread depth levels was roughly comparable to that which would normally accrue only when ice covers the roadway. Pavement conditions equivalent to those encountered on this polished concrete surface are seen on public roadways wherever traffic, itself, has thoroughly polished the aggregate or where the asphaltic binder has "bled" from bituminous pavements to create a minimally-textured surface.

4) Noting these findings in light of Section 393.75 of the Code of Federal Regulations which specifies a minimum tread depth of 2/32's on rear tires and 4/32's on the front tires of trucks in interstate transportation, the federal rule can be said to be:

    a) backwards, in the sense that the inevitable light-rear and heavy-front load distribution in the empty case suggests that the greater tread depth should be required *on rear-mounted tires*, rather than the fronts (note that only rear-mounted tires can achieve the very light loads at which hydrodynamic problems pose a special need for tread depth) and,

    b) permissive, in an absolute sense, insofar as it allows for the 2/32's tread depth value at which traction performance appears to be deteriorating radically, although the data produced here failed to quantify the deterioration at very low tread depths in confident statistical terms. (Concerning the absolute minimum issue, the authors recognize that traction loss vs. tread depth is a more or less continuous function and that a specific limit must be selected so that both the safety and economic implications of the choice are soberly balanced.)

7.0 References

1. Horne, W.B. "Predicting the Minimum Dynamic Hydroplaning Speed for Aircraft, Bus, Truck, and Automobile Tires Rolling on Flooded Pavements." Presentation to ASTM Committee E-17 at College Station, Texas, June 5, 1984.

2. Ivey, D.L. "Truck Tire Hydroplaning--Empirical Verification of Horne's Thesis." Presentation to the Technical Seminar on Tire Service and Evaluation, ASTM Committee F-9, Akron, Ohio, November 1984.

3. Sakai, H., Kanaya, O., and Okayama, T. "The Effect of Hydroplaning on the Dynamic Characteristics of Car, Truck, and Bus Tires." SAE Paper No. 780195, 1978.

4. Chira-Chavala, T. "Empty Trucks and Their Problems on Wet Pavements--Can Truck Hydroplaning Theory be Supported by Accident Data?" Texas Transp. Inst., Texas A&M Univ., April 1985.

5. Ervin, R., et al. "Impact of Specific Geometric Features on Truck Operations and Safety at Interchanges." Final Rept., FHWA Contract No. DTFH61-82-C-00054, Transp. Res. Inst., Univ. of Mich., Rept. No. UMTRI-85-33, August 1985.

6. Horne, W.B., et al. "Phenomena of Pneumatic Tire Hydroplaning." Langley Res. Center, Rept. No. N64 10521, November 1963.

Appendix A

Histograms showing the distribution of tread depth for fleet-worn tire samples that were received for testing.

Included are plots representing the following groupings:

- all tires tested in the fleet-worn portion of the program
- all Goodyear tires in the program
- all Michelin tires
- all tires having lug-type tread patterns
- all tires having rib-type tread patterns
- all Goodyear-lug type tires
- all Goodyear-rib type tires
- all Michelin-rib type tires
- all Michelin-lug type tires

Histogram of all the tires tested

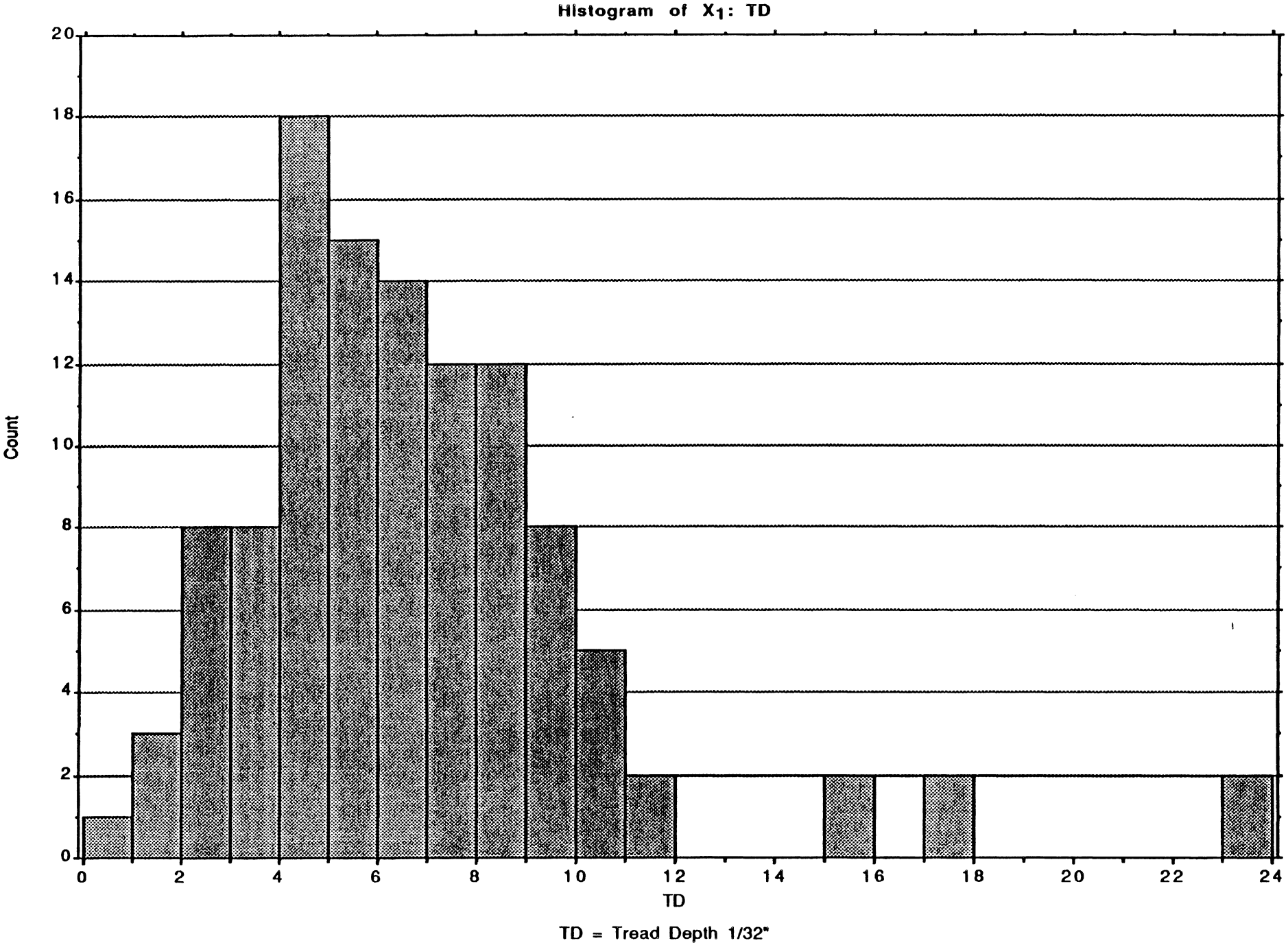

Histogram of all Goodyear tires

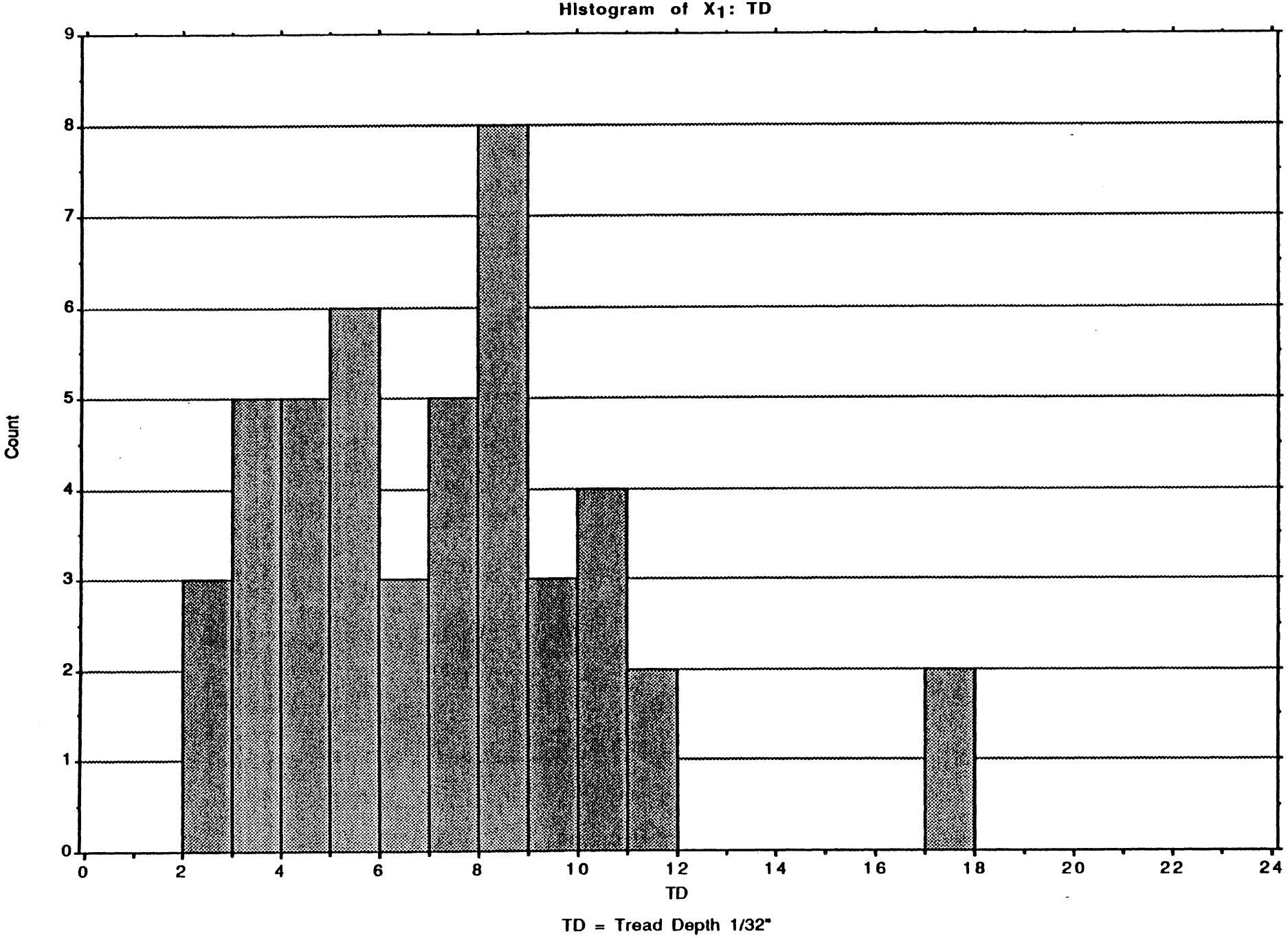

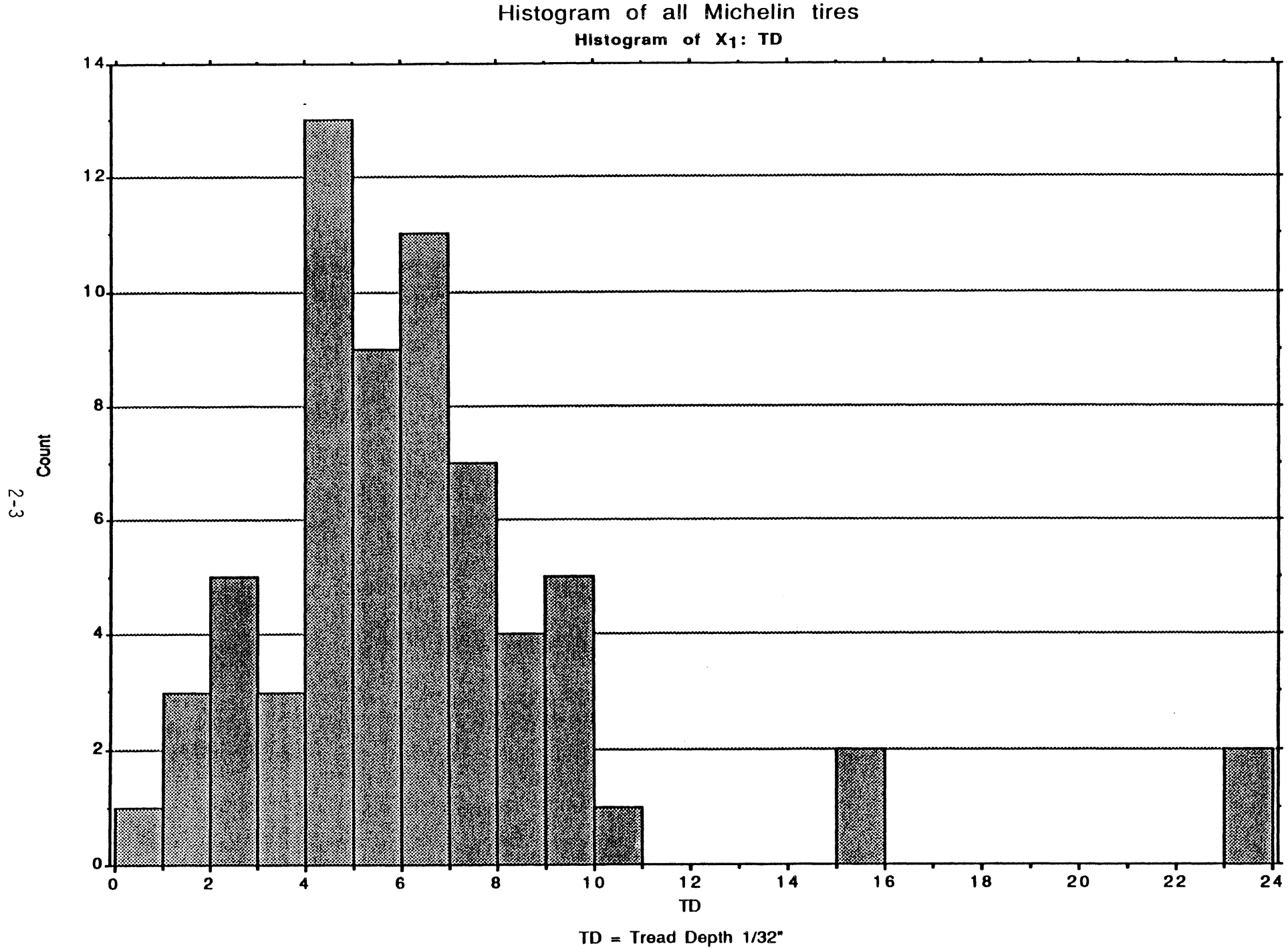
Histogram of all Michelin tires
Histogram of X1: TD
Count
TD
TD = Tread Depth 1/32"
0
2
4
6
8
10
12
14
16
18
20
22
24

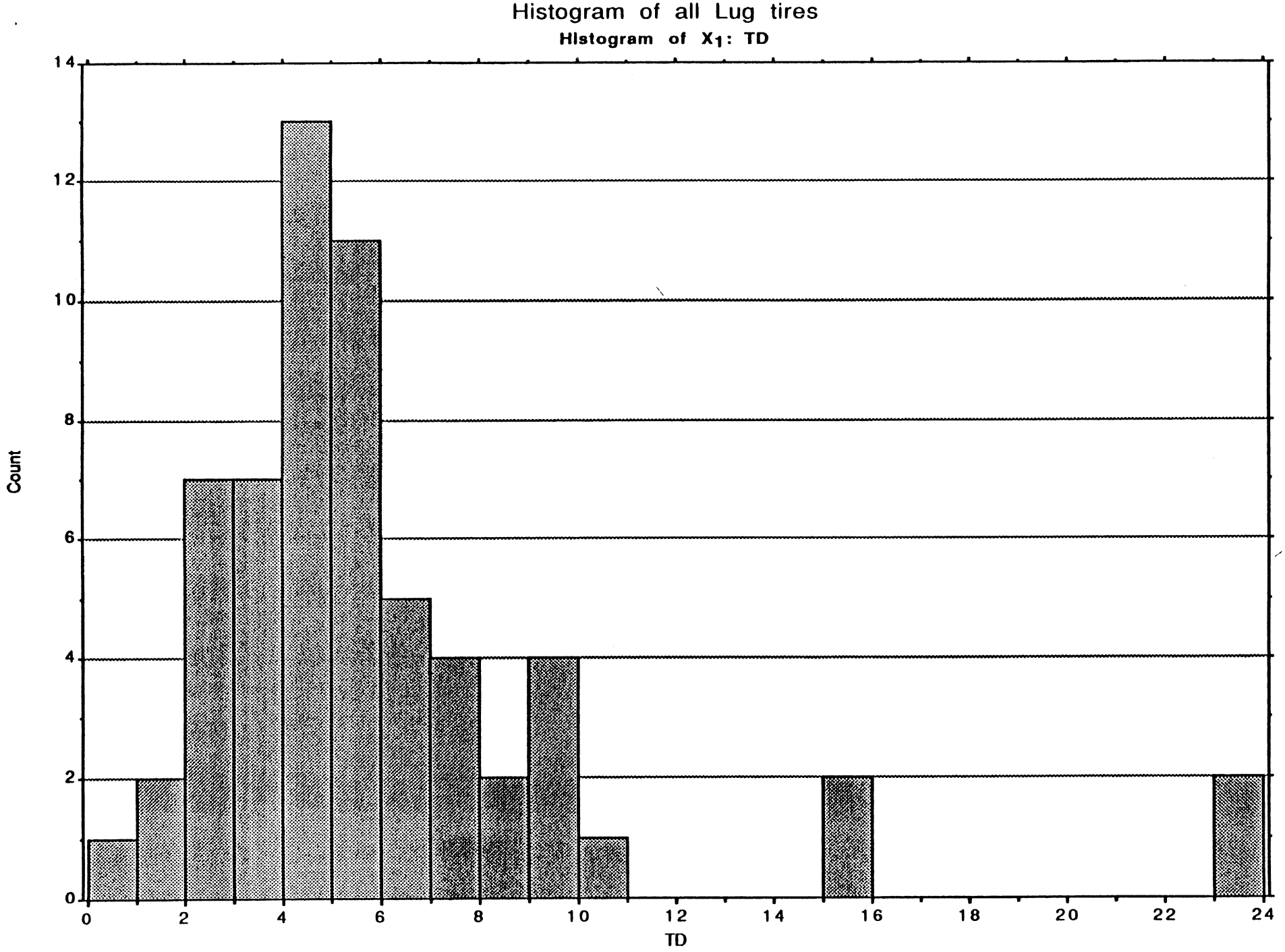
Histogram of all Lug tires
Histogram of X1: TD
Count
TD
0
2
4
6
8
10
12
14
16
18
20
22
24

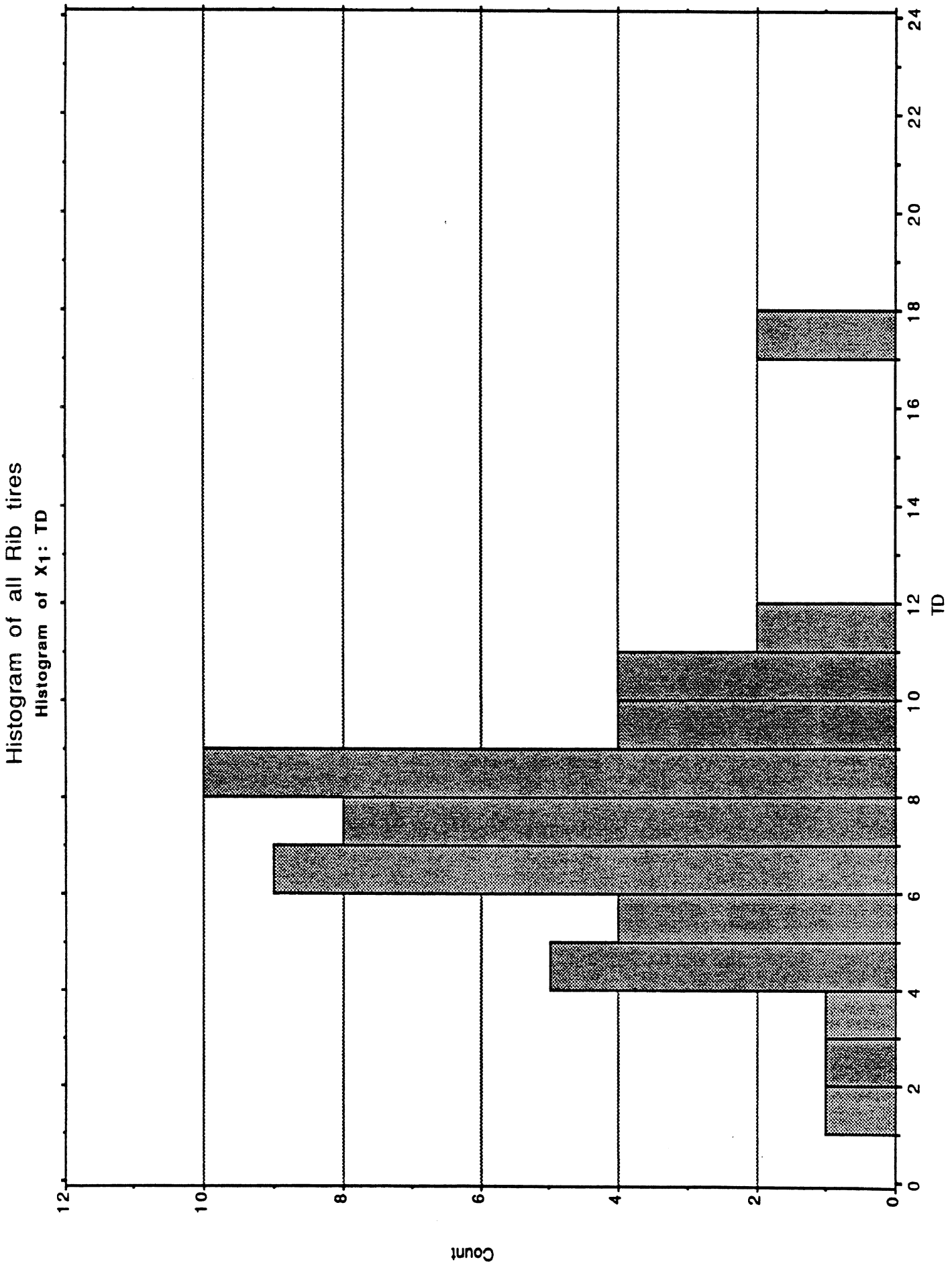
Histogram of all Rib tires
Histogram of X1: TD
Count
TD
0
2
4
6
8
10
12
14
16
18
20
22
24

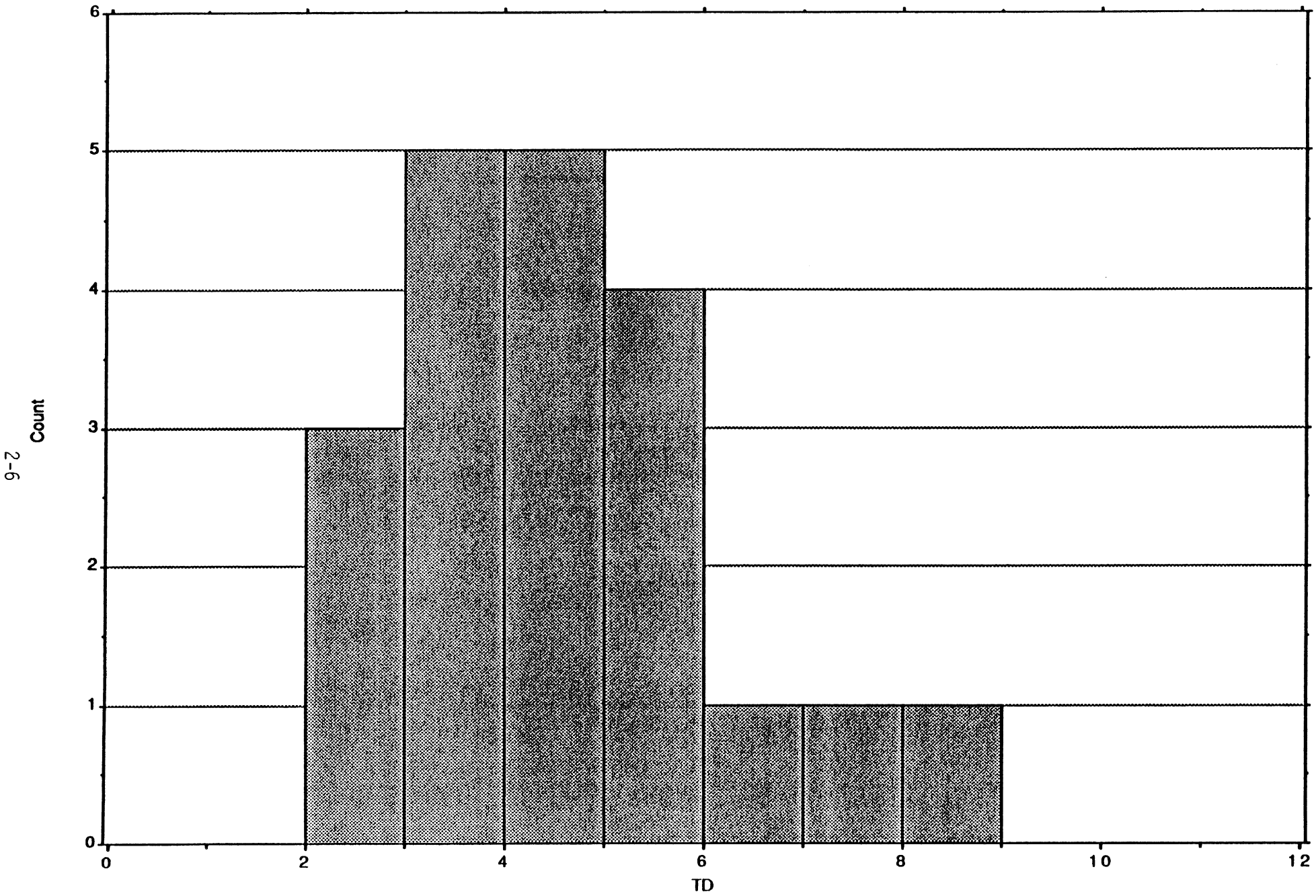
Histogram of Goodyear-Lug tires
Histogram of X1: TD
Count
TD
0
1
2
3
4
5
6
0
2
4
6
8
10
12

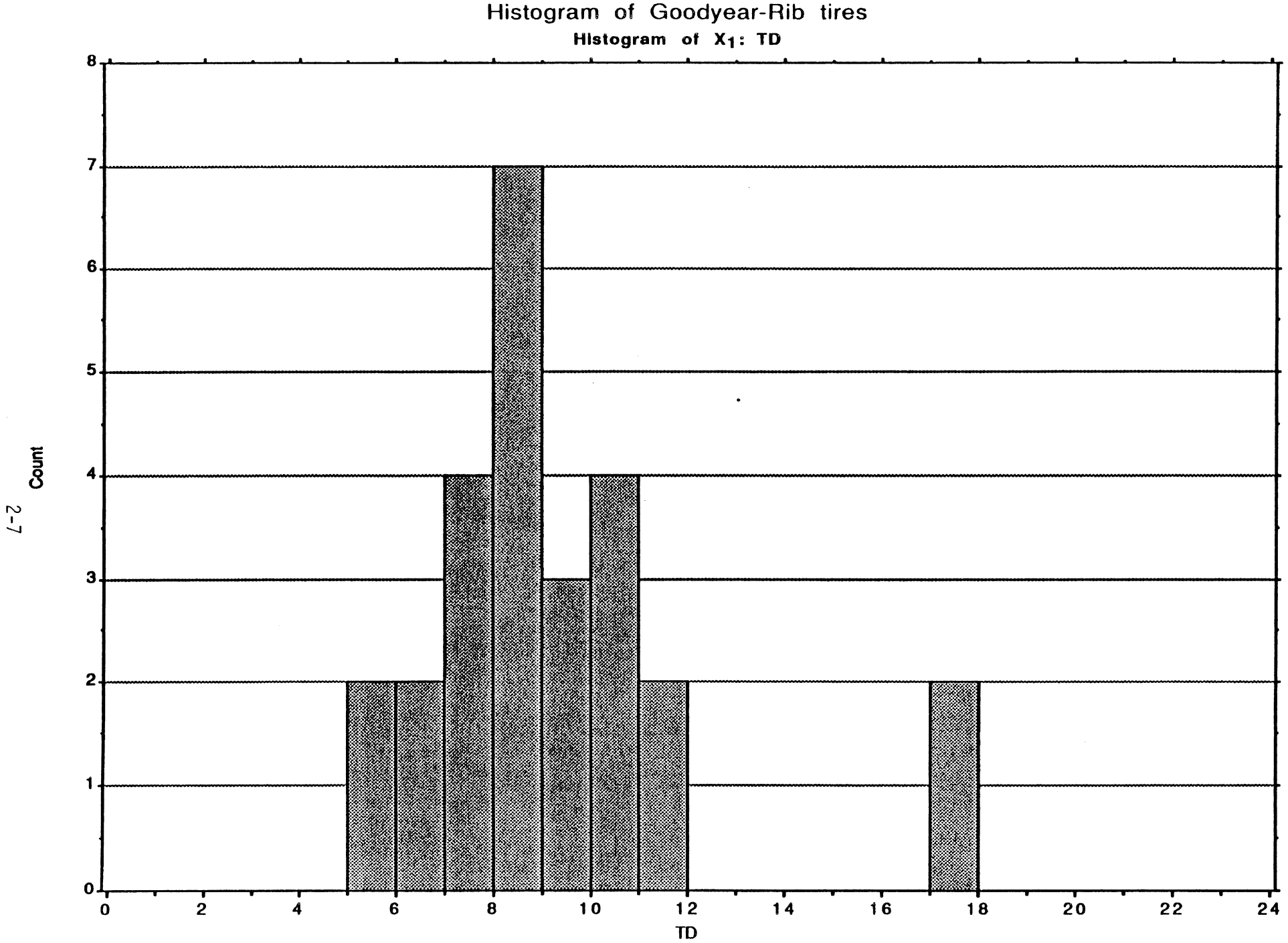
Histogram of Goodyear-Rib tires
Histogram of X1: TD
Count
TD
0
1
2
3
4
5
6
7
8
0
2
4
6
8
10
12
14
16
18
20
22
24

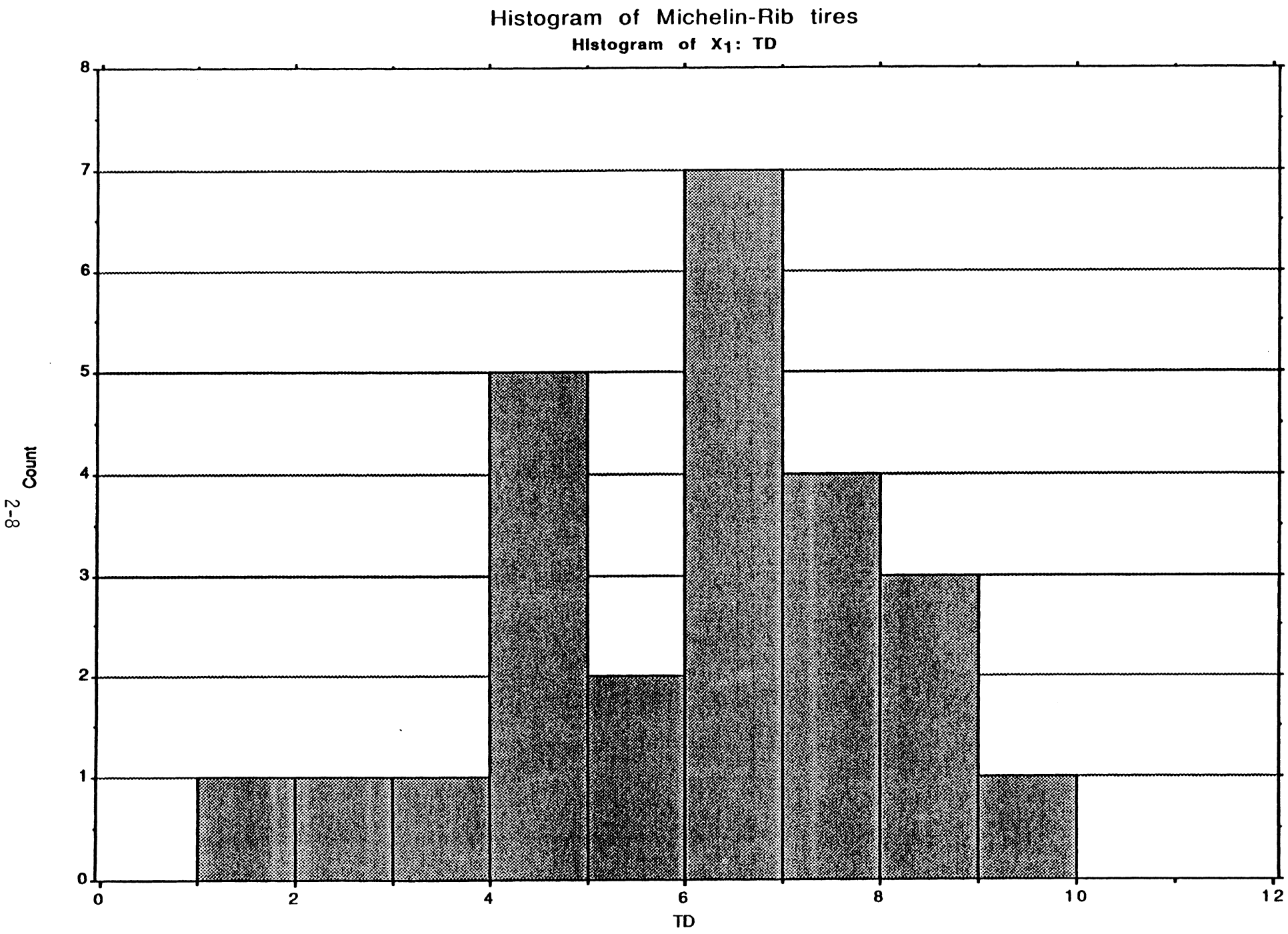
Histogram of Michelin-Rib tires
Histogram of X1: TD
Count
TD
0
1
2
3
4
5
6
7
8
0
2
4
6
8
10
12

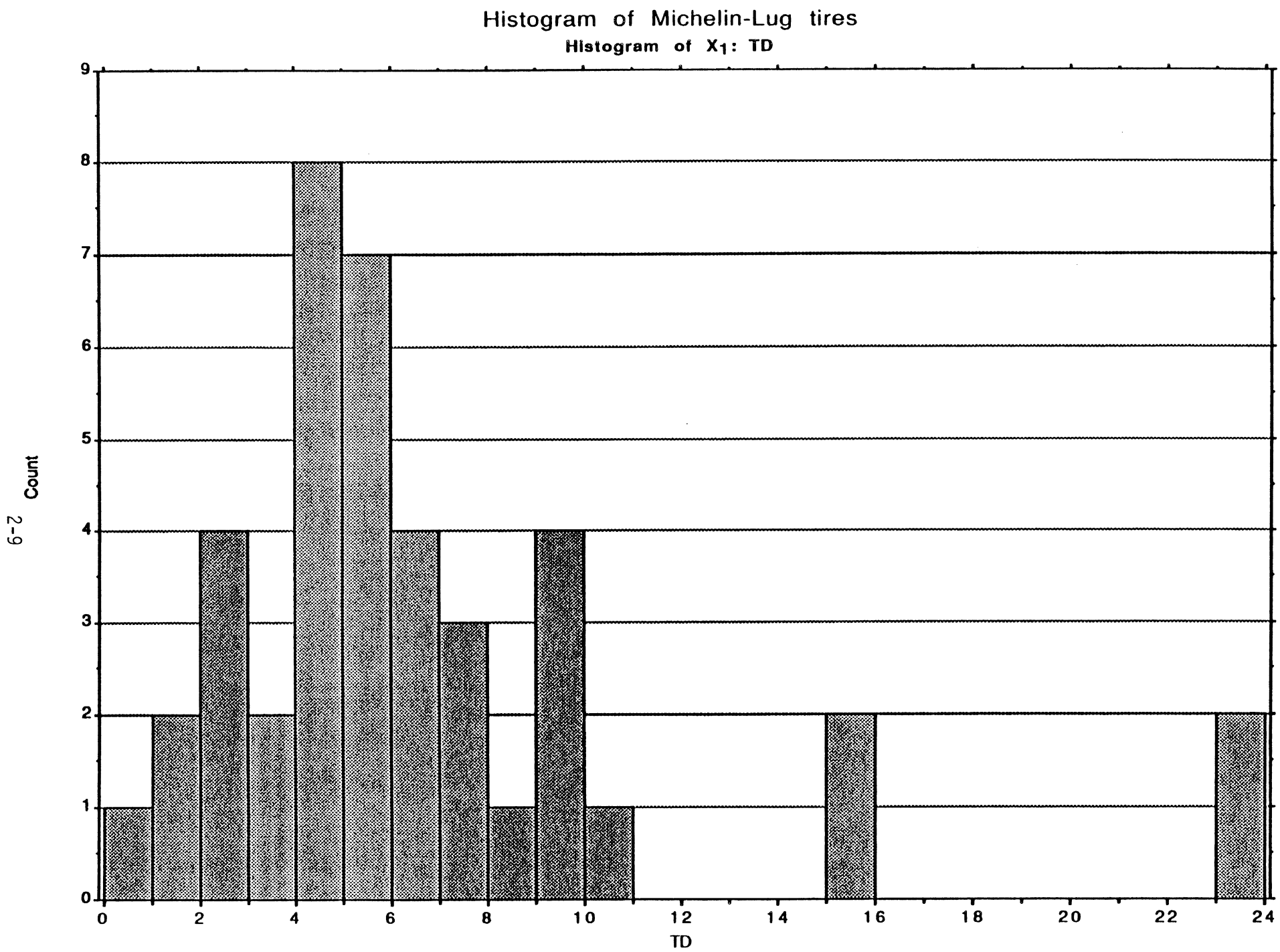
Histogram of Michelin-Lug tires
Histogram of X1: TD
Count
TD
0
1
2
3
4
5
6
7
8
9
0
2
4
6
8
10
12
14
16
18
20
22
24

Appendix B

The appendix presents a summary table of the traction measurements conducted with the Baseline and the Worn tire sets. The table includes entries denoting the test conditions as well as the results obtained on each pair of tires tested. Each row represents a dual tire pair involving the tire specimens whose assigned code numbers are listed in column six. The respective columns across the table portray the following variables:

- **Date** : the date at which the tests were performed.
- **Day** : the test-day number, with "0" being the first day of testing. As shown in the tables there were a total of 14 days of actual testing.
- **Brand** : the brand name of the test pair.
- **Name(s)** : the tire model name(s) represented in the test pair.
- **Tread** : the type of tread of the test pair, either Rib or Lug.
- **Tires** : a number designated to each tire making up the test pair. The first number corresponds to the tire mounted on the inside of the dual pair (right side, looking forward.)
- **TD** : the average tread depth of the test tire-pair,in 32^{nds} of an inch.
- Fz_{avg} : the average vertical load, in lbs, measured over all four lock-up cycles.
- V_{avg} : the average forward velocity, in mph, over the four lock-up cycles.
- V_{nom} : the nominal forward speed intended for the test, mph.
- μ_p : the reduced average μ_p value for all four lock-ups.
- S_p : the average value of the slip at the peak.
- μ_s: the reduced average μ_s value for all four lock-ups.
- **Press** : the inflation pressure, in psi, for the test pair.
- **Surface** : the test surface on which the measurements were performed (PA = asphalt, PS = polished concrete). The description of these two surfaces is given in section 3.
- **Wipe(s)** : the wipe tire designation used for this particular test, as explained in section 3.
- **Config.** : The wipe tire configuration, either dual or single.
- **TDw** : the average tread depth of the wipe tires, in 32^{nds} of an inch.
- **Press. W:** the inflation pressure of the wipe tires, in psi.

Date	Day No	Brand	Name(s)	Tread	Tires	TD	Fzavg(lb)	Vavg(mph)	Vnom	μp	Sp	μs	Press(psi)	Surface	Wipe(s)	Config.	TDw	Press. W
10/6/87	0	Goodyear	G159	Rib	1 - 2	18	2019.03	52.99	53	0.2711	0.2	0.1712	100	PS	RB1	Dual	18	95
10/6/87	0	Goodyear	G159	Rib	1 - 2	18	2022.76	47.97	48	0.3084	0.36	0.193	100	PS	RB1	Dual	18	95
10/6/87	0	Goodyear	G159	Rib	1 - 2	18	2023.35	42.98	43	0.3191	0.12	0.2147	100	PS	RB1	Dual	18	95
10/6/87	0	Goodyear	G159	Rib	1 - 2	18	2020.13	53.11	53	0.8356	0.14	0.4702	100	PA	RB1	Dual	18	95
10/6/87	0	Goodyear	G159	Rib	1 - 2	18	2057.44	48.73	48	0.87	0.12	0.4979	100	PA	RB1	Dual	18	95
10/6/87	0	Goodyear	G159	Rib	1 - 2	18	2064.16	43.13	43	0.7789	0.21	0.4504	100	PA	RB1	Dual	18	95
10/6/87	0	Goodyear	G159	Rib	1 - 2	18	2006.36	53.36	53	0.2384	0.29	0.1576	100	PS	RB1	Single	18	105
10/6/87	0	Goodyear	G159	Rib	1 - 2	18	2011.04	47.57	48	0.2931	0.27	0.1574	100	PS	RB1	Single	18	105
10/6/87	0	Goodyear	G159	Rib	1 - 2	18	2017.92	42.74	43	0.2822	0.35	0.1946	100	PS	RB1	Single	18	105
10/6/87	0	Goodyear	G159	Rib	1 - 2	18	2030.93	53.14	53	0.7418	0.14	0.4052	100	PA	RB1	Single	18	105
10/6/87	0	Goodyear	G159	Rib	1 - 2	18	2045.46	48.05	48	0.7319	0.09	0.447	100	PA	RB1	Single	18	105
10/6/87	0	Goodyear	G159	Rib	1 - 2	18	2056.77	42.97	43	0.7905	0.13	0.4672	100	PA	RB1	Single	18	105
10/6/87	0	Goodyear	G159	Rib	1 - 2	18	2035.31	52.5	53	0.2322	0.16	0.1493	100	PS	RB.5	Dual	14	95
10/6/87	0	Goodyear	G159	Rib	1 - 2	18	2080.08	47.62	48	0.2959	0.25	0.1851	100	PS	RB.5	Dual	14	95
10/6/87	0	Goodyear	G159	Rib	1 - 2	18	2089.19	42.6	43	0.2885	0.44	0.1989	100	PS	RB.5	Dual	14	95
10/6/87	0	Goodyear	G159	Rib	1 - 2	18	2014.28	52.82	53	0.849	0.12	0.4523	100	PA	RB.5	Dual	14	95
10/6/87	0	Goodyear	G159	Rib	1 - 2	18	2015.84	48.84	48	0.7902	0.19	0.4505	100	PA	RB.5	Dual	14	95
10/6/87	0	Goodyear	G159	Rib	1 - 2	18	2042.91	42.78	43	0.8212	0.24	0.4887	100	PA	RB.5	Dual	14	95
10/7/87	1	Goodyear	G159	Rib	1 - 2	18	2017.92	52.91	53	0.2273	0.13	0.1456	100	PS	RB.5	Single	14	105
10/7/87	1	Goodyear	G159	Rib	1 - 2	18	2027.11	47.61	48	0.2492	0.32	0.1578	100	PS	RB.5	Single	14	105
10/7/87	1	Goodyear	G159	Rib	1 - 2	18	2037.56	42.49	43	0.2607	0.21	0.1826	100	PS	RB.5	Single	14	105
10/7/87	1	Goodyear	G159	Rib	1 - 2	18	2034.48	52.42	53	0.7262	0.17	0.354	100	PA	RB.5	Single	14	105
10/7/87	1	Goodyear	G159	Rib	1 - 2	18	2043.39	48.4	48	0.765	0.12	0.4023	100	PA	RB.5	Single	14	105
10/7/87	1	Goodyear	G159	Rib	1 - 2	18	2063.29	42.94	43	0.761	0.18	0.4607	100	PA	RB.5	Single	14	105
10/8/87	2	Goodyear	G159	Rib	9 - 10	10.25	1985.47	51.74	53	0.2697	0.58	0.1581	100	PS	RB.5	Single	14	105
10/8/87	2	Goodyear	G159	Rib	9 - 10	10.25	1990.55	47.47	48	0.2871	0.2	0.1757	100	PS	RB.5	Single	14	105
10/8/87	2	Goodyear	G159	Rib	9 - 10	10.25	2008.94	42.64	43	0.2723	0.44	0.1759	100	PS	RB.5	Single	14	105
10/8/87	2	Goodyear	G159	Rib	9 - 10	10.25	1989.26	51.55	53	0.7937	0.11	0.3964	100	PA	RB.5	Single	14	105
10/8/87	2	Goodyear	G159	Rib	9 - 10	10.25	2021.67	47.91	48	0.7951	0.13	0.4321	100	PA	RB.5	Single	14	105
10/8/87	2	Goodyear	G159	Rib	9 - 10	10.25	2029.35	42.65	43	0.8057	0.14	0.4548	100	PA	RB.5	Single	14	105
10/8/87	2	Goodyear	G159	Rib	9 - 10	10.25	2013.57	52.29	53	0.3134	0.32	0.1748	100	PS	RB.5	Dual	14	95
10/8/87	2	Goodyear	G159	Rib	9 - 10	10.25	2013.45	47.54	48	0.2762	0.5	0.1665	100	PS	RB.5	Dual	14	95
10/8/87	2	Goodyear	G159	Rib	9 - 10	10.25	2020.53	42.56	43	0.29	0.47	0.1908	100	PS	RB.5	Dual	14	95
10/8/87	2	Goodyear	G159	Rib	9 - 10	10.25	2040.04	51.6	53	0.7788	0.11	0.4128	100	PA	RB.5	Dual	14	95
10/8/87	2	Goodyear	G159	Rib	9 - 10	10.25	2028.36	47.57	48	0.7992	0.13	0.4052	100	PA	RB.5	Dual	14	95
10/8/87	2	Goodyear	G159	Rib	9 - 10	10.25	2056.19	42.51	43	0.8136	0.16	0.4481	100	PA	RB.5	Dual	14	95
10/8/87	2	Goodyear	G159	Rib	9 - 10	10.25	2005.44	52.65	53	0.2345	0.21	0.1572	100	PS	RB1	Dual	18	95
10/8/87	2	Goodyear	G159	Rib	9 - 10	10.25	2006.33	47.54	48	0.2436	0.15	0.1555	100	PS	RB1	Dual	18	95
10/8/87	2	Goodyear	G159	Rib	9 - 10	10.25	2021.46	42.44	43	0.2789	0.24	0.175	100	PS	RB1	Dual	18	95
10/8/87	2	Goodyear	G159	Rib	9 - 10	10.25	2024.44	53.33	53	0.7243	0.14	0.414	100	PA	RB1	Dual	18	95

Date	Day No	Brand	Name(s)	Tread	Tires	TD	Fzavg(lb)	Vavg(mph)	Vnom	μp	Sp	μs	Press(psi)	Surface	Wipe(s)	Config.	TDw	Press. W
10/8/87	2	Goodyear	G159	Rib	9 - 10	10.25	2036.68	47.28	48	0.7811	0.19	0.4435	100	PA	RB1	Dual	18	95
10/8/87	2	Goodyear	G159	Rib	9 - 10	10.25	2053.95	42.83	43	0.7551	0.17	0.4545	100	PA	RB1	Dual	18	95
10/8/87	2	Goodyear	G159	Rib	9 - 10	10.25	2006.55	52.18	53	0.1781	0.74	0.1265	100	PS	RB1	Single	18	105
10/8/87	2	Goodyear	G159	Rib	9 - 10	10.25	2017.79	47.15	48	0.2025	0.44	0.1409	100	PS	RB1	Single	18	105
10/8/87	2	Goodyear	G159	Rib	9 - 10	10.25	2026.66	42.3	43	0.2156	0.16	0.1508	100	PS	RB1	Single	18	105
10/8/87	2	Goodyear	G159	Rib	9 - 10	10.25	2035.67	51.22	53	0.7495	0.12	0.353	100	PA	RB1	Single	18	105
10/8/87	2	Goodyear	G159	Rib	9 - 10	10.25	2042.83	47.14	48	0.7189	0.14	0.368	100	PA	RB1	Single	18	105
10/8/87	2	Goodyear	G159	Rib	9 - 10	10.25	2064.8	42.32	43	0.7655	0.13	0.4293	100	PA	RB1	Single	18	105
10/8/87	2	Goodyear	G159	Rib	7 - 8	8	1984.74	52.14	53	0.205	0.17	0.1452	100	PS	RB1	Single	18	105
10/8/87	2	Goodyear	G159	Rib	7 - 8	8	1984.96	47.22	48	0.2146	0.23	0.127	100	PS	RB1	Single	18	105
10/8/87	2	Goodyear	G159	Rib	7 - 8	8	1982.52	42.47	43	0.2421	0.27	0.1585	100	PS	RB1	Single	18	105
10/8/87	2	Goodyear	G159	Rib	7 - 8	8	2014.03	52.15	53	0.723	0.13	0.3407	100	PA	RB1	Single	18	105
10/8/87	2	Goodyear	G159	Rib	7 - 8	8	2001.67	46.95	48	0.7194	0.21	0.3674	100	PA	RB1	Single	18	105
10/8/87	2	Goodyear	G159	Rib	7 - 8	8	2010.78	42.19	43	0.7906	0.15	0.4276	100	PA	RB1	Single	18	105
10/8/87	2	Goodyear	G159	Rib	7 - 8	8	1983.52	52.69	53	0.2132	0.39	0.1358	100	PS	RB1	Dual	18	95
10/8/87	2	Goodyear	G159	Rib	7 - 8	8	1982.44	47.97	48	0.2397	0.47	0.1485	100	PS	RB1	Dual	18	95
10/8/87	2	Goodyear	G159	Rib	7 - 8	8	1983.01	42.93	43	0.2603	0.22	0.1604	100	PS	RB1	Dual	18	95
10/8/87	2	Goodyear	G159	Rib	7 - 8	8	1989.8	52.44	53	0.7196	0.19	0.3752	100	PA	RB1	Dual	18	95
10/8/87	2	Goodyear	G159	Rib	7 - 8	8	2002.09	48.06	48	0.7342	0.07	0.3687	100	PA	RB1	Dual	18	95
10/8/87	2	Goodyear	G159	Rib	7 - 8	8	1998.79	43.6	43	0.7603	0.12	0.4126	100	PA	RB1	Dual	18	95
10/8/87	2	Goodyear	G159	Rib	7 - 8	8	1995.49	52.53	53	0.1794	0.61	0.1165	100	PS	RB.5	Dual	14	95
10/8/87	2	Goodyear	G159	Rib	7 - 8	8	1989.6	47.78	48	0.1912	0.46	0.1301	100	PS	RB.5	Dual	14	95
10/8/87	2	Goodyear	G159	Rib	7 - 8	8	1979.85	42.86	43	0.2286	0.49	0.152	100	PS	RB.5	Dual	14	95
10/8/87	2	Goodyear	G159	Rib	7 - 8	8	2007.19	52.44	53	0.7114	0.13	0.3523	100	PA	RB.5	Dual	14	95
10/8/87	2	Goodyear	G159	Rib	7 - 8	8	1999.3	47.61	48	0.7305	0.18	0.3878	100	PA	RB.5	Dual	14	95
10/8/87	2	Goodyear	G159	Rib	7 - 8	8	2003.77	43.1	43	0.702	0.25	0.4349	100	PA	RB.5	Dual	14	95
10/9/87	3	Goodyear	G159	Rib	7 - 8	8	1991.02	52.51	53	0.1795	0.36	0.1039	100	PS	RB.5	Single	14	105
10/9/87	3	Goodyear	G159	Rib	7 - 8	8	1985.32	47.69	48	0.2039	0.49	0.1339	100	PS	RB.5	Single	14	105
10/9/87	3	Goodyear	G159	Rib	7 - 8	8	1998.11	42.61	43	0.2325	0.49	0.138	100	PS	RB.5	Single	14	105
10/9/87	3	Goodyear	G159	Rib	7 - 8	8	1991.42	52.02	53	0.5322	0.14	0.317	100	PA	RB.5	Single	14	105
10/9/87	3	Goodyear	G159	Rib	7 - 8	8	1988.16	47.97	48	0.5074	0.12	0.3023	100	PA	RB.5	Single	14	105
10/9/87	3	Goodyear	G159	Rib	7 - 8	8	2000.46	42.83	43	0.5766	0.24	0.3582	100	PA	RB.5	Single	14	105
10/9/87	3	Michelin	Pilot XDA	Lug	11 - 12	24	2031.69	52.33	53	0.3304	0.83	0.293	100	PS	RB.5	Single	14	105
10/9/87	3	Michelin	Pilot XDA	Lug	11 - 12	24	2029.31	47.4	48	0.356	0.62	0.3134	100	PS	RB.5	Single	14	105
10/9/87	3	Michelin	Pilot XDA	Lug	11 - 12	24	2036.74	42.93	43	0.3622	0.61	0.3249	100	PS	RB.5	Single	14	105
10/9/87	3	Michelin	Pilot XDA	Lug	11 - 12	24	2065.41	52.51	53	0.6783	0.19	0.4816	100	PA	RB.5	Single	14	105
10/9/87	3	Michelin	Pilot XDA	Lug	11 - 12	24	2045.58	47.07	48	0.7671	0.21	0.5109	100	PA	RB.5	Single	14	105
10/9/87	3	Michelin	Pilot XDA	Lug	11 - 12	24	2068.68	43.64	43	0.6651	0.17	0.4971	100	PA	RB.5	Single	14	105
10/9/87	3	Michelin	Pilot XDA	Lug	11 - 12	24	2036.98	52.57	53	0.3185	0.54	0.2373	100	PS	RB.5	Dual	14	95
10/9/87	3	Michelin	Pilot XDA	Lug	11 - 12	24	2038.3	48	48	0.3422	0.49	0.2519	100	PS	RB.5	Dual	14	95

Date	Day No	Brand	Name(s)	Tread	Tires	TD	Fzavg(lb)	Vavg(mph)	Vnom	μp	Sp	μs	Press(psi)	Surface	Wipe(s)	Config.	TDw	Press. W
10/9/87	3	Michelin	Pilot XDA	Lug	11 - 12	24	2036.74	43.19	43	0.3767	0.61	0.3074	100	PS	RB.5	Dual	14	95
10/9/87	3	Michelin	Pilot XDA	Lug	11 - 12	24	2032.55	52.08	53	0.6917	0.29	0.4804	100	PA	RB.5	Dual	14	95
10/9/87	3	Michelin	Pilot XDA	Lug	11 - 12	24	2042.7	47.97	48	0.7312	0.27	0.4921	100	PA	RB.5	Dual	14	95
10/9/87	3	Michelin	Pilot XDA	Lug	11 - 12	24	2059.2	42.62	43	0.7326	0.28	0.4978	100	PA	RB.5	Dual	14	95
10/9/87	3	Michelin	Pilot XDA	Lug	11 - 12	24	2034.69	53.46	53	0.3255	0.65	0.2415	100	PS	RB1	Dual	18	95
10/9/87	3	Michelin	Pilot XDA	Lug	11 - 12	24	2033.24	48.04	48	0.3473	0.45	0.2711	100	PS	RB1	Dual	18	95
10/9/87	3	Michelin	Pilot XDA	Lug	11 - 12	24	2031.38	43.1	43	0.3628	0.56	0.2828	100	PS	RB1	Dual	18	95
10/9/87	3	Michelin	Pilot XDA	Lug	11 - 12	24	2057.53	51.84	53	0.7385	0.29	0.4766	100	PA	RB1	Dual	18	95
10/9/87	3	Michelin	Pilot XDA	Lug	11 - 12	24	2060.46	47.75	48	0.7476	0.19	0.4594	100	PA	RB1	Dual	18	95
10/9/87	3	Michelin	Pilot XDA	Lug	11 - 12	24	2071.2	42.9	43	0.7399	0.22	0.487	100	PA	RB1	Dual	18	95
10/12/87	4	Michelin	Pilot XDA	Lug	11 - 12	24	2019.41	53.15	53	0.2946	0.65	0.2129	100	PS	RB1	Single	18	105
10/12/87	4	Michelin	Pilot XDA	Lug	11 - 12	24	2023.46	47.49	48	0.3104	0.35	0.2255	100	PS	RB1	Single	18	105
10/12/87	4	Michelin	Pilot XDA	Lug	11 - 12	24	2032.54	43.01	43	0.3318	0.6	0.2366	100	PS	RB1	Single	18	105
10/12/87	4	Michelin	Pilot XDA	Lug	11 - 12	24	2028.44	52.63	53	0.7493	0.15	0.4291	100	PA	RB1	Single	18	105
10/12/87	4	Michelin	Pilot XDA	Lug	11 - 12	24	2044.22	48.43	48	0.7383	0.23	0.4138	100	PA	RB1	Single	18	105
10/12/87	4	Michelin	Pilot XDA	Lug	11 - 12	24	2067.76	43.36	43	0.7059	0.27	0.4675	100	PA	RB1	Single	18	105
10/12/87	4	Michelin	Pilot XDA	Lug	15 - 16	2.05	1980.69	52.99	53	0.1102	0.61	0.0756	100	PS	RB1	Single	18	105
10/12/87	4	Michelin	Pilot XDA	Lug	15 - 16	2.05	1981.85	47.49	48	0.1254	0.48	0.0925	100	PS	RB1	Single	18	105
10/12/87	4	Michelin	Pilot XDA	Lug	15 - 16	2.05	1978.5	42.99	43	0.1433	0.45	0.0987	100	PS	RB1	Single	18	105
10/12/87	4	Michelin	Pilot XDA	Lug	15 - 16	2.05	2000.51	52.28	53	0.5294	0.07	0.2331	100	PA	RB1	Single	18	105
10/12/87	4	Michelin	Pilot XDA	Lug	15 - 16	2.05	2007.3	47.45	48	0.5742	0.05	0.3303	100	PA	RB1	Single	18	105
10/12/87	4	Michelin	Pilot XDA	Lug	15 - 16	2.05	2014.13	43.69	43	0.5821	0.12	0.3173	100	PA	RB1	Single	18	105
10/12/87	4	Michelin	Pilot XDA	Lug	15 - 16	2.05	1978.97	52.31	53	0.122	0.57	0.0868	100	PS	RB1	Dual	18	95
10/12/87	4	Michelin	Pilot XDA	Lug	15 - 16	2.05	1981.86	47.02	48	0.1279	0.52	0.0955	100	PS	RB1	Dual	18	95
10/12/87	4	Michelin	Pilot XDA	Lug	15 - 16	2.05	1985.26	42.82	43	0.1483	0.62	0.1137	100	PS	RB1	Dual	18	95
10/12/87	4	Michelin	Pilot XDA	Lug	15 - 16	2.05	1999.33	52.48	53	0.5418	0.12	0.3042	100	PA	RB1	Dual	18	95
10/12/87	4	Michelin	Pilot XDA	Lug	15 - 16	2.05	2010.52	47.31	48	0.5741	0.19	0.2981	100	PA	RB1	Dual	18	95
10/12/87	4	Michelin	Pilot XDA	Lug	15 - 16	2.05	2016.63	42.84	43	0.6246	0.16	0.3771	100	PA	RB1	Dual	18	95
10/12/87	4	Michelin	Pilot XDA	Lug	15 - 16	2.05	1980.79	52.11	53	0.1037	0.45	0.0754	100	PS	RB.5	Dual	14	95
10/12/87	4	Michelin	Pilot XDA	Lug	15 - 16	2.05	1983.16	46.98	48	0.1211	0.59	0.0866	100	PS	RB.5	Dual	14	95
10/12/87	4	Michelin	Pilot XDA	Lug	15 - 16	2.05	1985.34	42.51	43	0.1447	0.48	0.0877	100	PS	RB.5	Dual	14	95
10/12/87	4	Michelin	Pilot XDA	Lug	15 - 16	2.05	1990.46	52.95	53	0.6572	0.12	0.3475	100	PA	RB.5	Dual	14	95
10/12/87	4	Michelin	Pilot XDA	Lug	15 - 16	2.05	2010.99	48.2	48	0.5887	0.27	0.313	100	PA	RB.5	Dual	14	95
10/12/87	4	Michelin	Pilot XDA	Lug	15 - 16	2.05	2014.37	43.48	43	0.6653	0.16	0.3682	100	PA	RB.5	Dual	14	95
10/12/87	4	Michelin	Pilot XDA	Lug	15 - 16	2.05	1980.12	53.42	53	0.094	0.65	0.0614	100	PS	RB.5	Single	14	105
10/12/87	4	Michelin	Pilot XDA	Lug	15 - 16	2.05	1986.77	48.27	48	0.104	0.7	0.0801	100	PS	RB.5	Single	14	105
10/12/87	4	Michelin	Pilot XDA	Lug	15 - 16	2.05	1986.15	43.8	43	0.1356	0.54	0.0901	100	PS	RB.5	Single	14	105
10/12/87	4	Michelin	Pilot XDA	Lug	15 - 16	2.05	2015.8	53.33	53	0.4917	0.14	0.2592	100	PA	RB.5	Single	14	105
10/12/87	4	Michelin	Pilot XDA	Lug	15 - 16	2.05	2017.49	48.67	48	0.5831	0.17	0.3217	100	PA	RB.5	Single	14	105
10/12/87	4	Michelin	Pilot XDA	Lug	15 - 16	2.05	2024.73	43.26	43	0.6159	0.11	0.3356	100	PA	RB.5	Single	14	105

Date	Day No	Brand	Name(s)	Tread	Tires	TD	Fzavg(lb)	Vavg(mph)	Vnom	μp	Sp	μs	Press(psi)	Surface	Wipe(s)	Config.	TDw	Press. W
10/12/87	4	Michelin	Pilot XDA	Lug	13 - 14	16	2004.75	52.49	53	0.2767	0.51	0.1967	100	PS	RB.5	Single	14	105
10/12/87	4	Michelin	Pilot XDA	Lug	13 - 14	16	2016.03	47.78	48	0.3054	0.67	0.2227	100	PS	RB.5	Single	14	105
10/12/87	4	Michelin	Pilot XDA	Lug	13 - 14	16	2022.18	43.19	43	0.3105	0.49	0.2274	100	PS	RB.5	Single	14	105
10/12/87	4	Michelin	Pilot XDA	Lug	13 - 14	16	1989	54.01	53	0.6306	0.2	0.3832	100	PA	RB.5	Single	14	105
10/12/87	4	Michelin	Pilot XDA	Lug	13 - 14	16	1998.3	49.24	48	0.7126	0.16	0.4162	100	PA	RB.5	Single	14	105
10/12/87	4	Michelin	Pilot XDA	Lug	13 - 14	16	2007.41	43.83	43	0.7315	0.2	0.4304	100	PA	RB.5	Single	14	105
10/28/87	5	Michelin	Pilot XDA	Lug	13 - 14	16	2000.73	51.54	53	0.27	0.56	0.2057	100	PS	RB.5	Dual	14	95
10/28/87	5	Michelin	Pilot XDA	Lug	13 - 14	16	1997.28	47.42	48	0.2889	0.58	0.1843	100	PS	RB.5	Dual	14	95
10/28/87	5	Michelin	Pilot XDA	Lug	13 - 14	16	2007.3	42.2	43	0.329	0.54	0.2203	100	PS	RB.5	Dual	14	95
10/28/87	5	Michelin	Pilot XDA	Lug	13 - 14	16	2005.41	52.08	53	0.6476	0.18	0.3899	100	PA	RB.5	Dual	14	95
10/28/87	5	Michelin	Pilot XDA	Lug	13 - 14	16	2008.29	47.19	48	0.6812	0.17	0.3832	100	PA	RB.5	Dual	14	95
10/28/87	5	Michelin	Pilot XDA	Lug	13 - 14	16	2033.56	42.37	43	0.7029	0.19	0.4277	100	PA	RB.5	Dual	14	95
10/28/87	5	Michelin	Pilot XDA	Lug	13 - 14	16	1997.72	52.12	53	0.2779	0.62	0.1693	100	PS	RB1	Dual	18	95
10/28/87	5	Michelin	Pilot XDA	Lug	13 - 14	16	2001.21	47.14	48	0.2761	0.48	0.2223	100	PS	RB1	Dual	18	95
10/28/87	5	Michelin	Pilot XDA	Lug	13 - 14	16	2014.46	42.33	43	0.2977	0.54	0.2059	100	PS	RB1	Dual	18	95
10/28/87	5	Michelin	Pilot XDA	Lug	13 - 14	16	2018.46	52.46	53	0.6919	0.17	0.4107	100	PA	RB1	Dual	18	95
10/28/87	5	Michelin	Pilot XDA	Lug	13 - 14	16	2023.06	47.5	48	0.637	0.21	0.402	100	PA	RB1	Dual	18	95
10/28/87	5	Michelin	Pilot XDA	Lug	13 - 14	16	2033.62	42.47	43	0.677	0.21	0.4282	100	PA	RB1	Dual	18	95
10/28/87	5	Michelin	Pilot XDA	Lug	13 - 14	16	1997.42	52.13	53	0.2158	0.65	0.1533	100	PS	RB1	Single	18	105
10/28/87	5	Michelin	Pilot XDA	Lug	13 - 14	16	2010.4	47.26	48	0.2491	0.58	0.1542	100	PS	RB1	Single	18	105
10/28/87	5	Michelin	Pilot XDA	Lug	13 - 14	16	2018.88	42.22	43	0.2706	0.52	0.194	100	PS	RB1	Single	18	105
10/28/87	5	Michelin	Pilot XDA	Lug	13 - 14	16	2025.79	51.93	53	0.5135	0.35	0.3397	100	PA	RB1	Single	18	105
10/28/87	5	Michelin	Pilot XDA	Lug	13 - 14	16	2024.43	46.62	48	0.5407	0.37	0.3541	100	PA	RB1	Single	18	105
10/28/87	5	Michelin	Pilot XDA	Lug	13 - 14	16	2041.68	42.84	43	0.5469	0.17	0.3709	100	PA	RB1	Single	18	105

Worn Tires Study

Date	Day No	Brand	Name(s)	Tread	Tires	TD	Fzavg(lb)	Vavg(mph)	Vnom	μp	Sp	μs	Press(psi)	Surface	Wipe(s)	Config	TDw	Press. W
10/30/87	6	Goodyear	G159	Rib	27 - 31	5.5	2012.07	53.07	53	0.2057	0.43	0.095	50	PS	RB.5	Single	14	105
10/30/87	6	Goodyear	G159	Rib	27 - 31	5.5	2017.61	52.2	53	0.1736	0.57	0.1022	60	PS	RB.5	Single	14	105
10/30/87	6	Goodyear	G159	Rib	27 - 31	5.5	1994.02	52.19	53	0.1786	0.31	0.1033	70	PS	RB.5	Single	14	105
10/30/87	6	Goodyear	G159	Rib	27 - 31	5.5	1994.83	52.38	53	0.1706	0.47	0.0969	80	PS	RB.5	Single	14	105
11/2/87	7	Goodyear	G159	Rib	18 - 30	11.55	2030.83	51.47	53	0.1225	0.54	0.0815	80	PS	RB.5	Single	14	105
11/4/87	9	Goodyear	G167	Lug	40 - 55	7.85	2025.23	52.4	53	0.272	0.53	0.1888	80	PS	RB.5	Single	14	105
11/24/87	10	Goodyear	G167	Lug	48 - 53	2.45	2012.04	52.35	53	0.1429	0.58	0.1074	80	PS	RB.5	Single	14	105
10/30/87	6	Goodyear	G159	Rib	27 - 31	5.5	2008.67	52.08	53	0.167	0.34	0.095	85	PS	RB.5	Single	14	105
11/2/87	7	Goodyear	G159	Rib	18 - 30	11.55	2025.44	51.63	53	0.1234	0.61	0.0744	85	PS	RB.5	Single	14	105
11/4/87	9	Goodyear	G167	Lug	40 - 55	7.85	2027.54	52.87	53	0.2605	0.3	0.1799	85	PS	RB.5	Single	14	105
11/24/87	10	Goodyear	G167	Lug	48 - 53	2.45	2006.58	52.11	53	0.1596	0.81	0.1132	85	PS	RB.5	Single	14	105
10/30/87	6	Goodyear	G159	Rib	27 - 31	5.5	1998.93	51.89	53	0.1557	0.62	0.1041	90	PS	RB.5	Single	14	105
11/2/87	7	Goodyear	G159	Rib	18 - 30	11.55	2028.43	50.93	53	0.132	0.61	0.0814	90	PS	RB.5	Single	14	105
11/4/87	9	Goodyear	G167	Lug	40 - 55	7.85	2032.3	52.48	53	0.2515	0.23	0.1723	90	PS	RB.5	Single	14	105
11/24/87	10	Goodyear	G167	Lug	48 - 53	2.45	2005.71	52.1	53	0.1601	0.68	0.1211	90	PS	RB.5	Single	14	105
10/30/87	6	Goodyear	G159	Rib	27 - 31	5.5	1994.58	52.29	53	0.1637	0.21	0.1145	95	PS	RB.5	Single	14	105
11/2/87	7	Goodyear	G159	Rib	18 - 30	11.55	2020.77	51.58	53	0.1035	0.57	0.0604	95	PS	RB.5	Single	14	105
11/4/87	9	Goodyear	G167	Lug	40 - 55	7.85	2027.5	51.76	53	0.2787	0.5	0.19	95	PS	RB.5	Single	14	105
11/24/87	10	Goodyear	G167	Lug	48 - 53	2.45	2004.75	51.72	53	0.1792	0.5	0.1314	95	PS	RB.5	Single	14	105
11/24/87	10	Goodyear	G167	Lug	53 - 48	2.45	1980.22	52.29	53	0.1736	0.27	0.1125	100	PS	RB.5	Single	14	105
11/24/87	10	Goodyear	G167	Lug	48 - 53	2.45	2000.85	51.93	53	0.1684	0.64	0.1285	100	PS	RB.5	Single	14	105
11/4/87	9	Goodyear	G167	Lug	51 - 43	3.15	2001.79	52.53	53	0.2034	0.68	0.1487	100	PS	RB.5	Single	14	105
11/4/87	9	Goodyear	G167	Lug	43 - 51	3.15	2011.78	52.66	53	0.193	0.29	0.1154	100	PS	RB.5	Single	14	105
11/4/87	9	Goodyear	G167	Lug	52 - 50	3.5	2015.56	52.82	53	0.2176	0.17	0.1422	100	PS	RB.5	Single	14	105
11/4/87	9	Goodyear	G167	Lug	50 - 52	3.5	2008.56	52.53	53	0.2242	0.24	0.1473	100	PS	RB.5	Single	14	105
11/4/87	9	Goodyear	G167	Lug	44 - 38	3.75	2009.98	52.2	53	0.2424	0.43	0.1669	100	PS	RB.5	Single	14	105
11/4/87	9	Goodyear	G167	Lug	38 - 44	3.75	2024.67	52.12	53	0.1849	0.58	0.1415	100	PS	RB.5	Single	14	105
11/3/87	8	Goodyear	G167	Lug	39 - 54	4.2	2020.36	51.71	53	0.223	0.64	0.1561	100	PS	RB.5	Single	14	105
11/3/87	8	Goodyear	G167	Lug	54 - 39	4.2	2037.69	51.78	53	0.2141	0.44	0.1414	100	PS	RB.5	Single	14	105
11/3/87	8	Goodyear	G167	Lug	46 - 45	4.5	2008.21	51.59	53	0.2836	0.56	0.2106	100	PS	RB.5	Single	14	105
11/3/87	8	Goodyear	G167	Lug	45 - 46	4.5	2021.02	51.77	53	0.2459	0.46	0.1883	100	PS	RB.5	Single	14	105
11/3/87	8	Goodyear	G167	Lug	45 - 42	4.65	2014.91	52.34	53	0.2613	0.61	0.1731	100	PS	RB.5	Single	14	105
11/3/87	8	Goodyear	G167	Lug	42 - 45	4.65	2022.18	52.47	53	0.1992	0.69	0.1528	100	PS	RB.5	Single	14	105
11/3/87	8	Goodyear	G167	Lug	56 - 47	5.1	2017.63	53.03	53	0.2432	0.52	0.1632	100	PS	RB.5	Single	14	105
11/3/87	8	Goodyear	G167	Lug	47 - 56	5.1	2023.11	52.33	53	0.1797	0.84	0.1604	100	PS	RB.5	Single	14	105
11/3/87	8	Goodyear	G167	Lug	49 - 41	5.2	2029.73	52.6	53	0.1852	0.16	0.1258	100	PS	RB.5	Single	14	105
11/3/87	8	Goodyear	G167	Lug	41 - 49	5.2	2036.96	51.98	53	0.1965	0.61	0.1615	100	PS	RB.5	Single	14	105
11/4/87	9	Goodyear	G167	Lug	37 - 55	7.25	2009.1	52.67	53	0.2322	0.18	0.1579	100	PS	RB.5	Single	14	105
11/4/87	9	Goodyear	G167	Lug	55 - 37	7.25	2021.58	52.53	53	0.2715	0.55	0.196	100	PS	RB.5	Single	14	105
11/4/87	9	Goodyear	G167	Lug	55 - 40	7.85	2019.43	52.64	53	0.2721	0.61	0.184	100	PS	RB.5	Single	14	105
11/4/87	9	Goodyear	G167	Lug	40 - 55	7.85	2038.51	52.83	53	0.2624	0.47	0.1702	100	PS	RB.5	Single	14	105
10/30/87	6	Goodyear	G159	Rib	31 - 27	5.5	1975.42	51.98	53	0.2007	0.4	0.1108	100	PS	RB.5	Single	14	105
10/30/87	6	Goodyear	G159	Rib	27 - 31	5.5	1983.78	52.64	53	0.1555	0.64	0.0984	100	PS	RB.5	Single	14	105
10/30/87	6	Goodyear	G159	Rib	17 - 34	6.45	2010.96	52.61	53	0.177	0.48	0.0739	100	PS	RB.5	Single	14	105

Worn Tires Study

Date	Day No	Brand	Name(s)	Tread	Tires	TD	Fzavg(lb)	Vavg(mph)	Vnom	μp	Sp	μs	Press(psi)	Surface	Wipe(s)	Config	TDw	Press. W
10/30/87	6	Goodyear	G159	Rib	34 - 17	6.45	2026.22	52.61	53	0.2272	0.1	0.1129	100	PS	RB.5	Single	14	105
10/30/87	6	Goodyear	G159	Rib	23 - 21	7.59	2008.14	52.77	53	0.2058	0.2	0.0919	100	PS	RB.5	Single	14	105
10/30/87	6	Goodyear	G159	Rib	21 - 23	7.59	2012.93	52.81	53	0.1953	0.5	0.1132	100	PS	RB.5	Single	14	105
10/9/87	3	Goodyear	G159	Rib	7 - 8	8	1991.02	52.51	53	0.1795	0.36	0.1039	100	PS	RB.5	Single	14	105
11/2/87	7	Goodyear	G159	Rib	24 - 26	8.15	1993.05	51.77	53	0.1762	0.36	0.0944	100	PS	RB.5	Single	14	105
11/2/87	7	Goodyear	G159	Rib	26 - 24	8.15	2005.89	51.82	53	0.1929	0.31	0.119	100	PS	RB.5	Single	14	105
11/2/87	7	Goodyear	G159	Rib	35 - 20	8.6	2023.01	52.73	53	0.1652	0.6	0.1142	100	PS	RB.5	Single	14	105
11/2/87	7	Goodyear	G159	Rib	20 - 35	8.6	2030.22	53.07	53	0.2233	0.13	0.1099	100	PS	RB.5	Single	14	105
11/2/87	7	Goodyear	G159	Rib	29 - 32	8.85	2015.14	53.12	53	0.2049	0.5	0.1368	100	PS	RB.5	Single	14	105
11/2/87	7	Goodyear	G159	Rib	32 - 29	8.85	2031.31	52.68	53	0.2216	0.17	0.1077	100	PS	RB.5	Single	14	105
11/2/87	7	Goodyear	G159	Rib	32 - 33	8.9	2032.88	52.56	53	0.2434	0.12	0.1271	100	PS	RB.5	Single	14	105
11/2/87	7	Goodyear	G159	Rib	33 - 32	8.9	2032.27	52.26	53	0.2313	0.25	0.1437	100	PS	RB.5	Single	14	105
11/2/87	7	Goodyear	G159	Rib	36 - 19	9.3	2014.95	50.5	53	0.1642	0.23	0.1103	100	PS	RB.5	Single	14	105
11/2/87	7	Goodyear	G159	Rib	19 - 36	9.3	2019.48	52.45	53	0.161	0.46	0.126	100	PS	RB.5	Single	14	105
10/8/87	2	Goodyear	G159	Rib	9 - 10	10.25	1985.47	51.74	53	0.2697	0.58	0.1581	100	PS	RB.5	Single	14	105
11/2/87	7	Goodyear	G159	Rib	25 - 28	10.25	2028.44	52.28	53	0.1521	0.6	0.0939	100	PS	RB.5	Single	14	105
11/2/87	7	Goodyear	G159	Rib	28 - 25	10.25	2042.03	52.19	53	0.164	0.23	0.1007	100	PS	RB.5	Single	14	105
11/2/87	7	Goodyear	G159	Rib	28 - 22	10.5	2023.6	52.06	53	0.1601	0.33	0.0913	100	PS	RB.5	Single	14	105
11/2/87	7	Goodyear	G159	Rib	22 - 28	10.5	2034.02	51.78	53	0.1555	0.7	0.0944	100	PS	RB.5	Single	14	105
11/2/87	7	Goodyear	G159	Rib	30 - 18	11.55	2020.04	52.23	53	0.1464	0.61	0.1017	100	PS	RB.5	Single	14	105
11/2/87	7	Goodyear	G159	Rib	18 - 30	11.55	2033.26	51.51	53	0.114	0.57	0.0666	100	PS	RB.5	Single	14	105
10/7/87	1	Goodyear	G159	Rib	1 - 2	18	2017.92	52.91	53	0.2273	0.13	0.1456	100	PS	RB.5	Single	14	105
9/9/88	13	Michelin	Pilot(e) XDA,XDHT	Lug	108 - 83	1.43	2003.22	52.76	53	0.0528	0.96	0.0455	80	PS	RB.5	Single	14	105
9/9/88	13	Michelin	Pilot(e) XDHT,XDA	Lug	83 - 108	1.43	2001.11	52.08	53	0.1048	0.53	0.075	100	PS	RB.5	Single	14	105
9/9/88	13	Michelin	Pilot(e) XDA,XDHT	Lug	108 - 83	1.43	2001.01	52.24	53	0.0429	0.78	0.028	100	PS	RB.5	Single	14	105
10/12/87	4	Michelin	Pilot XDA	Lug	15 - 16	2.05	1980.12	51.72	53	0.094	0.65	0.0614	100	PS	RB.5	Single	14	105
9/8/88	12	Michelin	Pilot(e) XDA,XDHT	Lug	118 - 84	2.12	1992.82	52.25	53	0.1418	0.39	0.0833	100	PS	RB.5	Single	14	105
9/8/88	12	Michelin	Pilot(e) XDHT,XDA	Lug	84 - 118	2.12	1979.78	51.85	53	0.1409	0.51	0.1041	100	PS	RB.5	Single	14	105
9/8/88	12	Michelin	Pilot XDHT,XDA	Lug	61 - 93	2.97	2000.91	52.6	53	0.1317	0.44	0.1159	100	PS	RB.5	Single	14	105
9/8/88	12	Michelin	Pilot XDA,XDHT	Lug	93 - 61	2.97	1990.17	52.81	53	0.1293	0.61	0.1138	100	PS	RB.5	Single	14	105
9/8/88	12	Michelin	Pilot(e) XDHT,XDA	Lug	62 - 85	3.88	1996.39	52.93	53	0.1399	0.14	0.1054	100	PS	RB.5	Single	14	105
9/8/88	12	Michelin	Pilot(e) XDA,XDHT	Lug	85 - 62	3.88	1999.24	52.91	53	0.1165	0.74	0.0942	100	PS	RB.5	Single	14	105
9/9/88	13	Michelin	Pilot XDA	Lug	100 - 110	4.4	2012.75	52.33	53	0.1327	0.8	0.1037	100	PS	RB.5	Single	14	105
9/9/88	13	Michelin	Pilot XDA	Lug	110 - 100	4.4	2011.92	52.64	53	0.1454	0.5	0.1122	100	PS	RB.5	Single	14	105
9/9/88	13	Michelin	Pilot XDA	Lug	90 -109	4.61	1988.14	52.31	53	0.1208	0.9	0.1037	100	PS	RB.5	Single	14	105
9/9/88	13	Michelin	Pilot XDA	Lug	109 - 90	4.61	2007.37	51.99	53	0.1075	0.94	0.0948	100	PS	RB.5	Single	14	105
9/9/88	13	Michelin	Pilot XDHT,XDA	Lug	97 - 113	4.8	2012.49	52.12	53	0.179	0.9	0.1502	100	PS	RB.5	Single	14	105
9/9/88	13	Michelin	Pilot XDA,XDHT	Lug	113 - 97	4.8	1970.83	52.88	53	0.1252	0.66	0.1022	100	PS	RB.5	Single	14	105
9/8/88	12	Michelin	Pilot XDA	Lug	86 - 98	5.08	1996.27	52.24	53	0.1112	0.62	0.0928	100	PS	RB.5	Single	14	105
9/8/88	12	Michelin	Pilot XDA	Lug	98 - 86	5.08	1995.3	52.28	53	0.0914	0.74	0.0813	100	PS	RB.5	Single	14	105
11/24/87	10	Michelin	Pilot X	Lug	59 - 60	5.1	1965.91	52.03	53	0.1362	0.76	0.0814	100	PS	RB.5	Single	14	105
11/24/87	10	Michelin	Pilot X	Lug	60 - 59	5.1	1982.88	52.54	53	0.1499	0.7	0.0853	100	PS	RB.5	Single	14	105
9/8/88	12	Michelin	Pilot XDA	Lug	98 - 89	5.19	1996.39	52.48	53	0.0936	0.9	0.0868	100	PS	RB.5	Single	14	105
9/8/88	12	Michelin	Pilot XDA	Lug	89 - 98	5.19	2000.07	52.55	53	0.1051	0.7	0.0828	100	PS	RB.5	Single	14	105

Date	Day No	Brand	Name(s)	Tread	Tires	TD	Fzavg(lb)	Vavg(mph)	Vnom	μp	Sp	μs	Press(psi)	Surface	Wipe(s)	Config	TDw	Press. W
9/9/88	13	Michelin	Pilot(e) XDA	Lug	91 - 112	5.69	2014.67	52.54	53	0.1069	0.72	0.0985	100	PS	RB.5	Single	14	105
9/9/88	13	Michelin	Pilot(e) XDA	Lug	112 - 91	5.69	2023.89	52.8	53	0.1383	0.6	0.1199	100	PS	RB.5	Single	14	105
11/24/87	10	Michelin	Pilot(e) X	Lug	57 - 58	5.99	1967.98	52.96	53	0.1448	0.74	0.0948	100	PS	RB.5	Single	14	105
11/24/87	10	Michelin	Pilot(e) X	Lug	58 - 57	5.99	1998.99	53.14	53	0.1164	0.88	0.088	100	PS	RB.5	Single	14	105
9/12/88	14	Michelin	Pilot XDA	Lug	88 - 96	6.4	2012.12	51.99	53	0.1146	0.85	0.104	100	PS	RB.5	Single	14	105
9/12/88	14	Michelin	Pilot XDA	Lug	96 - 88	6.4	1979.59	52.29	53	0.1438	0.82	0.1217	100	PS	RB.5	Single	14	105
9/12/88	14	Michelin	Pilot XDA,XZA-1	Lug	94 - 115	6.83	2023.96	52.02	53	0.1545	0.7	0.1295	100	PS	RB.5	Single	14	105
9/12/88	14	Michelin	Pilot XZA-1,XDA	Lug	115 - 94	6.83	2014.51	52.14	53	0.1514	0.68	0.1273	100	PS	RB.5	Single	14	105
9/12/88	14	Michelin	Pilot XDA	Lug	92 - 95	7.29	2223.04	51.81	53	0.1022	0.51	0.0824	100	PS	RB.5	Single	14	105
9/12/88	14	Michelin	Pilot XDA	Lug	95 - 92	7.29	2013.03	51.9	53	0.1238	0.56	0.099	100	PS	RB.5	Single	14	105
9/12/88	14	Michelin	Pilot(e) XDA	Lug	99 - 116	8.97	2092.45	52.43	53	0.1596	0.7	0.1338	100	PS	RB.5	Single	14	105
9/12/88	14	Michelin	Pilot XDA	Lug	116 - 99	8.97	1834.25	52.31	53	0.0985	0.58	0.0944	100	PS	RB.5	Single	14	105
9/12/88	14	Michelin	Pilot XDA	Lug	111 - 117	9.34	2013.99	52.42	53	0.0987	0.86	0.0875	100	PS	RB.5	Single	14	105
9/12/88	14	Michelin	Pilot XDA	Lug	117 - 111	9.34	2065.5	52.54	53	0.0983	0.75	0.0894	100	PS	RB.5	Single	14	105
9/12/88	14	Michelin	Pilot XDA	Lug	87 - 114	9.96	2040.29	52.25	53	0.13	0.73	0.1011	100	PS	RB.5	Single	14	105
9/12/88	14	Michelin	Pilot XDA	Lug	114 - 87	9.96	2034.17	51.97	53	0.1592	0.61	0.1258	100	PS	RB.5	Single	14	105
10/12/87	4	Michelin	Pilot XDA	Lug	13 - 14	16	2004.75	52.49	53	0.2767	0.51	0.1967	100	PS	RB.5	Single	14	105
10/9/87	3	Michelin	Pilot XDA	Lug	11 - 12	24	2031.69	52.33	53	0.3304	0.83	0.293	100	PS	RB.5	Single	14	105
9/9/88	13	Michelin	Pilot XTA	Rib	67 - 70	2.19	2013.15	52.56	53	0.1408	0.19	0.0823	100	PS	RB.5	Single	14	105
9/9/88	13	Michelin	Pilot XTA	Rib	70 - 67	2.19	2004.74	52.42	53	0.1312	0.44	0.0895	100	PS	RB.5	Single	14	105
9/7/88	11	Michelin	Pilot XZA-1	Rib	71 - 79	4.28	1989.63	52.6	53	0.1524	0.45	0.0986	100	PS	RB.5	Single	14	105
9/7/88	11	Michelin	Pilot XZA-1	Rib	79 - 71	4.28	1972.75	52.5	53	0.1274	0.26	0.0952	100	PS	RB.5	Single	14	105
9/7/88	11	Michelin	Lng Ranger	Rib	81 - 82	4.62	1991.33	53.19	53	0.0734	0.48	0.0562	100	PS	RB.5	Single	14	105
9/7/88	11	Michelin	Lng Ranger	Rib	82 - 81	4.62	1982.38	53.16	53	0.0862	0.59	0.0649	100	PS	RB.5	Single	14	105
9/7/88	11	Michelin	Pilot XZA,XZA-1	Rib	79 - 106	4.62	1984.03	52.31	53	0.1183	0.49	0.086	100	PS	RB.5	Single	14	105
9/7/88	11	Michelin	Pilot XZA-1,XZA	Rib	106 - 79	4.62	1980.41	52.29	53	0.1522	0.41	0.104	100	PS	RB.5	Single	14	105
9/7/88	11	Michelin	Pilot XTA	Rib	76 - 69	4.72	1994.19	52.51	53	0.1345	0.67	0.0983	100	PS	RB.5	Single	14	105
9/8/88	12	Michelin	Pilot XTA	Rib	66 - 77	5.98	1990.46	52.22	53	0.159	0.47	0.1102	100	PS	RB.5	Single	14	105
9/8/88	12	Michelin	Pilot XTA	Rib	77 - 66	5.98	1998.26	52.25	53	0.1652	0.12	0.0947	100	PS	RB.5	Single	14	105
9/8/88	12	Michelin	Pilot XTA	Rib	65 - 78	6.3	1964.04	52.28	53	0.1911	0.14	0.1115	100	PS	RB.5	Single	14	105
9/8/88	12	Michelin	Pilot XTA	Rib	78 - 65	6.3	2006.38	52.21	53	0.1734	0.08	0.1009	100	PS	RB.5	Single	14	105
9/8/88	12	Michelin	Pilot XZA-1	Rib	80 - 104	6.95	2003.05	52.58	53	0.1366	0.6	0.0996	100	PS	RB.5	Single	14	105
9/8/88	12	Michelin	Pilot XZA-1	Rib	104 - 80	6.95	1989.51	52.22	53	0.149	0.65	0.0972	100	PS	RB.5	Single	14	105
9/8/88	12	Michelin	Pilot XTA	Rib	63 - 74	7.05	2009.14	52.07	53	0.1691	0.18	0.0933	100	PS	RB.5	Single	14	105
9/8/88	12	Michelin	Pilot XTA	Rib	74 - 63	7.05	1988.59	52.13	53	0.1461	0.16	0.0876	100	PS	RB.5	Single	14	105
9/7/88	11	Michelin	Pilot XTA	Rib	73 - 75	7.4	1983.72	52.62	53	0.182	0.28	0.1062	100	PS	RB.5	Single	14	105
9/7/88	11	Michelin	Pilot XTA	Rib	75 - 73	7.4	1981.95	52.74	53	0.1911	0.16	0.1102	100	PS	RB.5	Single	14	105
9/8/88	12	Michelin	Pilot(') XZA-1,XZA	Rib	72 - 103	7.51	2002.73	52.76	53	0.1895	0.43	0.1256	100	PS	RB.5	Single	14	105
9/8/88	12	Michelin	Pilot(') XZA,XZA-1	Rib	103 - 72	7.51	2025.35	52.63	53	0.1307	0.19	0.0915	100	PS	RB.5	Single	14	105
9/12/88	14	Michelin	Pilot XTA	Rib	64 - 68	7.98	2014.76	52.16	53	0.1842	0.36	0.1103	100	PS	RB.5	Single	14	105
9/12/88	14	Michelin	Pilot(') XZA-1,XZA	Rib	105 - 107	9.09	1989.82	52.22	53	0.1805	0.43	0.1014	100	PS	RB.5	Single	14	105
9/12/88	14	Michelin	Pilot(') XZA,XZA-1	Rib	107 - 105	9.09	1964.67	52.03	53	0.2013	0.33	0.1388	100	PS	RB.5	Single	14	105

Appendix C

μ-slip curves showing the contrast in response obtained when the two tires in a dual pair are "swapped".

All tires have been fleet-worn to a tread depth whose average value for the dual pair is listed below each figure. The notation on each figure indicates the code numbers of the tires which were installed within the dual pair, denoting the "inside" position, I, and the "outside" position, O.

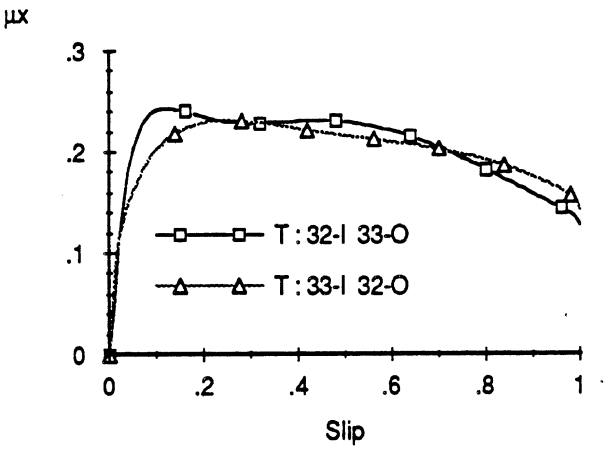

G159 TD = 8.90 on PS @ 53 mph

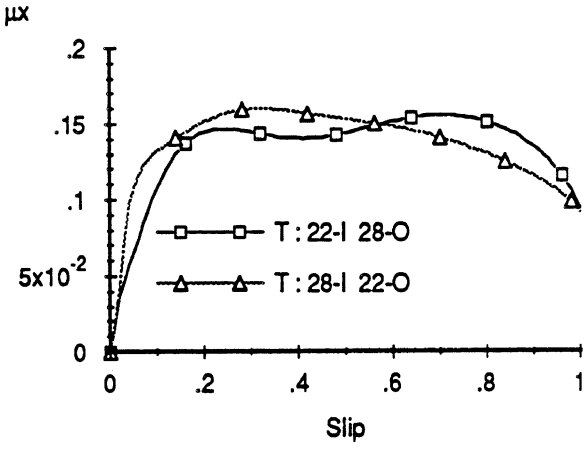

G159 TD = 10.50 on PS @ 53 mph

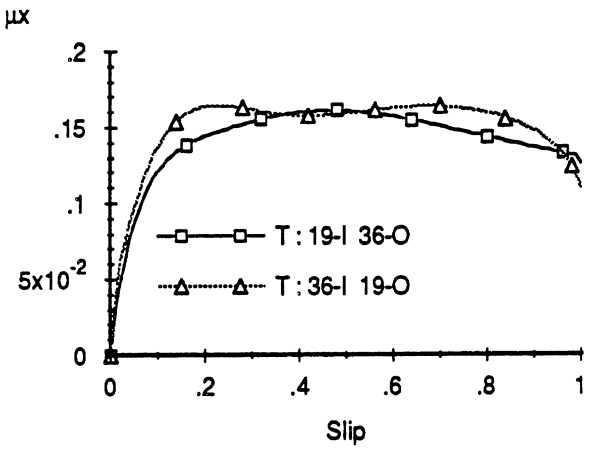

G159 TD = 9.30 on PS @ 53 mph

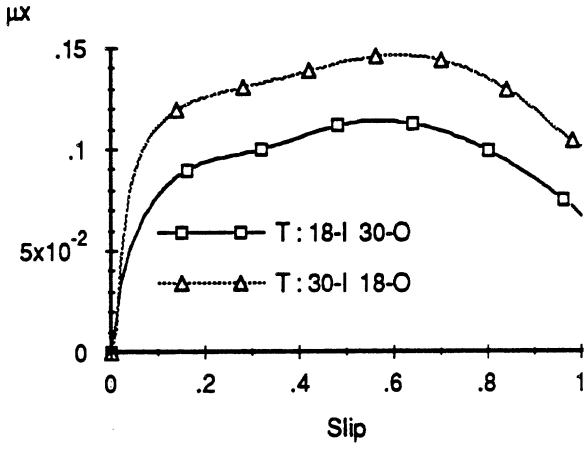

G159 TD = 11.55 on PS @ 53 mph

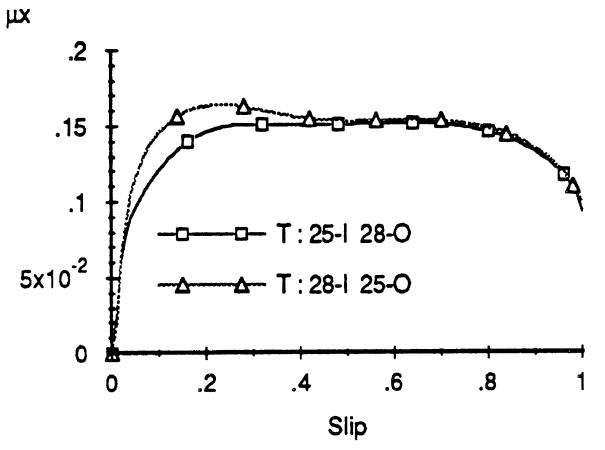

G159 TD = 10.25 on PS @ 53 mph

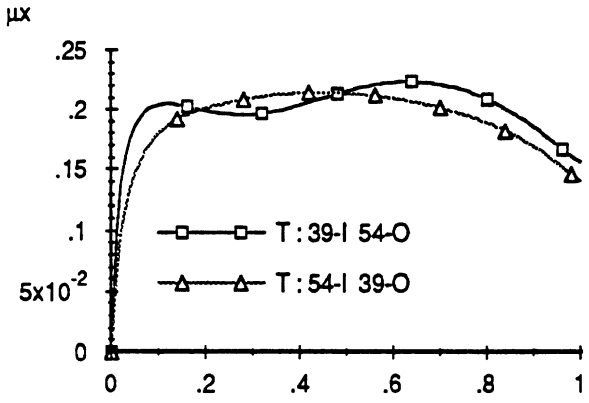

G167 TD = 4.20 on PS @ 53 mph

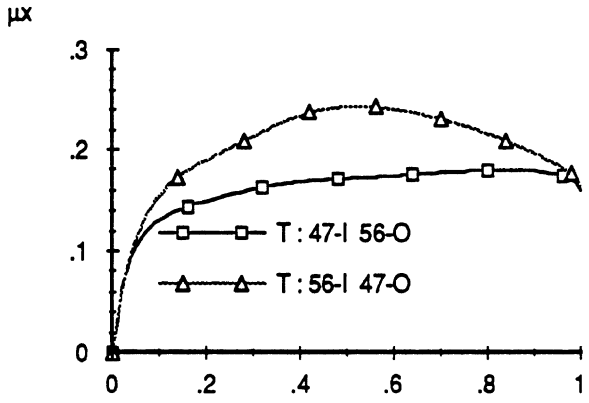

G167 TD = 5.10 on PS @ 53 mph

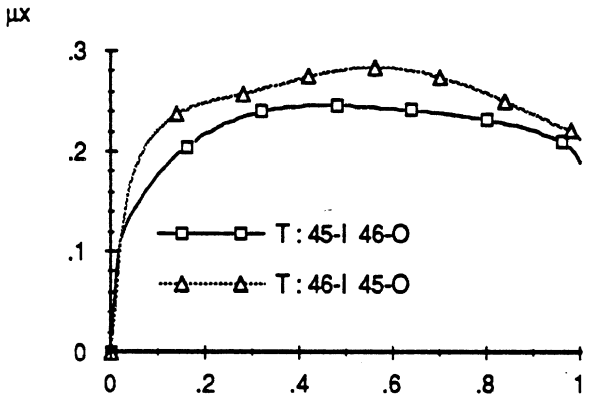

G167 TD = 4.50 on PS @ 53 mph

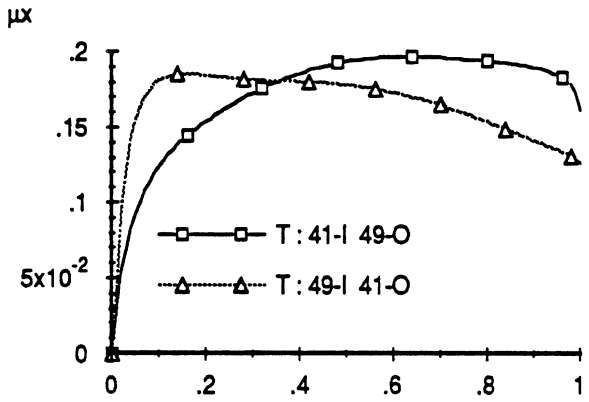

G167 TD = 5.20 on PS @ 53 mph

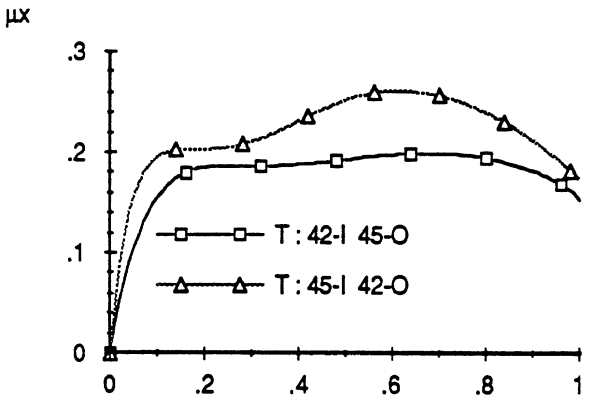

G167 TD = 4.65 on PS @ 53 mph

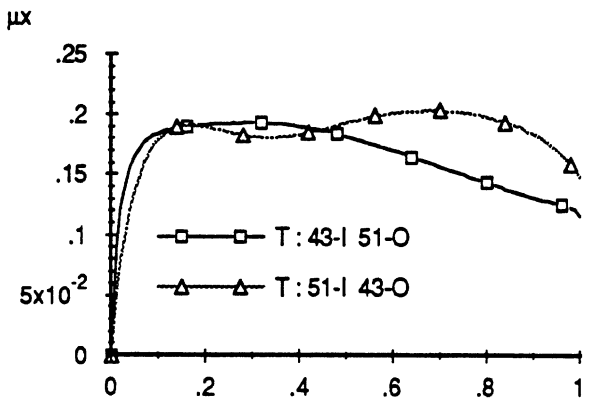

G167 TD = 3.15 on PS @ 53 mph

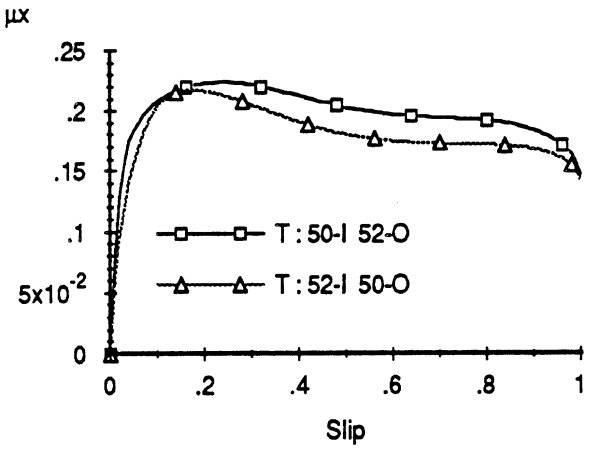

G167 TD = 3.50 on PS @ 53 mph

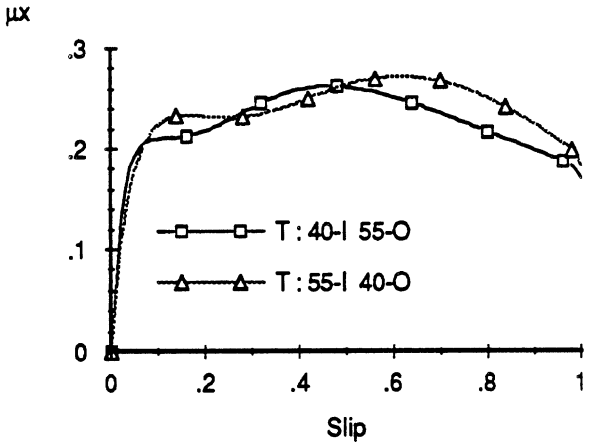

G167 TD = 7.85 on PS @ 53 mph

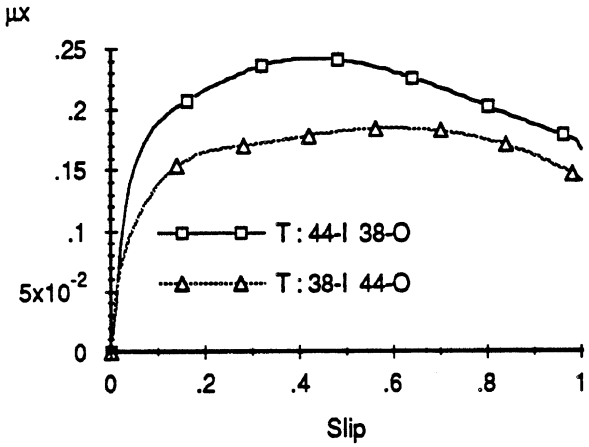

G167 TD = 3.75 on PS @ 53 mph

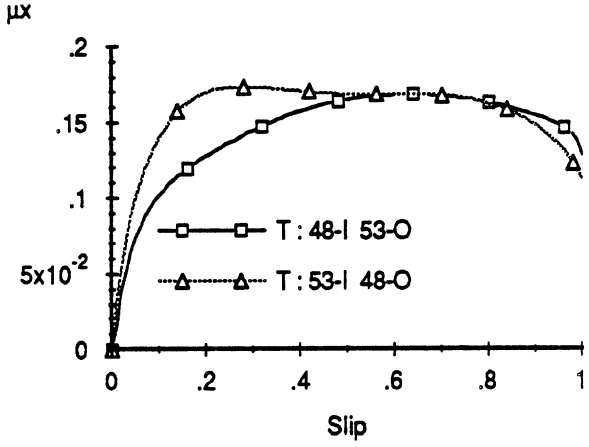

G167 TD = 2.45 on PS @ 53 mph

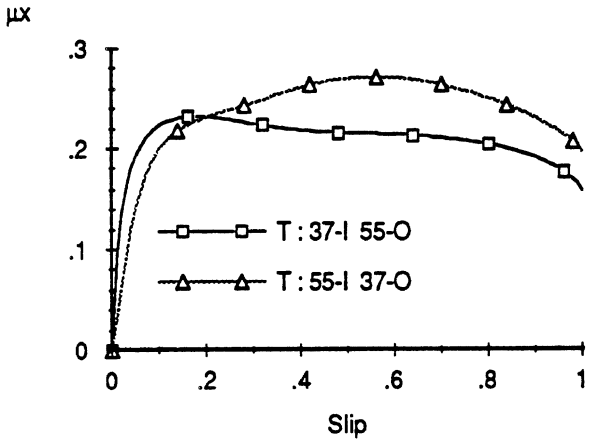

G167 TD = 7.25 on PS @ 53 mph

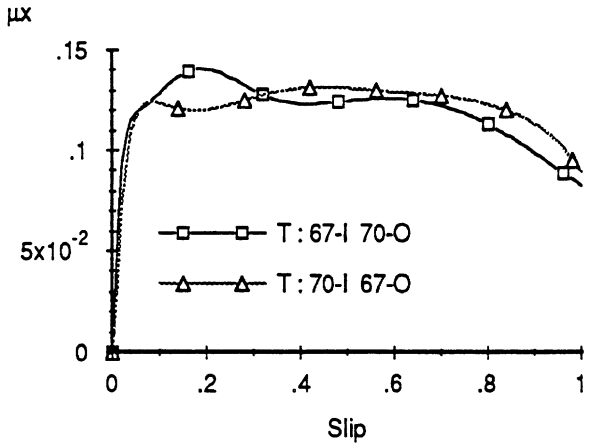

Michelin (XTA) TD = 2.19 on PS @ 53 mph

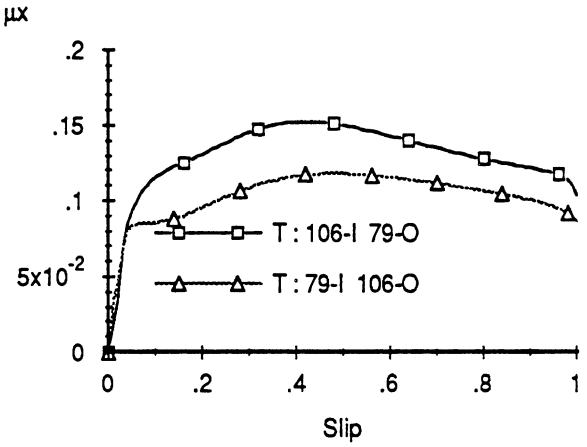

Michelin (XZA-XZA-1) TD = 4.62 on PS @ 53 mph

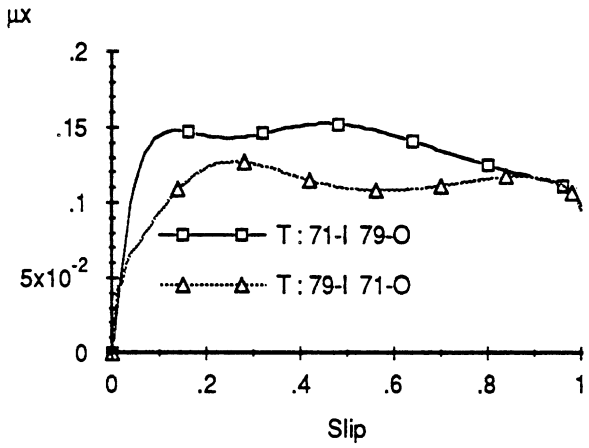

Michelin (XZA-1) TD = 4.28 on PS @ 53 mph

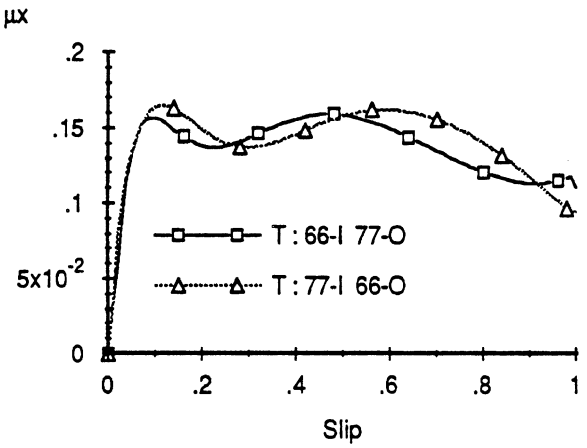

Michelin (XTA) TD = 5.98 on PS @ 53 mph

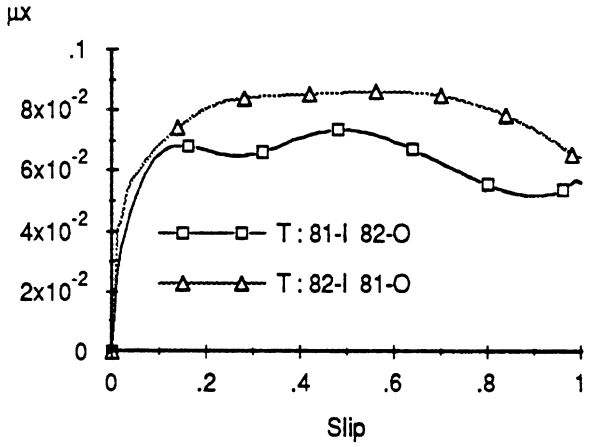

Michelin (Lng Rng) TD = 4.62 on PS @ 53 mph

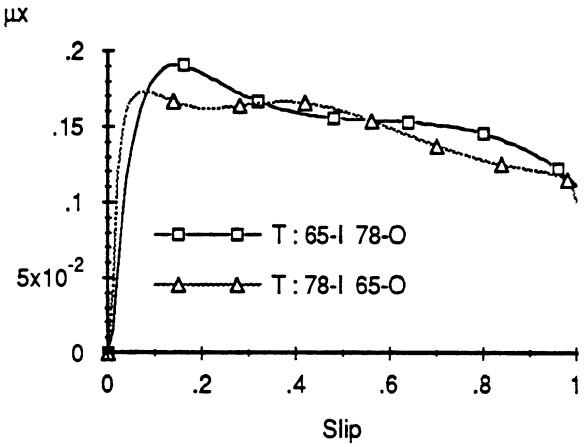

Michelin (XTA) TD = 6.30 on PS @ 53 mph

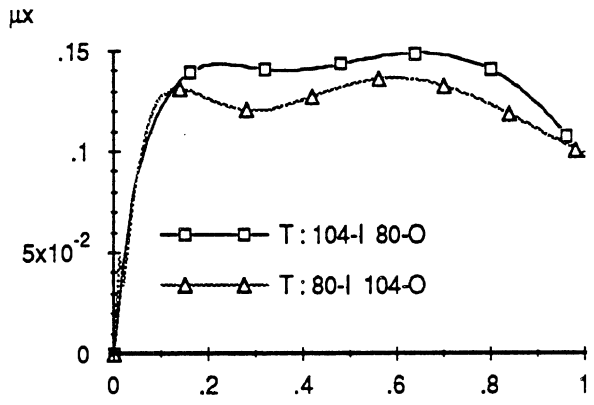

Michelin (XZA-1) TD = 6.95 on PS @ 53 mph

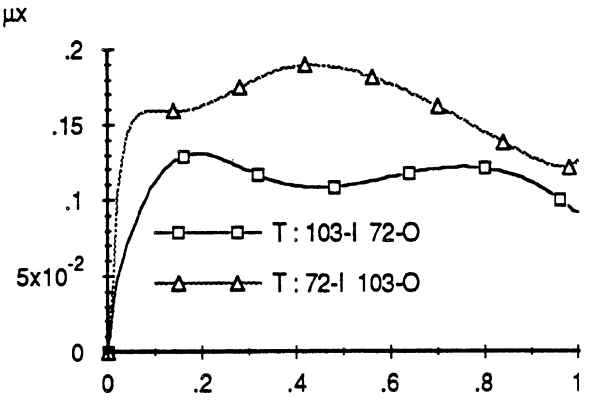

Michelin (XZA-XZA-1) TD = 7.51 on PS @ 53 mph

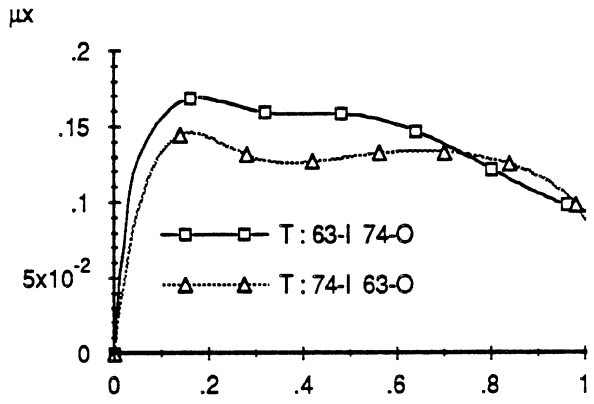

Michelin (XTA) TD = 7.05 on PS @ 53 mph

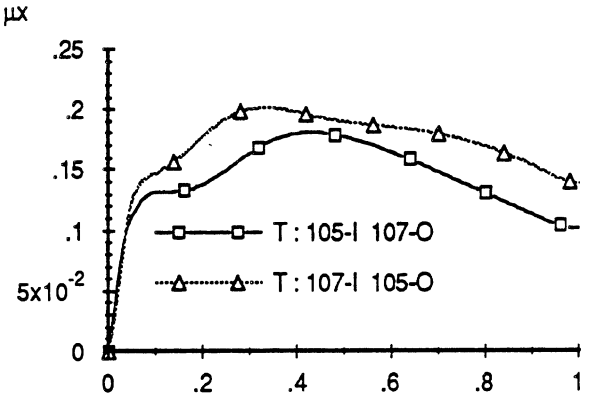

Michelin (XZA-1-XZA) TD = 9.09 on PS @ 53 mph

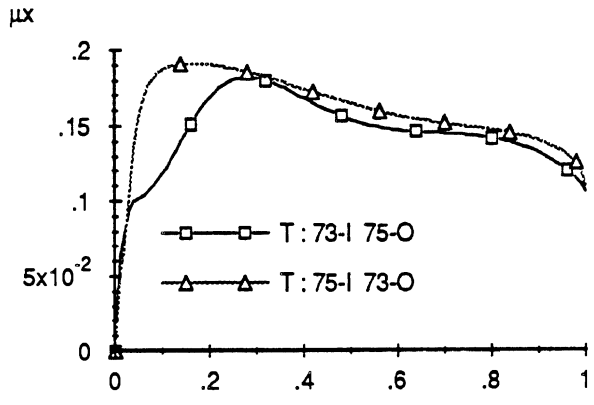

Michelin (XTA) TD = 7.40 on PS @ 53 mph

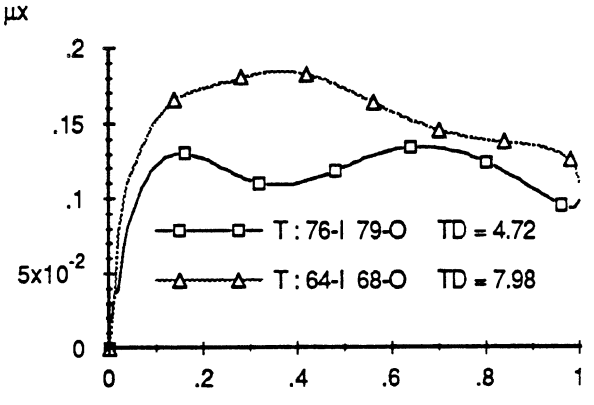

Michelin (XTA) on PS @ 53 mph

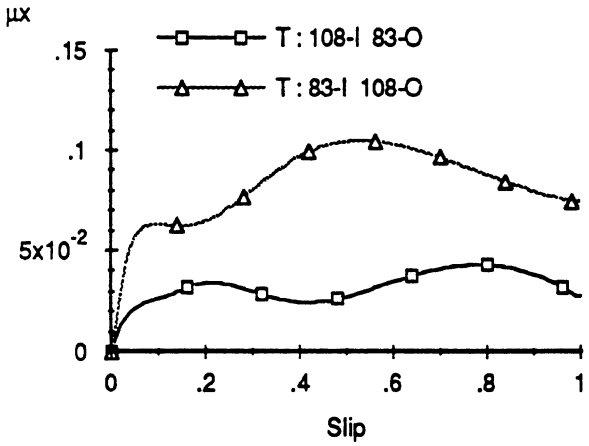

Michelin (XDA-XDHT) TD = 1.43 on PS @ 53 mph

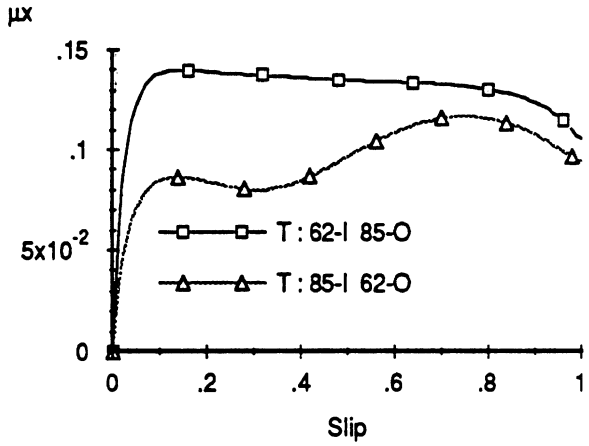

Michelin (XDHT-XDA) TD = 3.88 on PS @ 53 mph

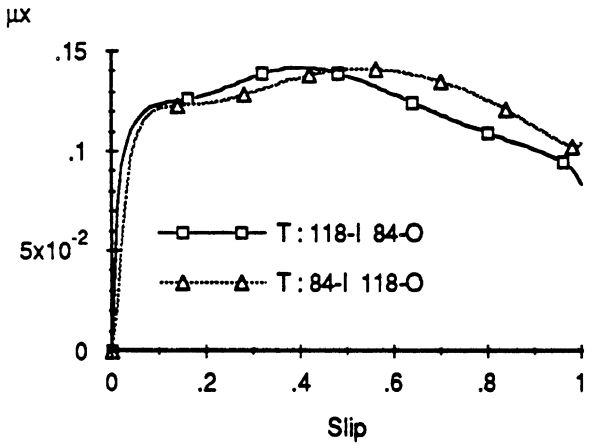

Michelin (XDA-XDHT) TD = 2.12 on PS @ 53 mph

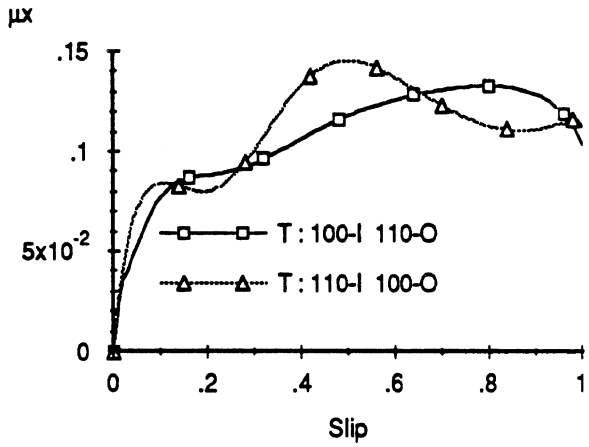

Michelin (XDA) TD = 4.40 on PS @ 53 mph

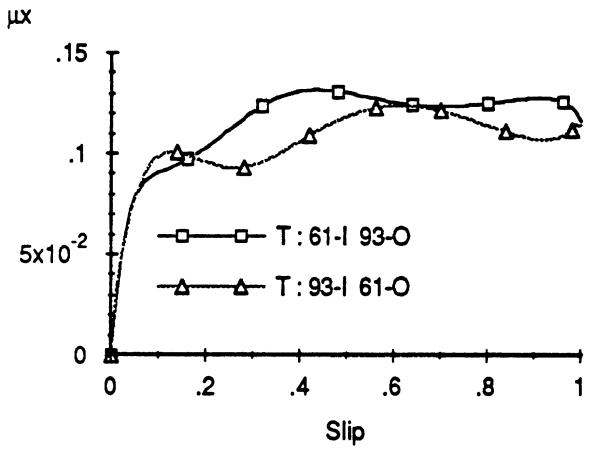

Michelin (XDHT-XDA) TD = 2.97 on PS @ 53 mph

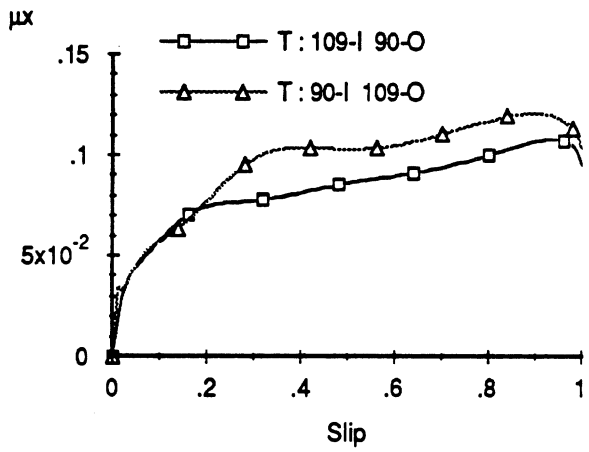

Michelin (XDA) TD = 4.61 on PS @ 53 mph

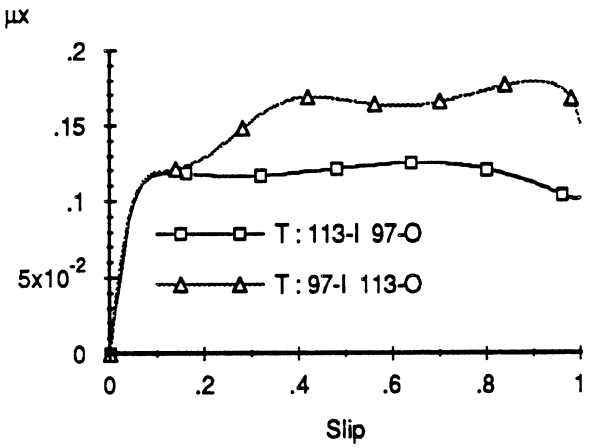

Michelin (XDHT-XDA) TD = 4.80 on PS @ 53 mph

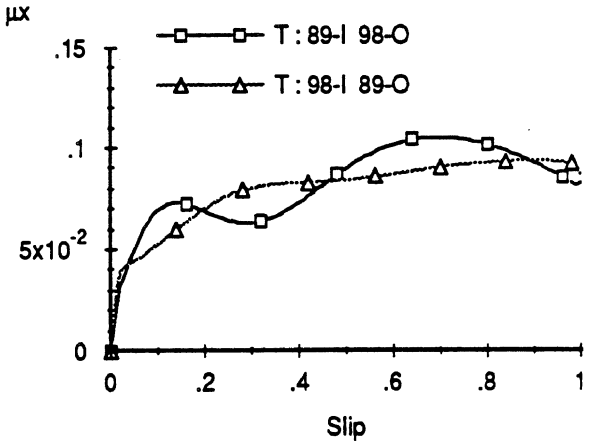

Michelin (XDA) TD = 5.19 on PS @ 53 mph

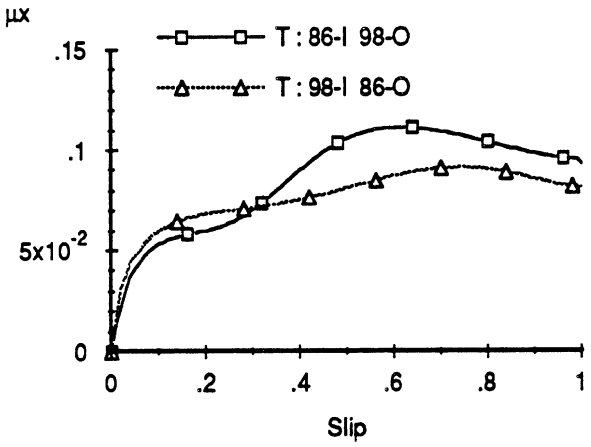

Michelin (XDA) TD = 5.08 on PS @ 53 mph

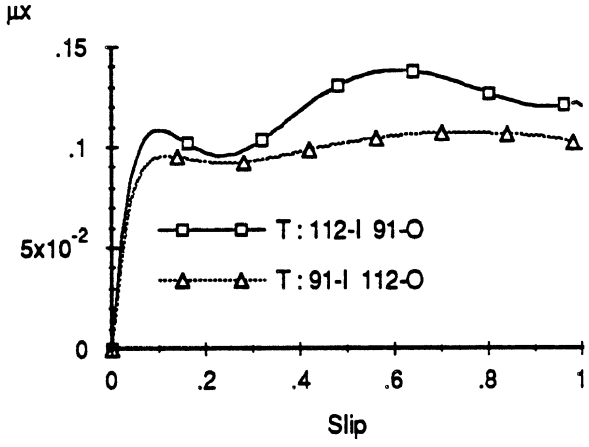

Michelin (XDA) TD = 5.69 on PS @ 53 mph

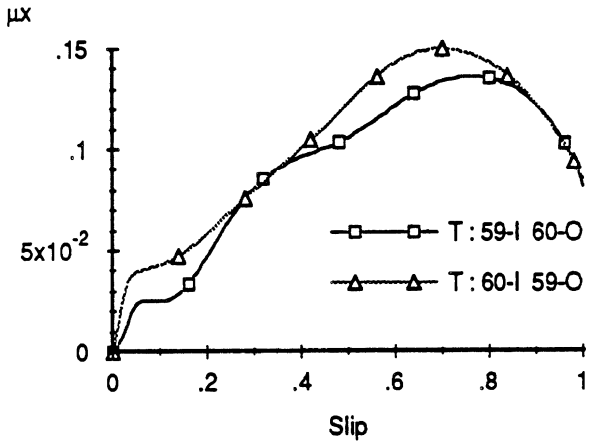

Michelin (X) TD = 5.10 on PS @ 53 mph

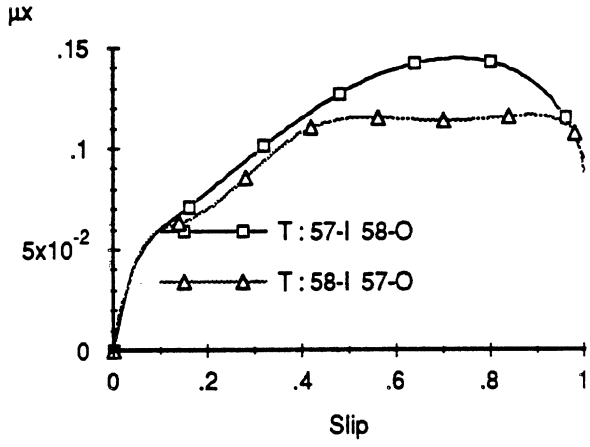

Michelin (X) TD = 5.99 on PS @ 53 mph

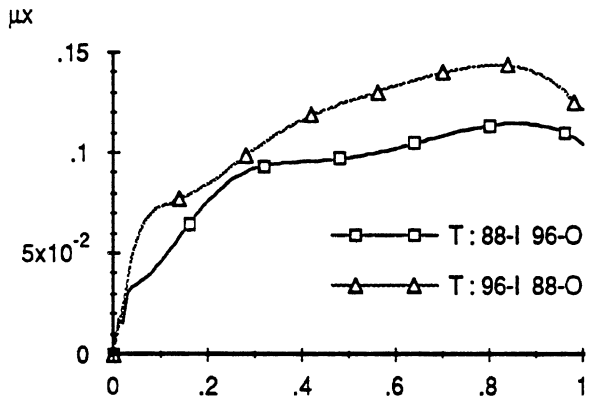

Michelin (XDA) TD = 6.40 on PS @ 53 mph

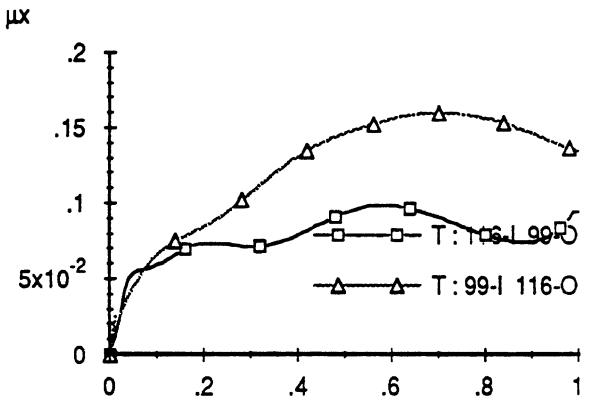

Michelin (XDA) TD = 8.97 on PS @ 53 mph

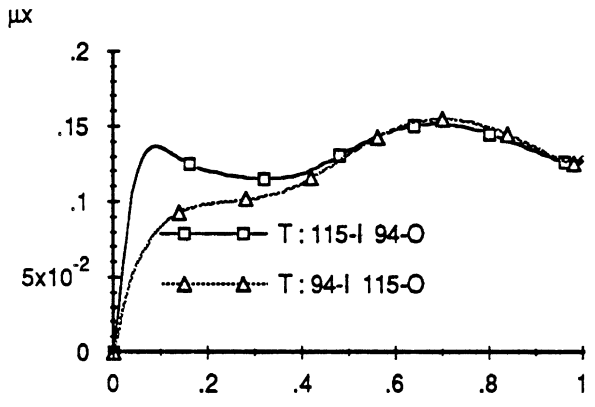

Michelin (XZA-1-XDA) TD = 6.83 on PS @ 53 mph

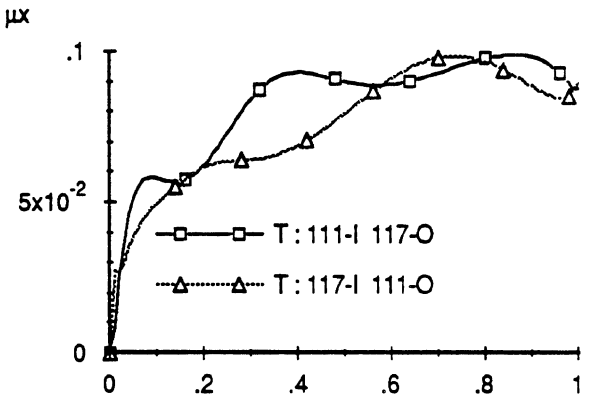

Michelin (XDA) TD = 9.34 on PS @ 53 mph

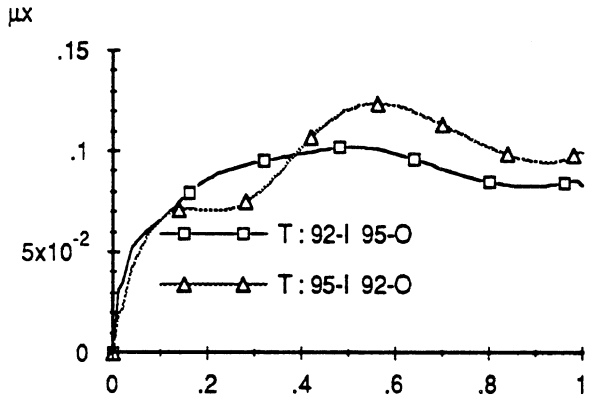

Michelin (XDA) TD = 7.29 on PS @ 53 mph

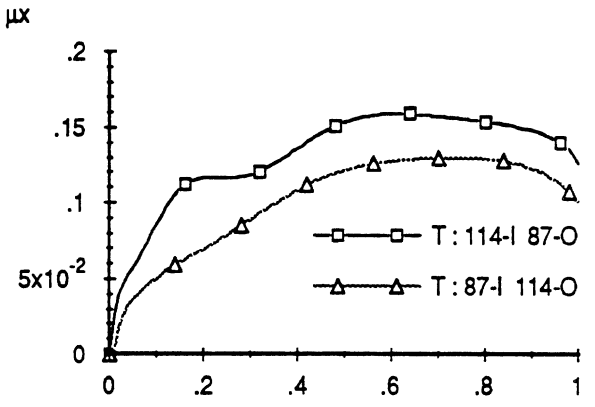

Michelin (XDA) TD = 9.96 on PS @ 53 mph

Appendix D

Plots of peak and slide μ for selected groupings of tires from the fleet-worn sample.

The plots cover the following groupings:

- all tires tested in the fleet-worn portion of the program
- all tires having a tread depth less than 4/32 inch
- all Goodyear tires having a tread depth less than 4/32 inch
- all Michelin tires having a tread depth less than 4/32 inch
- all lug-type tires having a tread depth less than 4/32 inch
- all Goodyear-lug type tires
- all Goodyear-rib type tires
- all Michelin-rib type tires
- all Michelin-lug type tires
- all Michelin-lug tires having less than 4/32 inch of tread depth

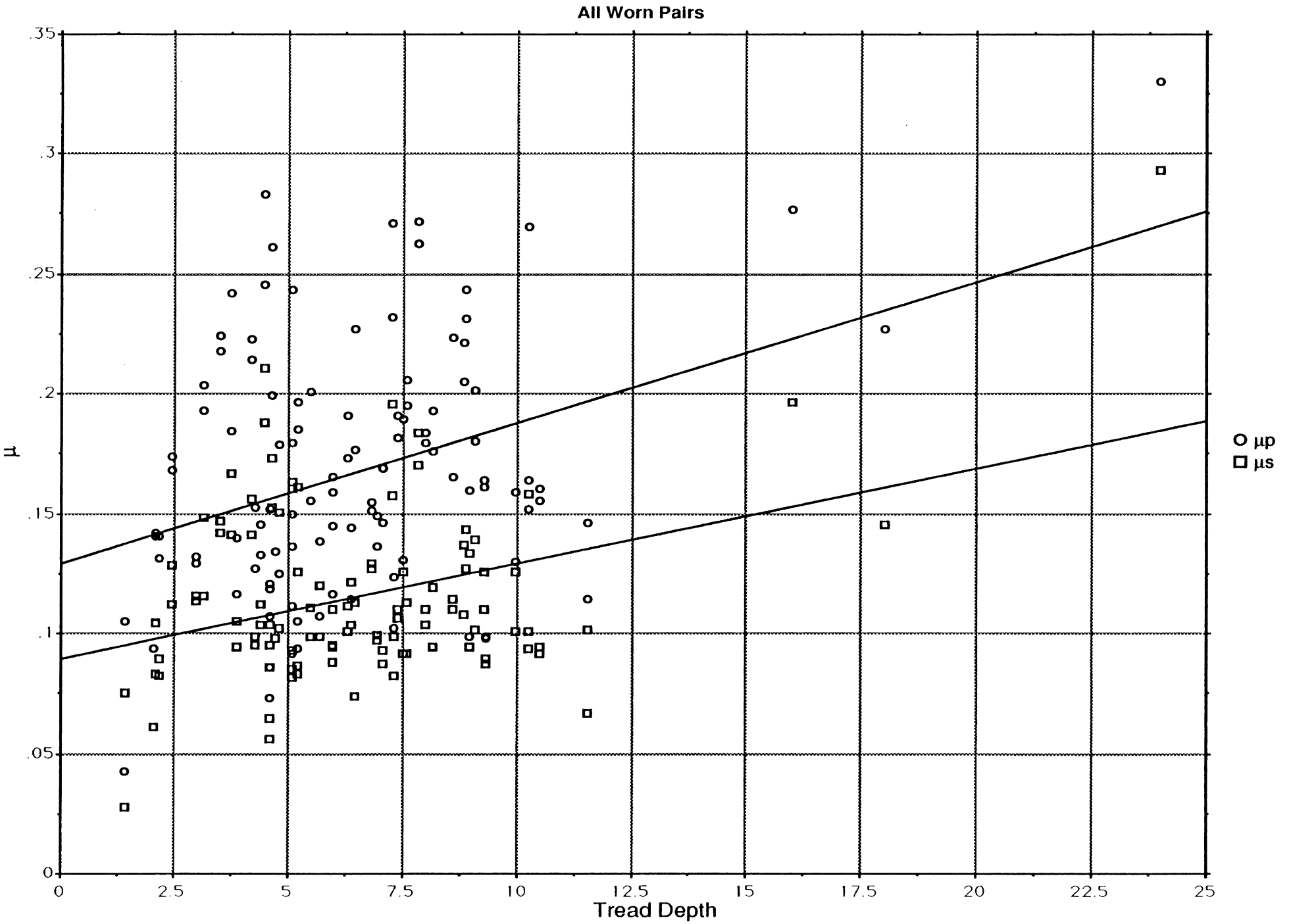
All Worn Pairs
.35
.3
.25
.2
.15
.1
.05
0
μ
0
2.5
5
7.5
10
12.5
15
17.5
20
22.5
25
Tread Depth
μp
μs

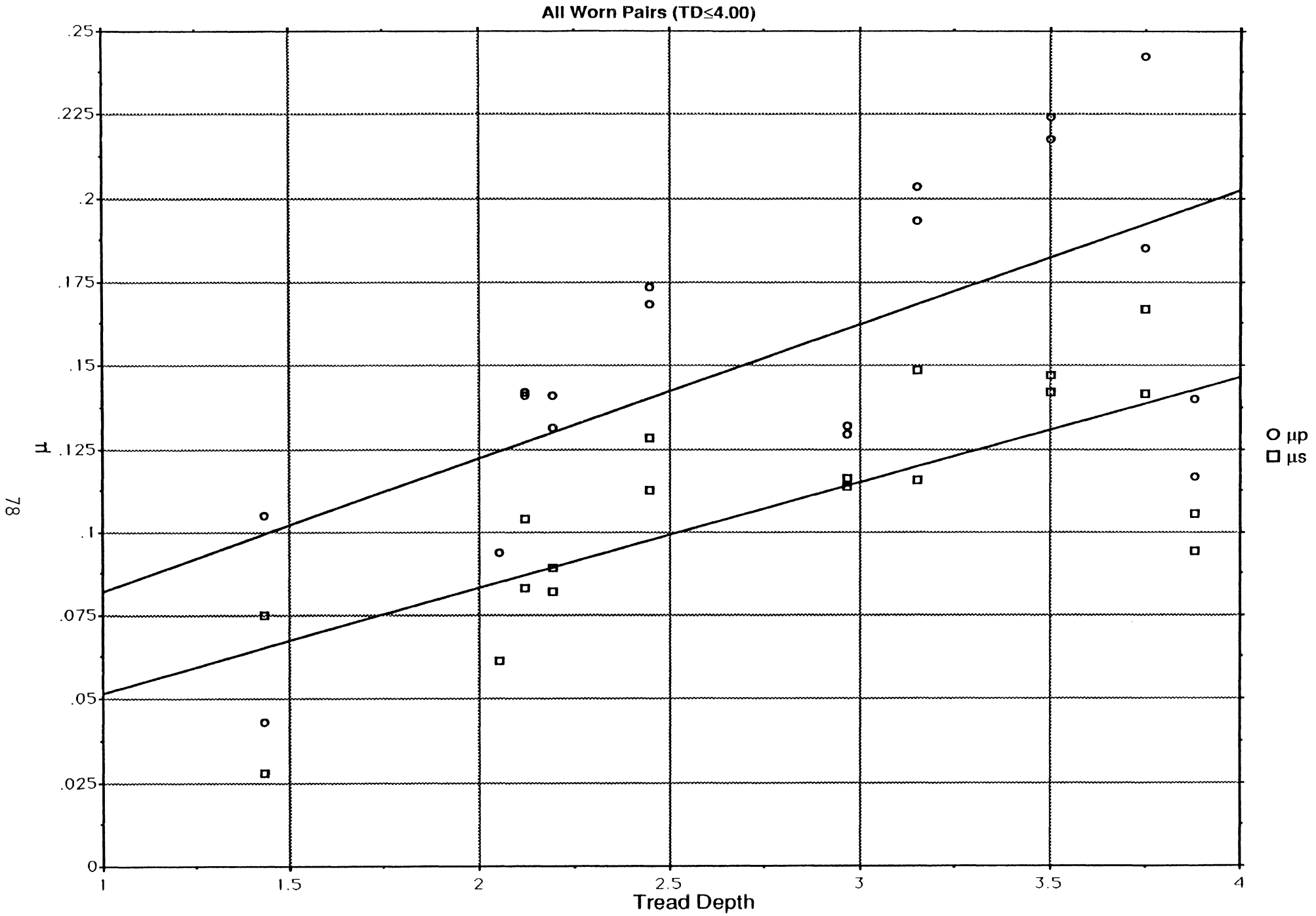
All Worn Pairs (TD≤4.00)
.25
.225
.2
.175
.15
.125
.1
.075
.05
.025
0
μ
1
1.5
2
2.5
3
3.5
4
Tread Depth
μp
μs

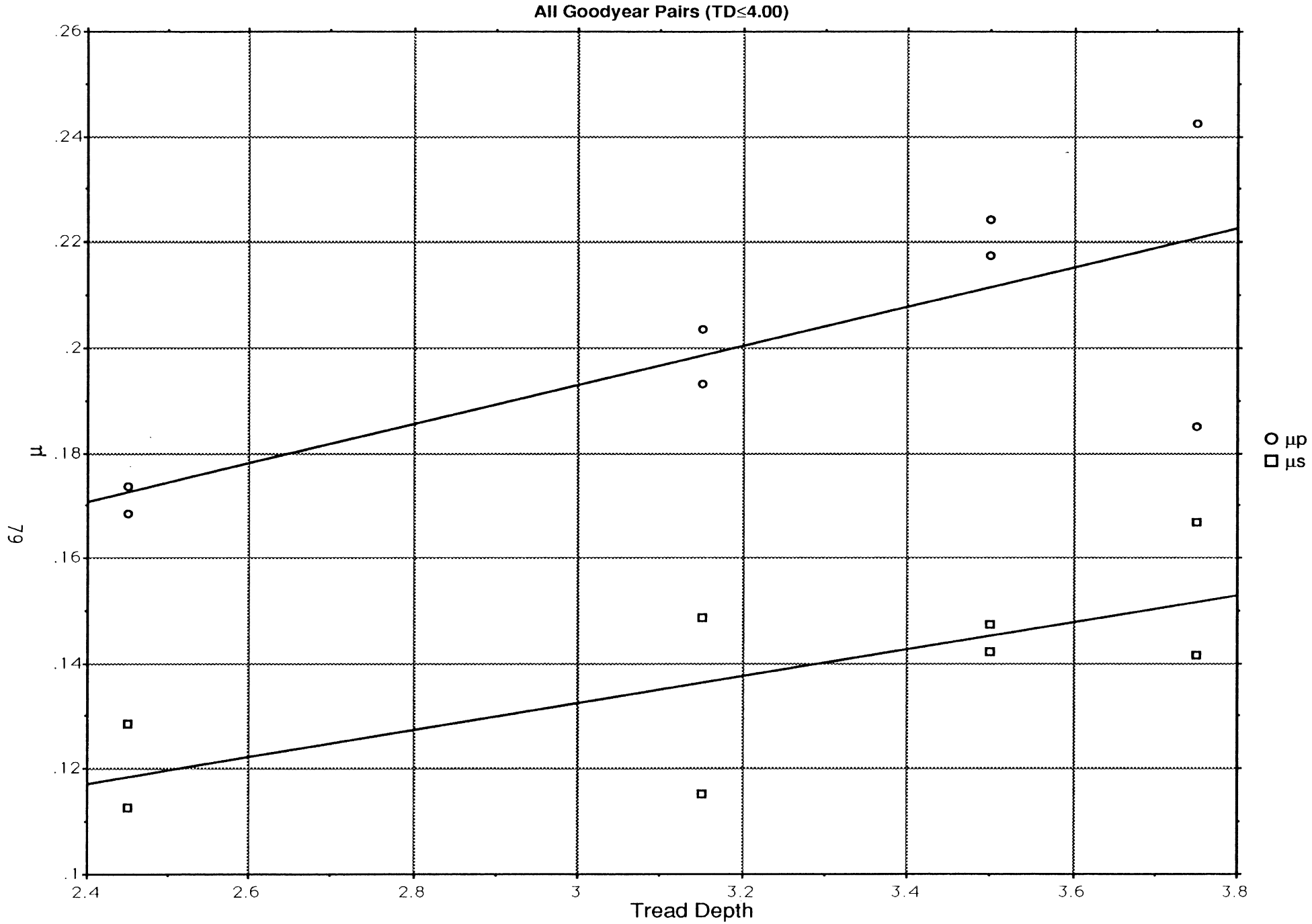
All Goodyear Pairs (TD≤4.00)
.26
.24
.22
.2
.18
.16
.14
.12
.1
μ
2.4
2.6
2.8
3
3.2
3.4
3.6
3.8
Tread Depth
μp
μs

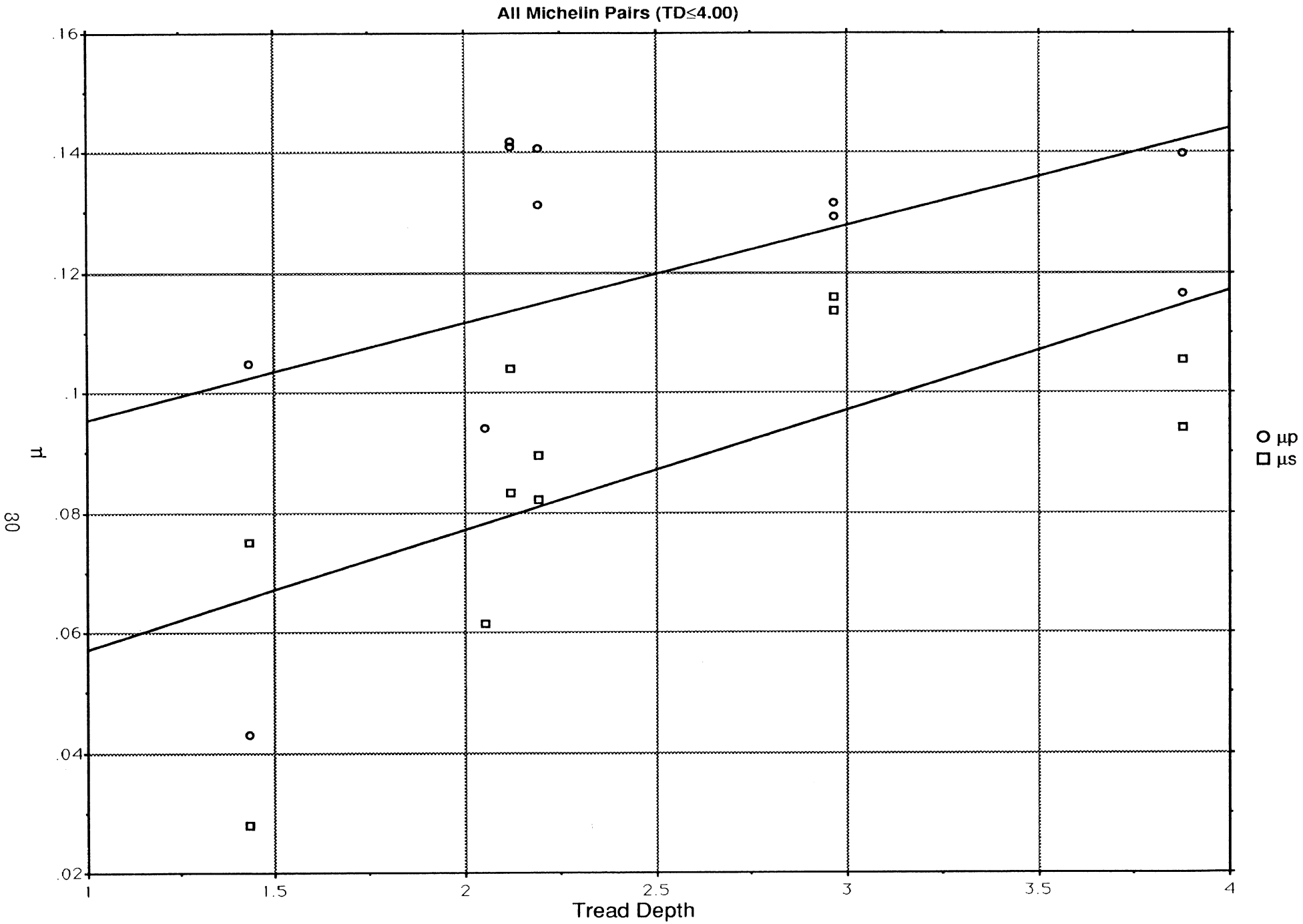
All Michelin Pairs (TD≤4.00)
.16
.14
.12
.1
.08
.06
.04
.02
μ
1
1.5
2
2.5
3
3.5
4
Tread Depth
μp
μs

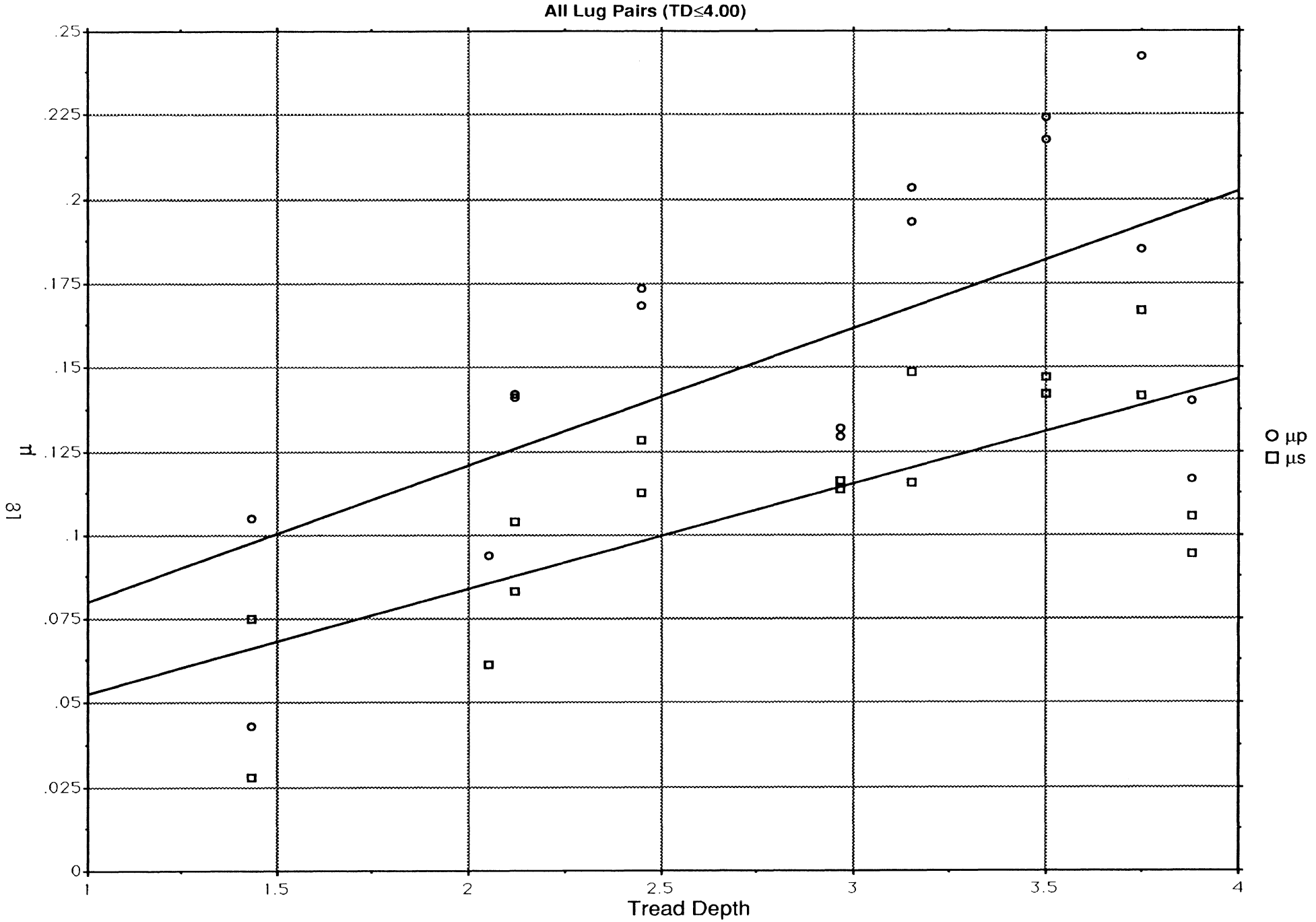
All Lug Pairs (TD≤4.00)
.25
.225
.2
.175
.15
.125
.1
.075
.05
.025
0
μ
1
1.5
2
2.5
3
3.5
4
Tread Depth
μp
μs

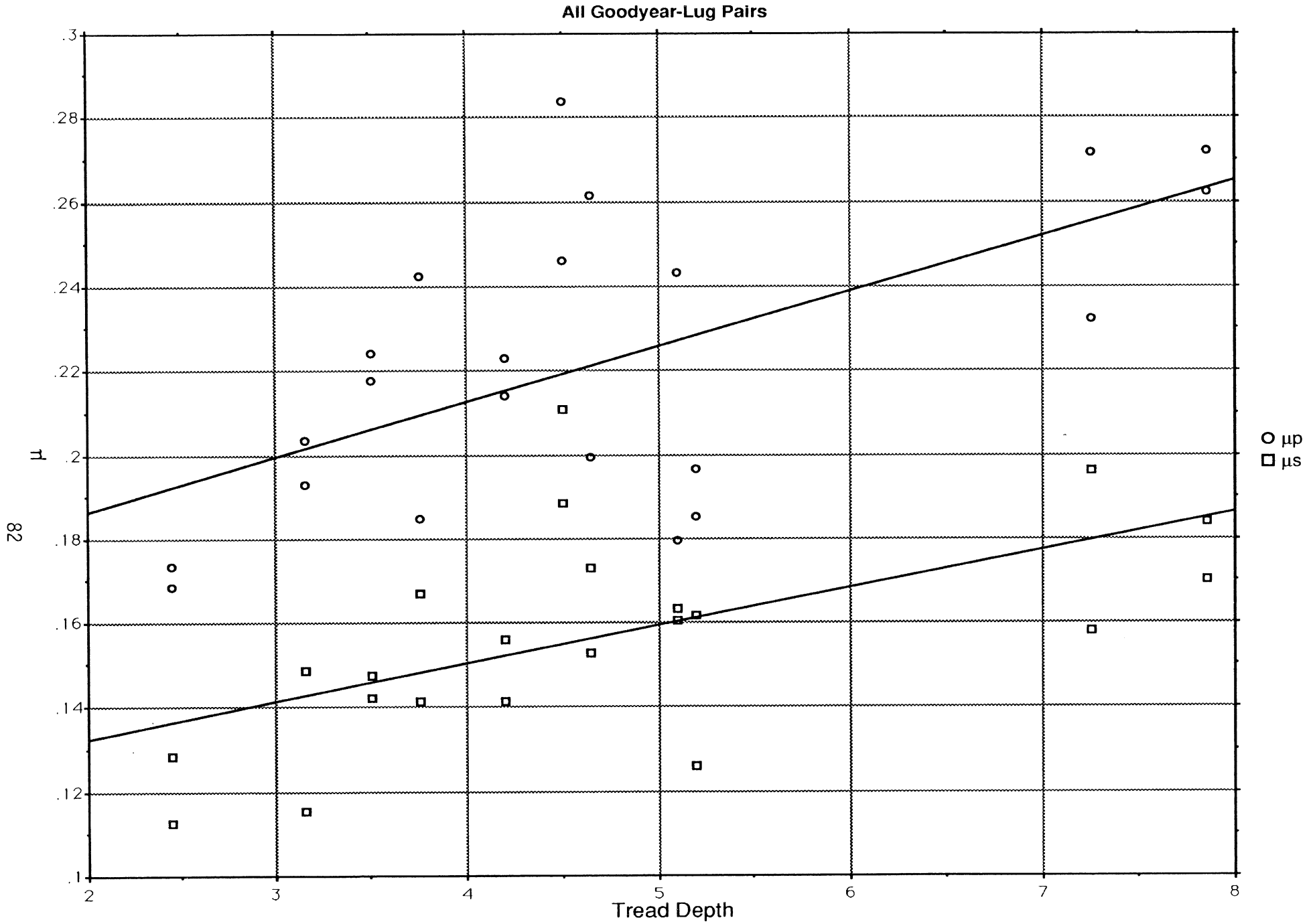
All Goodyear-Lug Pairs
μ
.3
.28
.26
.24
.22
.2
.18
.16
.14
.12
.1
2
3
4
5
6
7
8
Tread Depth
μp
μs

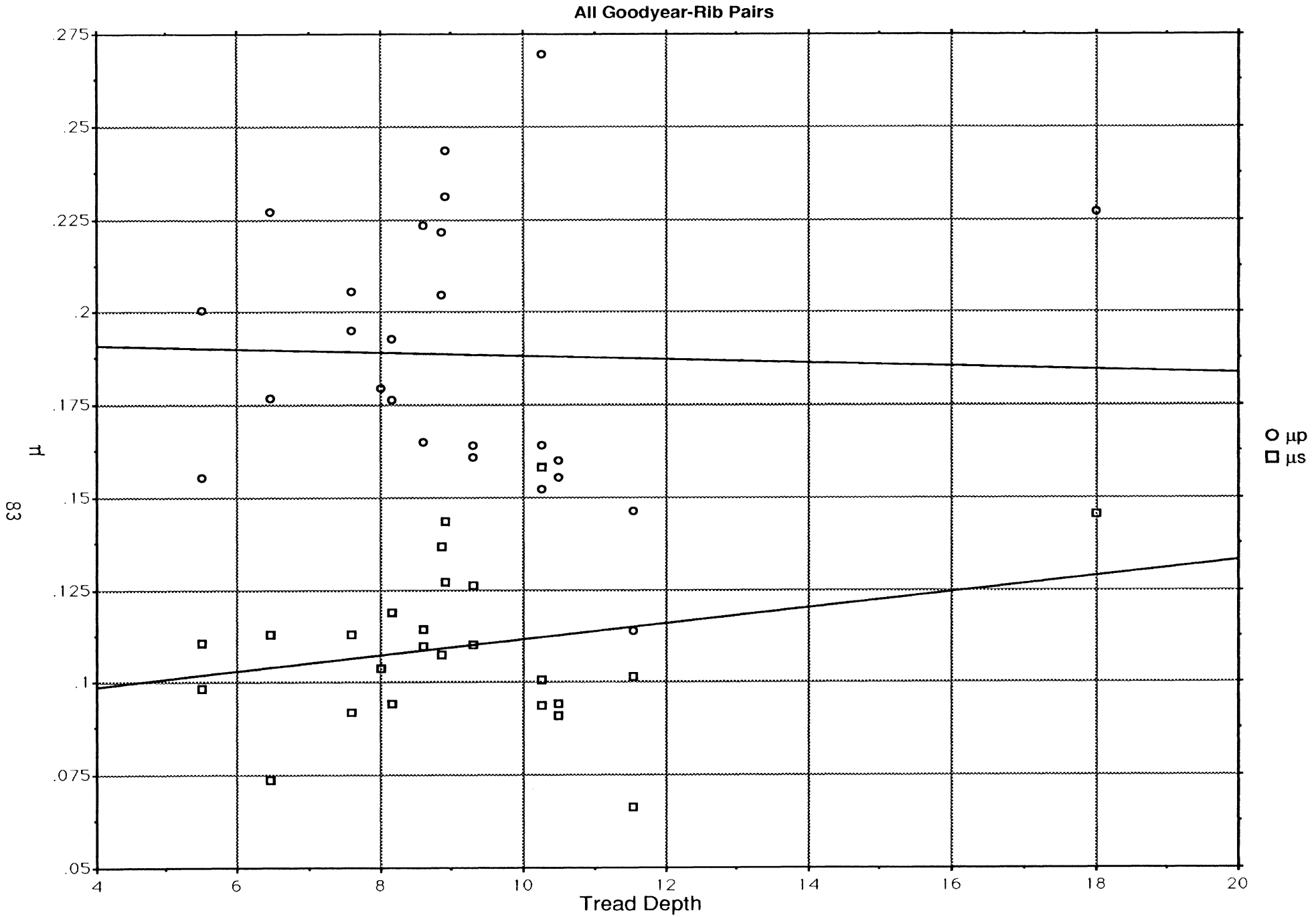
All Goodyear-Rib Pairs
.275
.25
.225
.2
.175
.15
.125
.1
.075
.05
μ
4
6
8
10
12
14
16
18
20
Tread Depth
μp
μs

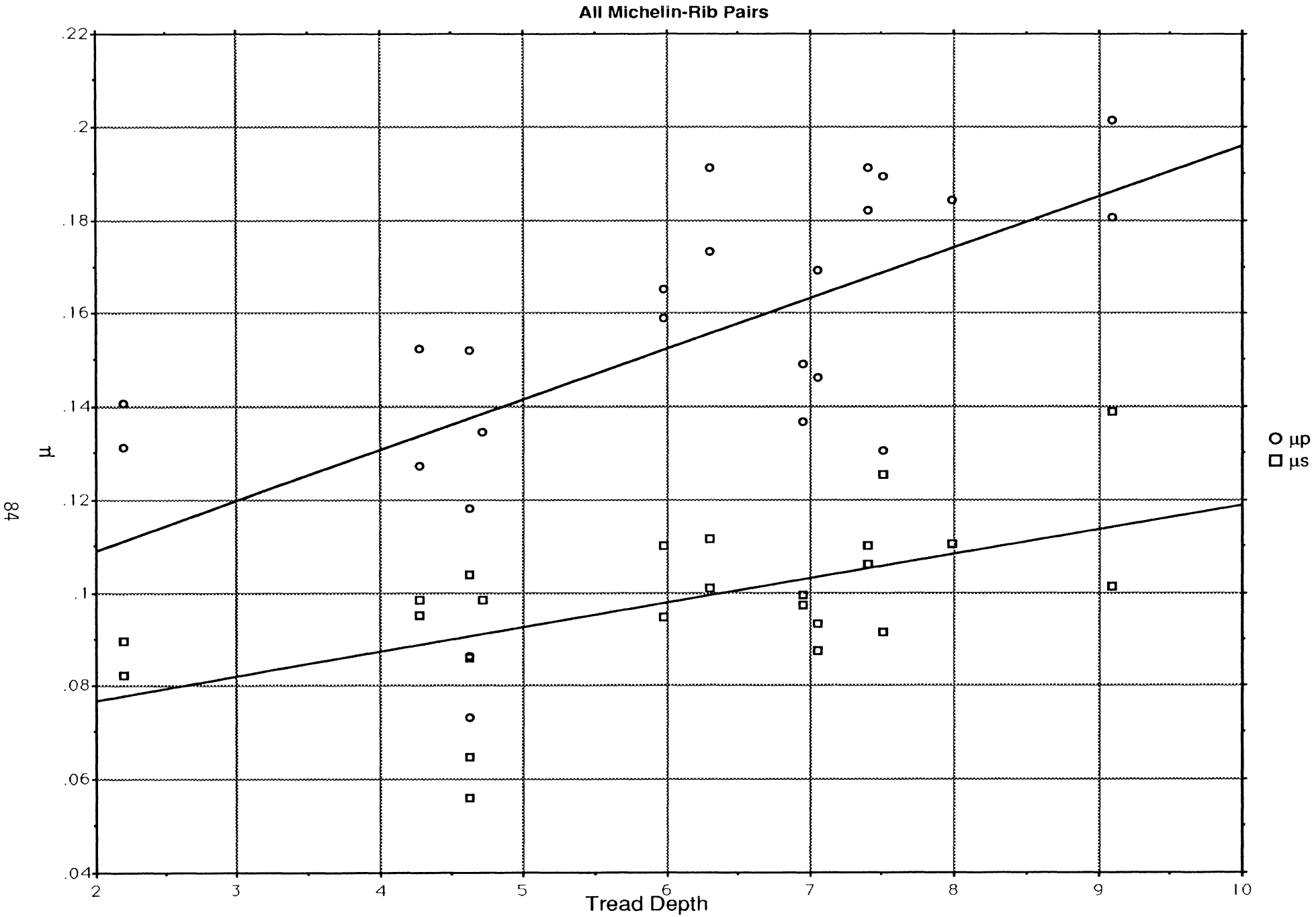
All Michelin-Rib Pairs
.22
.2
.18
.16
.14
.12
.1
.08
.06
.04
μ
2
3
4
5
6
7
8
9
10
Tread Depth
μp
μs

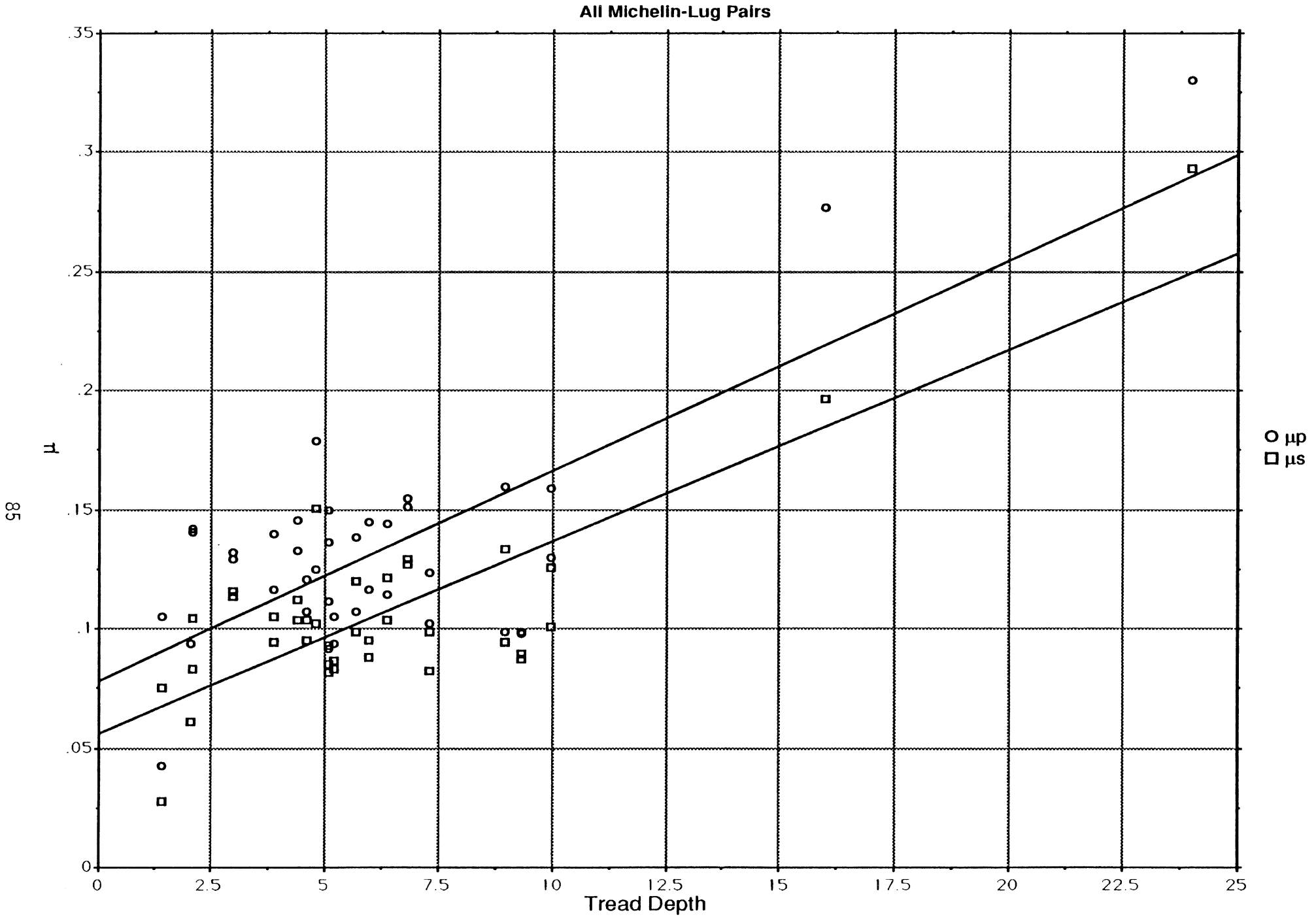
All Michelin-Lug Pairs
.35
.3
.25
.2
.15
.1
.05
0
μ
0
2.5
5
7.5
10
12.5
15
17.5
20
22.5
25
Tread Depth
μp
μs

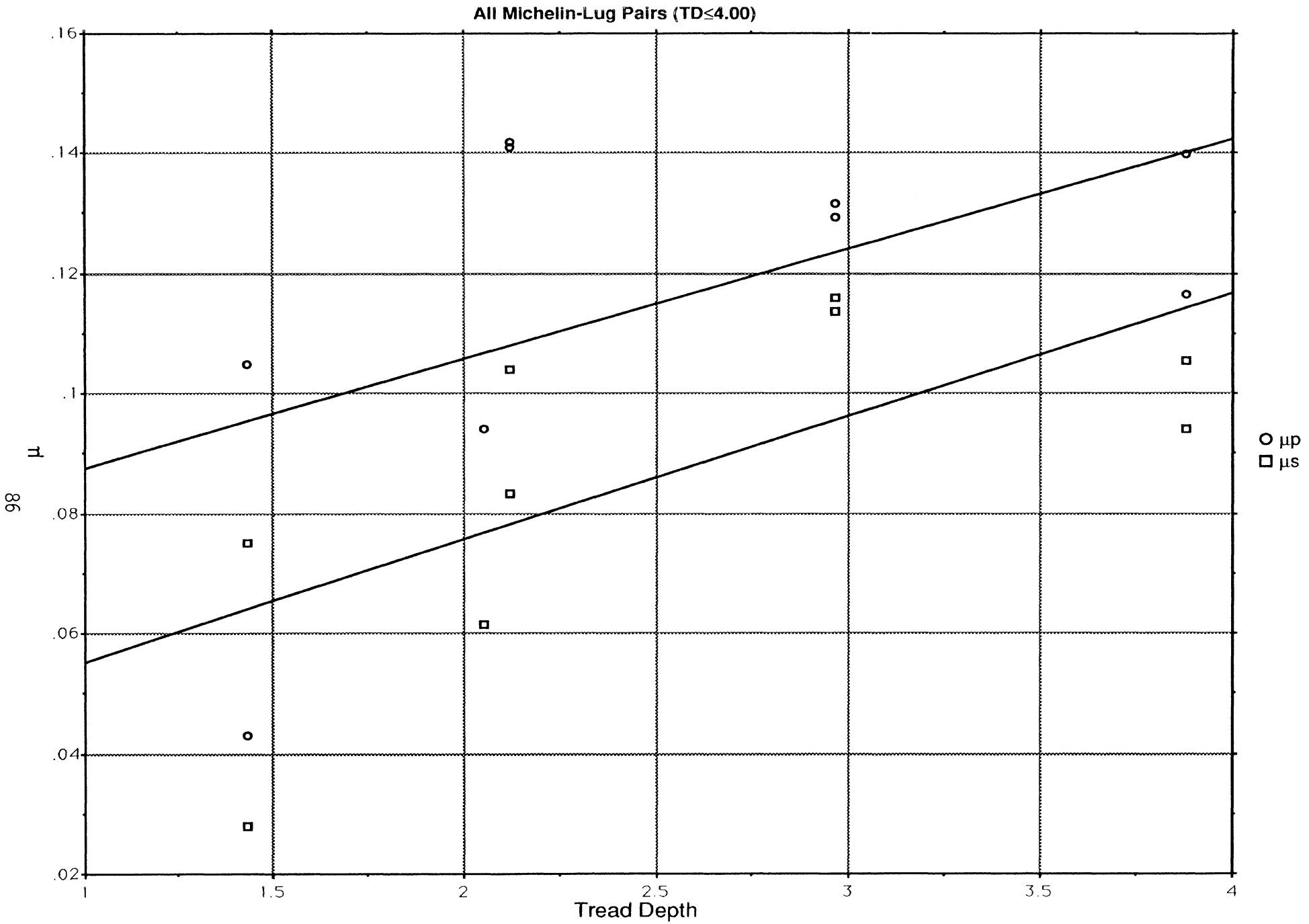
All Michelin-Lug Pairs (TD≤4.00)
.16
.14
.12
.1
.08
.06
.04
.02
μ
1
1.5
2
2.5
3
3.5
4
Tread Depth
μp
μs